

**THE PREDICTED PERFORMANCE OF
A TWO-SPOOL TURBOFAN ENGINE
IN RAINSTORMS**

By
Tarik Baki

Thesis presented for the degree of Masters of Science
MSc to the faculty of Engineering

Department of Mechanical Engineering
Glasgow University

April 1993.

© Tarik Baki.

ProQuest Number: 11007734

All rights reserved

INFORMATION TO ALL USERS

The quality of this reproduction is dependent upon the quality of the copy submitted.

In the unlikely event that the author did not send a complete manuscript and there are missing pages, these will be noted. Also, if material had to be removed, a note will indicate the deletion.



ProQuest 11007734

Published by ProQuest LLC (2018). Copyright of the Dissertation is held by the Author.

All rights reserved.

This work is protected against unauthorized copying under Title 17, United States Code
Microform Edition © ProQuest LLC.

ProQuest LLC.
789 East Eisenhower Parkway
P.O. Box 1346
Ann Arbor, MI 48106 – 1346

Thesis
9581
copy 1

GLASGOW
UNIVERSITY
LIBRARY

This thesis is dedicated to the memory of my kind and loving grand-mother Mama Hadja and my dear grand-father Hadj Tahar.

You will always be present in our hearts.

CONTENTS

ACKNOWLEDGEMENTS
NOMENCLATURE
STATION NUMBERING
SUMMARY

PAGE

CHAPTER I : GENERAL INTRODUCTION AND BACKGROUND

1.1. Introduction	4
1.1.1. Contribution made in the present investigation	6
1.2. Historical development of gas turbines	7
1.3. Modern developments	9
1.4. Turbojet engine development	10
1.5. Transient behaviour of aircraft gas turbine	11

CHAPTER II : PERFORMANCE PREDICTION PROGRAM FOR TWO-SPOOL TURBOFAN ENGINE

2.1. Modelling of gas turbines	13
2.1.1. The ICV method	14
2.1.2. The CMF method	15
2.1.3. Comparison of CMF and ICV methods	17
2.2. Non adiabatic modelling and heat transfer effects	18
2.2.1. Heat transfer effects	18
2.2.1.1. Effects on Fans, Turbines and Compressors	19
2.2.1.2. Effects on Combustion Chamber	20
2.2.1.3. Changes in Compressor characteristics	20

2.2.1.4. Tip clearance changes and effects on efficiency	21
2.2.1.5. Seal clearance changes	22
2.2.1.6. Combustion delay	22

CHAPTER III : SCALING OF COMPONENTS FOR TAY MK-650 ENGINE FROM TAY MK-610 COMPONENTS

3.1. Introduction	23
3.2. Scaling factors	24
3.3. Fan arrangements	26
3.3.1. Inner fan arrangements	27
3.3.2. Outer fan arrangements	30
3.4. IP compressor arrangements	35
3.5. HP compressor arrangements	37
3.6. HP turbine arrangements	40
3.7. LP turbine arrangements	42
3.8. Combustion chamber	43
3.9. Fuel system	43
3.10. Exhaust mixer	43
3.11. Bypass duct blockage	43
3.12. Automatic restoration of thrust system (A.R.T.S)	44
3.10. Summary of arrangements	44

CHAPTER IV : INTRODUCTION INTO THE TAY MK-650 OF WATER THERMODYNAMICS EFFECTS PREDICTION PROGRAM

4.1. Introduction	45
4.2. Performance prediction of Tay MK-650 using the intercomponent volume method "dry air case"	45
4.2.1. Fan	47

4.2.1.1. Outer fan	47
4.2.1.2. Inner fan	47
4.2.2. IP compressor	47
4.2.3. HP compressor	48
4.2.4. HP turbine	48
4.2.5. LP turbine	48
4.3. Performance of the engines "water ingestion case"	49
4.3.1. HP compressor	54
4.3.2. Combustion chamber	54
4.3.3. Bypass duct	55
4.4. Derivation of baseline	56

CHAPTER V : MATCHING OF PREDICTIONS TO TEST DATA FROM TAY MK-650 ENGINE

5.1. Engine test conditions	57
5.2. Engine core predictions	57
5.2.1. Water evaporation at plane between IP and HP compressors	58
5.2.2. Water evaporation at plane between HP compressor and Combustion chamber	60
5.3. Matching of predictions to Rolls-Royce engine tests	64
5.4. Use of matched model to predict surge	66

CHAPTER VI : APPLICATION OF PERFORMANCE OF ENGINE IN RAINSTORMS

6.1. Introduction	68
6.2. Rainstorm data	68
6.3. Application of rainstorm to Tay engine	70
6.3.1. Water distribution in Fan/Frontal area	71

6.3.2. Water evaporation effects at plane between mixer and final nozzle	72
6.3.4. Predicted performance in rainstorm	75

CHAPTER VII : CONCLUSION AND SUGGESTIONS FOR FURTHER WORK

7.1. Conclusion	79
7.1.1. Comment on above conclusions	80
7.2. Recommendations	81

REFERENCES	83
------------	----

APPENDIXES	87
------------	----

TABLES AND FIGURES	120
--------------------	-----

ACKNOWLEDGEMENTS

It is my great pleasure to express my extended gratitude to my supervisor Professor N.R.L. Maccallum for all the help, advice, guidance and encouragement displayed by him throughout this work.

My sincere thanks go to Rolls-Royce plc for providing me with the necessary information to base myself on throughout this thesis and to all the staff of the Mechanical Engineering Department at Glasgow University for their help and support.

Very special thanks go to my wife Marwah (Michele) for her care, understanding and encouragement.

Last but not least, I am grateful to my mother, my father and all my family for the love, patience and belief shown towards me at all times during my period of studies.

NOMENCLATURE

NOTATION :

A	aspect ratio of aerofoil
a	distance of point of maximum camber from blade leading edge
a/c	maximum camber
c	blade chord
C _p	specific heat at constant pressure
C ₁ ...C _n	scaling factors
D ₁ ...D _n	scaling factors
ΔP_{st}	stage pressure rise
ΔT	isentropic temperature rise
\dot{r}	fuel flow
f	ratio of heat transfer to the fluid to the work transfer from the fluid
FCSP	fraction of split
g	acceleration due to gravity
GEOM	fraction of the total engine frontal area
M	Mach number
m	polytropic index of non-adiabatic path
\dot{m}	mass flow rate of air or gas
N	shaft rotational speed
n	polytropic index of expansion or compression
P	stagnation pressure
P ₂ /P ₁	pressure ratio
P ₂₆ /P ₂₄	pressure ratio across the IP compressor
\dot{Q}	rate of heat transfer

R	compressor pressure ratio at surge, gas constant
s	space blading or pitch
s/c	pitch/chord ratio
T	stagnation temperature
T [*]	isentropic temperature
T1	inlet stagnation temperature
T24	IP compressor inlet stagnation temperature
T26	IP compressor outlet stagnation temperature
t	time, blade maximum thickness
(t/c)	maximum thickness to chord ratio of blade
U	tangential velocity
u	blade speed
Xn	thrust
r	compressor blade mean radius
awqtn	water quantity at HP compressor entry
qwticc	water quantity at Combustion chamber entry
qwtibp	water quantity in bypass duct
H	enthalpy

GREEK SYMBOLS :

α	air angle
α_1	fluid inlet angle
α_2	fluid outlet angle
β	blade angle, air/gas angle
β_1	blade inlet angle
β_2	blade outlet angle
ε	deflection = $\alpha_1 - \alpha_2$
λ	non-dimensional clearance (δ / h)

ρ	density
ψ	blade loading ($2C_p \Delta T / u^2$)
γ	ratio of specific heat
η	efficiency
φ	flow coefficient (V_a/u)
δ	deviation = $\alpha_2 - \beta_2$
\mathcal{E}	total
Δ	variation

SUBSCRIPTS :

a	axial
act	actual
ad	adiabatic
AMB	ambient
b	blade
bp	bypass
c	compressor
chics	characteristics
ENG	engine
ht	heat transfer
hp	HP compressor
ip	IP compressor
i	inner, inlet
ISEN	isentropic
C.V.	fuel calorific value
o	overall, outer
p	propulsive, polytropic
Ref	reference
w	water

s	static
st	stage
ss	superheated steam
t	thermal
T	turbine
650	engine under study
610	reference engine

SUMMARY

The present work makes an attempt at predicting the performance of a gas turbine under the ingestion effects of rainwater. Such study was achieved with the aid of appropriate mathematical models which have been devised to enable the forecasting of a gas turbine engine performance during steady running behaviour. The models can also be used to forecast transient performance, although they were not used for this purpose in the present work.

This research was based on the simulation of two conditions. The first simulation was of an engine test carried out by Rolls-Royce. The engine was a twin spool turbofan with mixed exhaust called the Tay MK-650. The engine test involved water injection into the engine core only, ie the water was introduced after the fan and only into the air entering the Intermediate pressure (IP) Compressor.

The second simulation accounted for the ingestion of water through the whole frontal area of the engine.

The conditions of flight corresponded to an altitude of 6,000 m, Mach Number 0.8 and the water mass flow was 2.3% of the total inlet mass flow - this corresponding to the heaviest rainfall conditions that have been measured.

The lay out of this research would therefore be presented as follows:

Chapter (I) : General background and recent development of gas turbines, with a brief introduction to the problem and definition of the contribution of the present work are exposed in this chapter.

Chapter (II) : This chapter deals with a briefing about previously studied ways of aircraft simulation and defining the appropriate methods

undertaken to tackle this problem for engines under normal conditions (no water ingestion).

Chapter (III) : Scaling of the main components for the TAY MK-650 engine, from the TAY MK-610 and description of performance prediction programs set for the two-spool turbofan engine during steady running state are presented here.

Chapter (IV) : This deals with water thermodynamics introduction into the simulation program for the Tay MK-650 engine. A study is made of possible evaporation and drag locations in the engine. Mathematical models are introduced into the engine prediction program to describe these effects of evaporation and drag. A derivation of baseline was necessary in order to establish a link and a comparison between test observations obtained from Rolls-Royce and the simulated results produced in this research.

Chapter (V) : The complete engine prediction program developed in Chapter (IV) is applied to the conditions of the core ingestion tests carried out by Rolls-Royce. From the comparison between the predictions and the test results it was concluded that the major (90%) location for evaporation of the core flow water was at the plane after the High Pressure (HP) Compressor ie at entry to the combustors. The first 10% of evaporation was regarded as taking place at entry to or within the HP Compressor. This evaporation distribution coupled with drag due to water impingement on all three blade rows in the IP Compressor then gave the best match between predicted and observed shaft speed and turbine temperature changes. At the water injection rate of 2% by mass of the core air flow, it was predicted that there would be a 40% reduction in surge margin in the HP Compressor. This agreed reasonably with the engine test results where a 3.5% water injection rate caused the HP compressor to surge.

Chapter (VI) : The aim of this chapter was to give the best indication of the appropriate combination of models which would represent water ingestion through the whole frontal area of the engine. Different methods based on different models are investigated to allow for the comparison of results from the clean engine and its counter-part the water injected engine. General discussions of all results obtained from different simulations, and various assumptions at conditions of 6,000 m altitude, Mach Number 0.8 are presented here as well. For a more realistic high rainfall situation, 2.3% by mass of the engine inlet flow was considered as water. That quantity of water was divided after the fan as 90% into the bypass duct and 10% into the core. Evaporation then took place at corresponding planes and it was found that the steady running line for the HP Compressor had risen by 20% of the initial surge margin at lower fuel flows and as much as 75% at higher fuel flows. It could be said that the main reason for this behaviour was once more due to the evaporation at plane between HP Compressor and Combustion Chambers with other evaporation planes having little to no effects on the HP Compressor surge margin.

Chapter (VII) : This Chapter displays a brief conclusion drawn from all assumptions and investigations as well as suggestions for further study. Finally, it was realised that this issue needs dedicated and continuous efforts in order to accomplish positive and highly accurate results in the future.

CHAPTER I

GENERAL INTRODUCTION AND BACKGROUND

1.1 INTRODUCTION

Engineers have come a long way to build and improve Gas Turbines for Aeronautical purposes, and research on that field still goes on. Crucial measures need to be taken into consideration in order to ensure the safety of the customer. The aircraft undergoes a thorough study at design stages, the former examination applies by respecting aircraft safety regulations, providing maximum reliability and minimum risk.

One major safety hazard is the induction of foreign flying objects. Such objects could get sucked into the frontal area of the aircraft's engine and cause considerable damage. Since weather conditions are impossible to control, a method of designing an engine to accommodate for water ingestion and limit its consequences and effects on all major components becomes a high priority. This Thesis describes a study that has been made of the effects of water ingestion in an engine. The engine which has been selected for this investigation is a modern two-spool Turbofan having mixed exhaust. The engine is given the reference name "Tay MK-650" by the manufacturer Rolls-Royce. The Bypass ratio of the engine is 3 and the engine develops about 15,100 lbf thrust at sea level static conditions (on an ISA day).

The Rolls-Royce Tay MK-650 would be a derivative engine based on the Tay MK-610 engine and used for purposes of water ingestion testing. It was considered practical to derive a modified version to investigate and analyse the problem of rain water ingestion and propose an engine with an even better response and a wider safety margin in case of trouble occurrence.

Water ingestion into an Aircraft gas turbine arises due to two circumstantial reasons:

- a) Wheel-Generated spray clouds entering the engine inlet during take-off and landing from a rough runway with puddles of water; and
- b) Rain entering the engine inlet during various part of a flight in a rain storm.

A number of studies (Refs 1-6) have shown that adverse effects can arise in engine performance due to such ingestion of water at engine inlet, when the engine has been designed for operation with air flow.

In particular the engine may surge or may suffer blow-out, or unsteadiness in the main burner or after-burner. Simple corrective steps, such as resetting the throttle, have generally been ineffective in overcoming the problems of loss of power and non-steady behaviour of the engine. In the case of wheel-spray ingestion, it has again become clear that basic changes in engine installation may be necessary in relation to inlets and landing wheels. In the current investigation, there is no particular emphasis on the precise cause for the presence of water at the engine inlet, it was assumed to enter the compressor along with air in droplet form. Furthermore, it is felt that the response of the compressor in the engine to water ingestion plays a determining and crucial role in the response of the engine as a whole in view of two considerations :

- 1) The compressor receives the ingested water directly and, as a rotating machine, is most strongly affected by the ingested water, and also the "state of water" before the fluid enters the combustion chamber.
- 2) The compressor performance most directly affects the operating point of the engine under steady and transient state conditions. However, the compressor performance is affected by the presence of an inlet through the changes in the flow field introduced by it.

While noting such strong interaction between the inlet and the compressor flow fields, the most important aspect of the problem of water ingestion is still considered to be that pertaining to changes in the compressor performance itself.

In the present case of Turbo-fan engines, the air-water mixture upon entering the inlet becomes divided between the fan and the compressor, both in which the effects of water ingestion are important, although perhaps, more so in the latter. In establishing the response of a compressor to water ingestion, it seems therefore useful to divide the total problem into two parts:

- A) The compressor as a machine itself; and
- B) The compressor as part of the engine system.

In that fashion one can separate the problems associated with engine matching (steady or transient) from those dependent upon the design of the compressor itself. Once those problems have been investigated in detail, the engine as a whole may be studied from a system point of view.

After making the necessary alterations needed, the prediction of the characteristics of both the IP and HP compressor as well as the Inner and Outer fan would be in order. These characteristics would be used to define and predict the behaviour of the Tay MK-650 during steady state performance under the effects of accumulating water droplets over a period of time.

1.1.1. CONTRIBUTION MADE IN THE PRESENT INVESTIGATION

In the present work, which is based on mathematical simulations of the behaviour of gas turbines, existing simulation programs for gas turbines operating under normal conditions have been considered

(Chapter II). These simulation models have been extended in this work to include the effects of water ingestion (Chapters III and IV). These extended models have then been used to predict a typical turbofan engine's performance under two specific conditions -

- (i) with water injection into the engine core flow only (Chapter V)
- (ii) heavy rainstorm at 6,000 m, Mach 0.8, water as 2.3% by mass of inlet flow (Chapter VI).

Chapter (V) includes a comparison between predictions and engine observations taken by Rolls-Royce in equivalent tests.

1.2. HISTORICAL DEVELOPMENT OF GAS TURBINES

The use of a turbine driven by the rising flue gases above a fire dates back to Hero of Alexandria in 150 BC and the Chinese were operating windmills at about the same period. The year 1808 saw the implementation of the first explosion type of gas turbines, these were operated successfully but inefficiently by Karavodine and Holzwarth from 1906 onwards. The type died out after a Brown Boveri constant pressure cycle gas turbine was designed in 1939. The lack of understanding of aerodynamic properties prior to the advent of aircraft, resulted in failures at very early stages of gas turbine design, even though different configurations were tried, none of them was successful due to lack of knowledge, which resulted in highly inefficient components.

The concept of gas turbine engines for aircraft propulsion dates from 1930, when Whittle designed his first engine. A German Jet Engine propelled plane flew in August 1939. Whittle's first flying engine was given the identification number W1 and developed 850 lb thrust, in 1941. At this time several multinational companies took a serious interest in trying out various configurations and several jet engines were operational by the end of the second World War. The first civil plane propelled by gas turbines did not enter service until 1953.

The quest for higher speeds at high altitudes with less fuel consumption is a continuous process for manufacturers. The principal of the jet engine is very straight forward. The working medium, which in this case is air is passed through a compressor and is pressurised, fuel then is either sprayed or injected and burnt in the combustion chamber, which in turn flows out of the turbine which extracts not more than the necessary energy to work the compressor by the use of a shaft running through the centre of the engine, the remaining of that energy produced is used to move the aircraft forward, in other words to create thrust, by the use of an open nozzle through which expand the gases exiting the turbine.

Since the early days there have been two main types of jet engines. The first type used by Whittle and built by British Thomson-Houston used a double-sided centrifugal compressor, a long combustion chamber which was curled round the outside of the turbine and an exhaust nozzle just behind the turbine. This model provides small to moderate air flows (up to about 50 kg/s) at a pressure ratio of up to about 5. The second engine type uses the axial compressor and is built up with a number of stages. It can handle much larger flows than the former, as its inlet occupies most of its frontal area. In practice, it is more convenient to use an axial compressor in order to achieve higher pressure ratios, however small engines still account for centrifugal compressors.

There are two types of gas turbine cycles:

Aircraft gas turbine cycles and Shaft power cycles, or they could be distinguished into Open cycles (Figs 1.1, 1.2) and Closed cycles (Fig 1.3).

The main differences between these two cycles are stated as follows: Initially the expected life of an industrial engine or shaft power cycles without a major overhaul is much greater than that for an Aircraft engine. Secondly the size and weight of an industrial engine is not as important as that for an Aircraft engine, as there are limitations to be

considered. Finally, the kinetic energy of the gases leaving the turbine are used to provide thrust whereas it is wasted in some form or other in all the remaining gas turbines. Aircraft gas turbines are now made by about fifty companies, mostly in a few, well known configurations. They may be considered as variations of the single or multi-spool turbojet, in which the combustion system is squeezed between the compressor and turbine to minimise weight and frontal area. In turboshaft form, its shaft may drive the rotors of a helicopter. If the reduction gear is built into the engine to drive propellers, it becomes a turboprop or prop-jet engine. Enlargement of the LP compressor makes a bypass-jet engine if the excess LP air is ducted to mix with the exhaust, or a fan-jet or turbo-fan if it emerges separately, this has the advantage of increasing the propulsive efficiency, see section 1.4. This thesis concentrates on a two-spool Turbo-fan Engine with Mixed exhaust and the reasons for this are given in section 1.3.

1.3. MODERN DEVELOPMENTS

A more efficient engine will require less weight of fuel, resulting in a lower airframe structural weight, less thrust to propel the aircraft, hence the engine can be smaller with a lower weight. The reduction in total aircraft weight reduces the first cost of the aircraft. Thus a very powerful escalating process stems from improving the engine fuel efficiency. The next section will outline some of the very basic design parameters influencing the fuel efficiency of the conventional gas turbine aero engine.

The aero gas turbine engine can be considered, for simplicity, to consist of three components. The power producing section (gas generator), the propulsive jet system and the transmission system which conveys the power from the gas generator to the propulsive jet.

The overall efficiency can be written simply as:

$$\eta_o = \eta_t * \eta_p * \eta_{tr}$$

where ;

η_t = thermal efficiency

η_{tr} = transmission efficiency

η_p = propulsive efficiency

Thermal efficiency is controlled basically by the design parameters of the Joule or Brayton cycle, Figs 1.3(a),(b), with the benefit of high pressure ratio and high turbine entry temperature, Fig 1.4, see section 1.4. The Thermal efficiency is maximized by means of increasing the pressure ratio (equation (4a), Appendix A). The magnitude of the final jet velocity selected for the engine not only determines the level of propulsive efficiency, but also determines the mechanical configuration of the engine. This configuration can vary from a simple high velocity pure jet engine, through turbofan configurations of modest jet velocity, to the propeller engine of very low jet velocity. By decreasing the jet velocity the propulsive efficiency could be maximized (equation (3), Appendix A). Transmission efficiency in the case of the bypass engine is a function of the fan turbine efficiency and the fan efficiency, and also depends on the proportion of the gas generator output transferred to the bypass stream (Ref 10).

In order to achieve a high overall efficiency it is necessary to maximize both the Thermal Efficiency and the Propulsive Efficiency.

1.4. TURBOJET ENGINE DEVELOPMENT

As it was already shown, thermal efficiency of a gas turbine improves with increased engine pressure ratio. Hence, it becomes a necessity to develop higher pressure ratio engines. Attempts were made to design one-spool engines with higher pressure ratio but that led to mechanical and aerodynamic problems in the compression process. At

low speeds stalling was likely to occur at the front end stages of the compressor, but at high speeds, it occurred at the rear stages which represented a major problem at the time. One way to solve this problem was to design a two-spool engine which uses "aerodynamic coupling" between the shafts and that allowed for pressure ratios of up to twenty or even thirty to be attained, see section 1.3. Propulsive efficiencies can be increased by means of a by-pass engine as well, this principle is based on a separate air intake area which would allow air to be split between the engine core and the outer fan section 1.2, these design requirements were an incentive to model a three-spool engine more complex than the former but more compact, see Figs 1.5, 1.6.

1.5. TRANSIENT BEHAVIOUR OF AIRCRAFT GAS TURBINE

The present research has concentrated on the effect of water ingestion on steady running behaviour of the engine. The transient behaviour of aero-gas turbines is also of considerable importance, and a brief outline of how this transient performance may be analysed and predicted is now given. In later research, the effect of water ingestion on transient performance may be investigated.

Since aircraft engines have to accelerate from idling speed to maximum speed and from maximum speed to an idling one in as short periods of time as possible. It would be necessary to predict engine response and performance during these periods of time which are called transients, in order to ensure that the engine is working inside the safety margin. Two dangerous situations are to be avoided during a transient response. First surge in a compressor or excessive turbine entry temperatures. When a compressor is forced to operate at too high pressure ratio for the corresponding value of non-dimensional rotational speed, the compressor would surge. By matching all components of the

engine so that the steady-running line falls well below the surge line, surge situations can be alleviated. However, for an engine to be efficient with good fuel consumption, it is essential for it to operate at high pressure ratio. For optimum engine performance, transient behaviour must be fully and well understood before being used. During the steady-running state, the fuel flow is fixed at known flight conditions, that would fix the rotational speed and other parameters of the engine, due to the power balance between components. During acceleration or deceleration this power balance loses its effect, because in the acceleration mode the turbine power exceeds the compressor one, causing the turbine entry temperature to rise, for which the fuel flow rises above the corresponding equilibrium value. For a deceleration mode the opposite happens, turbine producing less power than the compressor, forcing the fuel flow to drop below the equilibrium value. Hence for a given flight condition, the acceleration and deceleration performances of the engine are a function of a non-dimensional rotational speed and non-dimensional fuel flow which represent independent variables.

CHAPTER II

PERFORMANCE PREDICTION PROGRAM FOR TWO-SPOOL TURBOFAN ENGINE

2.1. MODELLING OF GAS TURBINES

As gas turbines were first designed, it became necessary to predict the performance of the various components. When test data for the performance of the individual components was obtained, the predicted performance was revised to align it with the test results. For component performance prediction, experimental cascade information and aerofoil theory were used, once this was achieved the prediction of the steady state performance from the predicted component characteristics was obtained, then the evaluation of the steady running performance of the whole engine was accomplished. However, that was not enough, given the need to predict the performance of aircraft gas turbines to accelerate and decelerate in as short time as possible, this is called the Transient behaviour, research on this field has been pursued since very early history of aircraft development.

In order to develop the prediction of both steady running and transient performances, theoretical models were used by means of the characteristics of the components. Component characteristics of an engine are available at early design stages, which makes simulation of the engine over its entire range possible to realise. It became virtually manageable to meet the customers requirements with regard to the size, purpose and the performance of the aircraft by means of this reliable and accurate model. Two types of prediction procedures based on component models have evolved during these years of research :

(1) The Inter-Component Volumes method (ICV); which assumes mismatches of flow occurring at various stations in the engine. These

mismatches produce pressure changes.

(2) The Continuity of Mass Flow method (CMF); which assumes a constant mass flow at any given instant throughout the engine.

2.1.1. THE ICV METHOD

In this method, allowances are made for the accumulation of mass within the components and ducts of the engine. Volumes are introduced between the various components and all flow imbalances are assumed to occur in these volumes. Inter-component volumes include an appropriate proportion of the preceding component and an appropriate proportion of the next component. The corresponding size is the volume of the space between any two components plus the half of the volume of each adjacent component.

The procedure requires an initial estimate of the pressure distribution along the engine at the conditions corresponding to the state of performance of the engine. The initially provided pressure distribution will give mass flows into and out of the inter-components volumes. These mass flow imbalances are used to evaluate the accumulation or diminishment of the air/gas, and the rise or fall of the pressure in that volume during the subsequent time interval. This new data represents the starting point of the following calculation at the next time interval. Once all the components have been analysed in the previous manner, the power delivered or absorbed by the components is evaluated, which then gives the work imbalance on the shafts. The new shaft speeds are then calculated to be used for the next process, at the next time interval throughout all the components of the engine. The calculation is a straight-through procedure with no iterations, and it is repeated throughout a steady running or a transient until neither mismatches of flow nor work imbalance along the shafts occurs and thus the engine has stabilised and performance completed.

The computing time for this method is significantly longer than for the CMF one described next. Also, poor initial guesses would lead to erroneous results for the first number of time intervals. This can be overcome by having a "stabilisation" period prior to the transient or the steady state performance. Basically, the flight conditions and shaft speeds are known, a value for the initial pressure is guessed within these volumes. These starting parameters allow compressor inlet temperature and pressure to be determined. In order to find parameters such as mass flow rate and temperature at exit from the compressor, gas dynamics calculations are used. The same procedure is used for other components. This method has been used for simulations of turbo-fan engines, (Ref 11). The aim in this research is to consider steady running performance only, and for that a transient (ICV) program set for steady running conditions is used, with a set value for the fuel flow and the same starting parameters.

After the engine had stabilised at a specific fuel flow, readings for shaft speeds and exit pressures and temperatures are found.

2.1.2. THE CMF METHOD

This method is based on the fact that the flight conditions and the rotational speed of the compressors are known. The inlet conditions of mass flow, pressure and temperature to the compressor or fan, can be calculated from the known values of flight Mach number, and rotational speed. By guessing a mass flow rate value going into the engine or the pressure ratio across the first compressor and interpolating using the inlet conditions by means of gas dynamics equations, the outlet thermodynamic values from any component can be calculated. These represent the starting conditions for the next component and so on. An energy balance is used to obtain the outlet temperature for the combustion chamber using the fuel flow rate already known. A pressure loss factor is applied to the inlet pressure in order to give the outlet pressure. The former

calculations determine the turbine entry conditions, in addition to that, the shaft speeds and characteristics of the turbine are known. From these the outlet conditions can be found. As a test at the final nozzle, the area required for air flow is compared to the area available, if these two areas do not match and they hardly do at the first iteration, a revision of the initial conditions is called for. A series of iterations would then follow until the area required and the area available coincide. The mass flow out of the engine would then be known and the assumption that this mass flow matches the mass flow into the engine at any given instant has to hold, with allowances made for bleeds and fuel flow. If the mass flows do not satisfy the continuity, which is often the case, the initial guessed value of mass flow or pressure ratio would be revised until convergence is achieved. Although no accuracy is needed when the first guesses are made, in general, tests will cause iterations in which the initial guesses of pressure ratios or mass flows are revised until continuity of mass flow is achieved. Energy balances are then carried out on the shafts and instantaneous acceleration rates determined. This acceleration would apply throughout the next time interval according to Newton's law, that would give new shaft speeds which would form the initial conditions for the next time interval.

It is much easier to apply this method to less complex engines. One iterative loop would be needed for a single-spool engine, whereas for a two-spool turbo-fan with mixed exhausts five iterative loops may be needed. Difficulties have been experienced in achieving convergence for the complex configurations, Figs 2.1, 2.2. But at the same time computing time is significantly less than that for the ICV method, Figs 2.3, 2.4. However, there are no allowances for the accumulation of air, or gas mass within the components and ducts of the engine during transient.

Even though the ICV method was used for the purpose of this research, the CMF would have been equally satisfactory. However, the ICV method gave more accurate overall results since it allowed for the

accumulation of air, or gas.

For steady running prediction, the CMF method is exactly as valid as the ICV one, however, when predicting a transient performance, the ICV method becomes more practical due to reasons explained above. Further description of the CMF method is available in Ref 10.

2.1.3. COMPARISON OF CMF AND ICV METHODS

The main difference between the two methods is due to mass accumulation of air or gas in the engine. This effect is large during the first instants of a transient response but tends to reduce with time. For a single-spool engine, both methods gave similar results (Ref 10), except for the first fractions of a second which was explained earlier.

For a two-spool turbofan engine with mixed exhausts (Ref 11), comparisons have been carried out to find out that for all components, the steady running states for both methods coincided. However, the thrust and the speed responses during accelerations and decelerations predicted by the CMF method were approximately 4% faster than for the ICV method. For both the Inner and Outer fan, trajectories were identical. For the IP compressor the results predicted were very similar with the exception of the very start of the deceleration. This was mostly due to the CMF prediction of an instantaneous change in the pressure ratio while at the same non-dimensional speed line at the start of a deceleration.

The ICV prediction is a more stable one. For the HP compressor, the trajectory predicted by the CMF method was further down from the working line than that predicted by the ICV method.

To conclude, it could be said that both methods for transient predictions are in general agreement. However, the ICV method was chosen in this research because it accommodates for air/gas mass accumulation, the CMF does not. The main deficiency of the chosen method was that it required ten times more computing time than the CMF

method. See Fig 2.5 for a summary on comparing predictions from the two methods.

So far thermal effects in this research were not included in order to simplify the work. The next paragraph gives an insight onto the effects of heat transfer and non adiabatic modelling.

2.2. NON ADIABATIC MODELLING AND HEAT TRANSFER EFFECTS

The gas turbine simulation has to match as closely as possible the transient performance of a real engine. The main discrepancies that occurred between actual and program run engines during previous results were due to the neglect of heat transfer effects. To get an accurate prediction, allowances for thermal effects must be incorporated in the computer models (Ref 13).

2.2.1. HEAT TRANSFER EFFECTS

During transient, the effects which take place are:

- (i) Heat absorption in different components (fans, compressors and turbines)
- (ii) Heat absorption in the combustion chamber
- (iii) Changes due to effects of heat transfer in compressor characteristics
- (iv) Changes in compressors and turbines efficiencies due to tip clearance
- (v) Changes in seal clearances
- (vi) Combustion process response delay

Ommiting these effects would lessen the accuracy of the predictions. Whereas including them would alter the performance of the engine by changing components responses (Ref 14). Mainly, changes would occur in the transient trajectories of compressors, hence, in the performance

predicted by the engine. What follows is a general description of the former effects in a more detailed way. However, not as detailed as some researchers work on that specific field (Ref 16, Ref 17 and Ref 18).

2.2.1.1. EFFECTS ON FANS, TURBINES AND COMPRESSORS

The small stage or polytropic efficiency η_{pT} relate to temperature and pressure calculations in fans and or compressors for adiabatic flow. A straight forward method to explain the adiabatic expansion is listed below:

$$C_p dT = \eta_{pT} v dP \quad (1)$$

The relation between the index of expansion, n and the isentropic index γ would then be :

$$\frac{n-1}{n} = \eta_{pT} \frac{\gamma-1}{\gamma} \quad (2)$$

In the case of a non-adiabatic expansion where heat transfer takes place between the air and the components materials during transient, equation (1) then becomes:

$$C_p dT = (1 - f) \eta_{pT} v dP \quad (3)$$

$$\frac{m-1}{m} = (1 - f) \eta_{pT} \frac{\gamma-1}{\gamma} \quad (4)$$

Where f is the ratio of the heat transfer to the air in an element to the work transfer from the air in that element. Providing that the ratio f is constant along the turbine, equation (4) represents the non-adiabatic polytropic expansion with the symbol m as its index.

The non adiabatic flow in the compressor could be analysed in a similar manner to yield the equation of polytropic expansion in a compressor

$$\frac{m-1}{m} = \frac{1-f}{\eta_{PC}} \frac{\gamma-1}{\gamma} \quad (5)$$

The ratio, f , can be of considerable importance as it could rise to a value equal to 0.2 in a compressor and 0.35 in a turbine for two-spool engines, whereas for single spool engines it was of the order of 0.01 for a compressor and 0.03 for a turbine for sea level transients.

2.2.1.2. EFFECTS ON COMBUSTION CHAMBER

As the air/gas mixture passes through the chamber during a transient there would be a heat exchange between it and the materials that form the combustion chamber flame tube and casing. This can have a significant effect on the fuel flow changes during the first instants of a transient. A descriptive study of this problem is given in (Ref 19).

2.2.1.3. CHANGES IN COMPRESSOR CHARACTERISTICS

Several effects take place when accelerating a cold engine, causing changes in the compressor's overall characteristics. As heat effects take place, the density of the air passing through the components of the engine would differ at different subsequent stages, hence the ratio of axial velocity to blade speed would change in the last stages. The matching between stages would then vary which would affect the overall pressure rise at that corresponding non-dimensional inlet mass flow. That would be the first effect, (Refs 17 and 20). Secondly, an earlier separation of the air may occur (Refs 21 and 22), due to a more rapid thickening of the boundary layer which would be caused by the heat transfer from the suction surface of a blade to the air during a deceleration. A third effect is that the heat transfer at the casings and hubs will alter the end wall boundary layers development which would in return change the pressure rise capability of the stages. The previous effects on the overall

characteristics of a compressor were studied. When accelerating a "cold" engine it is observed that the constant speed characteristic is moved to a higher value as well as the surge pressure ratio at a specific mass flow. These effects were studied and quantified (Ref 23).

For change in effective speed:

$$\frac{\Delta N}{N} = C_1 \frac{T_b}{T_{air}} - \frac{T_{air}}{T_{air}} + C_2 \frac{\dot{Q}}{\dot{m} T_m C_p} \quad (6)$$

and for the revised surge pressure ratio:

$$\frac{R_{ht} - 1}{R_{ad} - 1} = 1 + C_3 f - C_4 \frac{\Delta(\delta)}{g} \quad (7)$$

For a two-spool turbo-fan HP Compressor C_1 , C_2 , C_3 and C_4 have the corresponding values of 0.1, -0.1, 0.36 and 1.1 respectively, Ref 24.

2.2.1.4. TIP CLEARANCE CHANGES AND EFFECTS ON EFFICIENCY

This is a brief summary on how tip clearance effect efficiency, and how the model for its study was developed. A more detailed study is given in Ref 25. Tip clearance changes depend on radial and axial growth (or shrinkage) during transient. Tip clearances movements depend on the growth of discs, blades, and casings. A disc is represented by a massive hub, a thin diaphragm and an outer rim to which the blade is attached. The hub and diaphragm temperatures are controlled by the air from an appropriate stage in a compressor. The influence of both the internal air and the external gas flow control the rim temperature. Appropriate heat transfer calculations are used for all surfaces. Disc tip expansions were then calculated with the assumption that the interfaces do not move apart. After using a finite element method as an alternative to calculate the whole disc, both methods were then compared.

The result was that the simplified method gave results which were less

than the predictions of the finite element analysis by a factor of 1.3, and had to be scaled up. Centrifugal growth and the expansions of the blades which were easily calculated, had also been accounted for. Finally, the expansions for the casing were found as its temperature related to the temperature of the internal gas flow and external air flows in the bypass duct. The work of Lakshminarayana (Ref 26) led to the following relationship which is used to determine the efficiency losses due to tip clearances:

$$\Delta\eta = \frac{0.7 \lambda \psi}{\cos \beta_m} \left[1 + 10 \left(\frac{\phi \lambda A}{\psi \cos \beta_m} \right) \right] \quad (8)$$

A tightening in the tip clearance of 0.1 mm gave an estimate of 0.6 per cent improvement in compressor efficiency.

2.2.1.5. SEAL CLEARANCE CHANGES

A two-spool turbo-fan was used to illustrate the methods and model used for tip clearance calculations, the same model could be adapted to find seal clearance movements. The most important ones are an outer seal at the HP Compressor final stage and a seal on the HP Turbine disc. Both these seals have been included as a model in the final program used to predict the transient performance of the engine.

2.2.1.6. COMBUSTION DELAY

One main suggestion was that there may be a delay between an alteration in fuel flow and the subsequent change in the effective heat release rate in the combustion chamber. However, Saravanamuttoo found that only in engines that used vapourising burners, that this effect takes place. The two-spool turbo-fan used for the purpose of this research uses pressure jet burners and is not affected, (Ref 27) saravanamuttoo.

CHAPTER III

SCALING OF COMPONENTS FOR THE TAY MK-650 ENGINE USING TAY MK-610 COMPONENTS

3.1. INTRODUCTION

The main performance prediction program used in this investigation (Paragraph 2 and Appendix E) can generally, be applied to any two-spool turbofan engine with mixed exhaust, provided that the appropriate component characteristics are used. The Rolls-Royce "Tay" series of engines are of this configuration.

For instance, the detailed characteristics of the components for a compressor;

$$\frac{\dot{m} \sqrt{T_1}}{P_1}, \frac{P_2}{P_1} \text{ and } \eta \text{ as functions of } \frac{N}{\sqrt{T_1}} \text{ and } \beta$$

were available to the author only for the MK-610 version of the engine. This MK-610 version is called in this Thesis the "Reference Engine".

However, the water ingestion tests carried out by Rolls-Royce in Reference 7 were on a MK-650 version of the Tay Engine. This engine was, geometrically, significantly different from the MK-610 Tay Engine. For example the Front Fan is of a larger diameter, therefore some form of scaling of the performance data of the components of the MK-610 was necessary in order to achieve a performance prediction program which aligned with the performance of the MK-650. To enable these scaling factors to be found, Rolls-Royce provided a set of performance parameters - pressures, temperatures, speeds and so on - which aligned with the actual tested performance of the MK-650 engines (Ref 8). This Chapter explains how these scaling factors were found, it will be seen that

these factors in many cases are not constant over the speed range of the engine. It would also be appropriate to define the features which had been uprated from the Tay MK-620 to produce the Tay MK-650 Engine. The prediction program was based on the Tay MK-650 during this research. A description of every component of this engine would be suitable in order to get familiar with its functions.

3.2. SCALING FACTORS

Dimensional analysis has enabled great simplification in the representation of the performance of turbomachinery such as a compressor or a turbine, (Ref 9). For example, for a compressor, the pressure ratio as given by dimensional analysis ;

$$\frac{P_2}{P_1} = \text{fn}\left(\frac{\dot{m}\sqrt{RT_1}}{P_1 D^2}, \frac{ND}{\sqrt{RT_1}}\right)$$

similarly the isentropic efficiency is given by ;

$$\eta_{1-2} = \text{fn}\left(\frac{\dot{m}\sqrt{RT_1}}{P_1 D^2}, \frac{ND}{\sqrt{RT_1}}\right)$$

in order to facilitate the handling of the numerical data to be read as input to the program, an additional dimensionless parameter, β , is introduced, so that in practice;

$$\begin{aligned} \frac{P_2}{P_1} &= \text{fn}\left(\beta, \frac{ND}{\sqrt{RT_1}}\right) \\ \frac{\dot{m}\sqrt{RT_1}}{P_1 D^2} &= \text{fn}\left(\beta, \frac{ND}{\sqrt{RT_1}}\right) \\ \eta_{1-2} &= \text{fn}\left(\beta, \frac{ND}{\sqrt{RT_1}}\right) \end{aligned}$$

It is clear that, if the diameter D for a Fan is increased then for a particular shaft speed N , while the so called "non-dimensional speed" $(N / \sqrt{T_1})$ will still have the same apparent value, the true non-dimensional speed $(ND / \sqrt{RT_1})$ will be higher. The tabulated numerical values which described the performance of the original component on the MK-610 engine were based on :

$$\frac{P_2}{P_1} = \text{fn}\left(\beta, \frac{ND}{\sqrt{RT_1}}\right),$$

$$\frac{\dot{m} \sqrt{RT_1}}{P_1 D^2} = \text{fn}\left(\beta, \frac{N}{\sqrt{T_1}}\right) \text{ and}$$

$$\eta_{1-2} = \text{fn}\left(\beta, \frac{N}{\sqrt{T_1}}\right)$$

It will therefore be possible, ignoring the effects of changes in gamma γ to insert scaling factors into both parameters of

$$\left(N / \sqrt{T_1}\right), \left(\dot{m} \sqrt{T_1} / P_1\right)$$

so that the original set of values for engine performance may be used to determine the performance of the larger-size Fan. There is another factor which is of considerable importance and which should be considered-the performance of the component when installed in the engine may differ significantly from that when measured on its own on a test rig or from the performance predicted from the design if no component test were yet carried out.

Once the full engine test data become available, the necessary scaling factors can be found to quantify the combined effects of the two types of changes which are linear and installation changes described above.

3.3. FAN ARRANGEMENTS

The concept of having an engine with a different configuration which requires higher thrust, would allow for the flow area to be increased accordingly. Since characteristics for blade hub and blade tip differ, separate characteristics had to be considered as the outer fan compresses the by-pass flow and the inner fan, the main core flow. Another reason for having separate characteristics is that the main intake, which would be a combined flow of air and water would be split into two streams, one going into the by-pass which even though is droplet laden, is not going to have a major effect on the engine's performance. However the other stream which would consist of air and water as well would be of utmost importance. The reason being that, the mixed intake of air and water would flow past the engine's components causing therefore an important change in the engine performance which normally would have air as its main working medium.

In order to achieve the condition of increased Fan size, the true non-dimensional speed group, which would be the original Tay MK-610 non-dimensional speed group has to be used. As assumptions were made by making no corrections on the non-dimensional speeds for both the inner and outer fan, both reference and new engines would have similar non-dimensional speeds.

For equivalent performance points:

$$\frac{ND}{\sqrt{RT_{in}}}_{650} = \frac{ND}{\sqrt{RT_{in}}}_{610}$$

Or

$$\frac{N}{\sqrt{T_{in}}}_{650} = \frac{N}{\sqrt{T_{in}}}_{610} * \frac{D_{610}}{D_{650}}$$

But assumptions were taken as to no corrections would be made on non-dimensional speed groups, that would mean:

$$\frac{D_{610}}{D_{650}} = 1$$

So the multiplying factor of 1.000 means that both sets of non-dimensional speeds for the reference engine Tay MK-610 and the Tay MK-650 are equal. $C_{9} = 1.000$ and $C_{42} = 1.000$ for the inner and the outer fans respectively. Based on an uprate features of the Tay MK-650 from the Tay MK-620, the Fan would consist of blades which would be 0.400" longer and will be mounted on the standard disc. To accommodate the longer blades a new fan containment casing will be required.

3.3.1. INNER FAN

Similar conditions at take-off apply for non-dimensional speeds. For example a value of 350.843 for the engine (Tay MK-650), taken from the list of data of parameters consisting of pressure ratios, mass flows, isentropic efficiencies and non-dimensional speeds provided by Rolls-Royce, would remain exactly the same as a characteristic value for the reference engine, Tay MK-610.

$$\frac{N}{\sqrt{T_{IN}}_{610}} = \frac{N}{\sqrt{T_{IN}}_{650}} * \frac{1}{C_9}$$

The value of pressure ratio corresponding to a non-dimensional speed value of (350.843) is obtained from the list mentioned above for the MK-650 engine, and is found to be:

$$\frac{P_{24}}{P_1}_{650} = 1.3487$$

whereas the reference engine MK-610 has a value of pressure ratio which could have been extrapolated from either the block of characteristics data or the characteristics graph ;

$$\frac{P_{24}}{P_1}_{610} = 1.0896$$

A combination of both these values would provide the pressure ratio scaling factor C_{21} . This combination is given by:

$$C_{21} = \frac{\frac{P_{24}}{P_1} - 1_{650}}{\frac{P_{24}}{P_1} - 1_{610}}$$

After allowing for the Tay MK-650 speed range to be covered, it was found that these scaling factors were not constant, hence an average including the whole range of the engine was calculated to suit the prediction of the performance needed. The average taken was found to be $C_{21} = 1.0344$, this coefficient is applied to the pressure rise component (pressure ratio - 1) for the reference engine Tay MK-610.

The corresponding design point would consist of values of pressure ratio, non - dimensional speed and mass flow, in order to locate that specific design point, the following method is considered. A value of a pressure ratio and corresponding mass flow are already supplied for the MK-650 engine data, that specific point would be located on a reference engine characteristics graph representing mass flows against pressure ratios. The design point value would correspond to a specific non-dimensional speed line found by means of an interpolation between the two values of non-dimensional speed lines nearest to the design point value. The scaled pressure ratio would be a value different from the original one found by using C_{21} , that new value is then projected onto the

previously mentioned speed line to give a point which then would be projected onto the mass flow axis and finally locate the characteristics new mass flow reading. For example the non-dimensional mass flow of the engine is given to equal 84.3206, the equivalent non-dimensional mass flow of the characteristics is equal to 79.0036 and was obtained by following the procedure described above using the graph of corresponding characteristics.

The scaling factor for mass flow requirements would be the ratio of the mass flow for the MK-650 engine data provided by Rolls-Royce for that corresponding case and the mass flow value found by means of interpolation using the reference MK-610 engine characteristics graph. The range of fuel flows was considerably large, this helped provide a reasonable number of cases in order to avoid erroneous results. After finding a separate scaling factor for each case on its own, an average was taken and applied in the performance prediction program for the Tay MK-650 Inner Fan. An average value of $C_{18} = 1.0166$ was found, that value would be generally applied in the equation below :

$$\frac{\dot{m} \sqrt{T_{IN}}}{P_{IN}}_{650} = \frac{\dot{m} \sqrt{T_{IN}}}{P_{IN}}_{610} * C_{18}$$

Finally, a scaling factor for efficiency had to be calculated. The efficiency of the engine MK-650 was provided by Rolls-Royce engine data for each single case of the fifteen different cases observed. Rolls-Royce data allowed the new scaled value for efficiency to be found. Given the pressure ratio, the original isentropic efficiency and the non-dimensional speed for a specific case, it was possible to obtain the positioning of non-dimensional speed lines from the reference engine MK-610 characteristics block. By means of interpolation between speed lines, a corresponding value of efficiency was found, that value would represent the new scaled isentropic efficiency. In order to cover a wider

range and to reduce any chance of serious mistakes, the whole range of speeds from Rolls-Royce data MK-650 were considered. The first case provided the optimum value for the difference between η_{650} and η_{610} , whereas the final case gave the minimum difference. Using both of the previous values as well as the corresponding optimum and minimum non-dimensional speeds for the engine Tay MK-650, The following equation was applied To give the efficiency scaling factor D_g . This was given as follows:

$$D_g = 0.1405 - 0.1064 * \left\{ \frac{\text{ZNDLPC}_{650} - \text{ZNDLPC}_{650_{MIN}}}{\text{ZNDLPC}_{650_{MAX}} - \text{ZNDLPC}_{650_{MIN}}} \right\}$$

The values of 0.1405 and 0.1064 were given by

$$0.1405 = (\eta_{650} - \eta_{610})_{MIN}$$

And :

$$0.1064 = (\eta_{650} - \eta_{610})_{MIN} - (\eta_{650} - \eta_{610})_{MAX}$$

The previous equation shows how the scaling factor for isentropic efficiency was dependent on maximum, minimum and varying case values of non-dimensional speeds from Rolls-Royce case study, as well as maximum and minimum increments between the MK-650 engine efficiency and the reference MK-610 characteristics efficiency.

3.3.2. OUTER FAN ARRANGEMENTS

Once more no correction on the non-dimensional speed was assumed, this is to say that:

$$\frac{N}{\sqrt{T_{IN}}}_{650} = \frac{N}{\sqrt{T_{IN}}}_{610}$$

For example, if at take-off conditions at the design point, the non-

dimensional speed for the MK-650 engine was equal to 350.843, then the characteristics non-dimensional speed for the reference MK-610 engine would be equivalent to 350.843. As far as the pressure ratio is concerned, the appropriate method is described next. A non-dimensional engine speed of 364.802 was considered, this value was pinpointed on a characteristics graph for the reference engine. This would allow for the determination of its location between any two characteristics non-dimensional speeds which are closest to it. In this case, the value 350.843 fell between a minimum of 326.15 and a maximum of 372.74. By means of interpolation, it was found that the engine speed line lay by 0.8296 off the minimum non-dimensional speed line. This small increment was found by applying the equation of interpolation described below:

$$\text{speed increment} = \frac{\frac{N}{\sqrt{T_{650}}} - \frac{N}{\sqrt{T_{\text{MIN}}_{610}}}}{\frac{N}{\sqrt{T_{\text{MAX}}_{610}}} - \frac{N}{\sqrt{T_{\text{MIN}}_{610}}}}$$

A numerical example explaining the previous increment would be:

$$(364.802 - 326.15) / (372.74 - 326.15) = 0.8296$$

Using the corresponding MK-610 characteristics graph for the Outer Fan component, the non-dimensional speed line for the Tay MK-650 engine was drawn. That line, drawn using approximate methods, would at some stage cross a working line provided by Rolls-Royce for the series of Tay engines and always represented on the characteristics graph. The intersection of the MK-650 engine non-dimensional speed line and the reference MK-610 engine working line provides a specific point, this point would then be projected onto the axis of pressure ratio values and would thus give an estimated pressure ratio value for the Tay MK-650 using the reference characteristics.

For example an engine with a non-dimensional speed of :

$$\frac{N}{\sqrt{T_{650}}} = 364.8$$

the corresponding pressure ratio from Rolls-Royce data for the Tay MK-650 engine would be :

$$\frac{P_{13}}{P_1} = 1.429$$

However, the corresponding pressure ratio found using the reference engine characteristics graph would be;

$$\frac{P_{13}}{P_1} = 1.40$$

so the equivalent scaling factor would be applied to the pressure rise component and would equal to:

$$C_{43} = \frac{\frac{P_{13}}{P_1} - 1_{650}}{\frac{P_{13}}{P_1} - 1_{610}} = 1.0725$$

There are different characteristics blocks of values (paragraph 3.2), defined by $\beta_1, \beta_2, \beta_3, \dots$, etc. These values represent the distance between successive non-dimensional speed lines. Using interpolation, a specific Beta value corresponding to a specific pressure ratio would be calculated. By finding a Beta value on the block of reference characteristics values, it would then be easy to define the corresponding row of non-dimensional speed lines and Hence find the block of mass flows (capacity). In order to calculate the scaling factor for the capacity, this method is followed. The pressure ratio at non-dimensional engine

speed was obtained using the working line on the characteristics graph, and was equal to 1.40. For every Beta value at the engine non-dimensional speed there is a corresponding pressure ratio value:

$$\frac{N}{\sqrt{T}}_{650}$$

$\beta = 1$	$\beta = 2$	$\beta = 4$	$\beta = 5$
$\frac{P_{13}}{P_1} = 1.4213$	$\frac{P_{13}}{P_1} = 1.4176$	$\frac{P_{13}}{P_1} = 1.4087$	$\frac{P_{13}}{P_1} = 1.3924$

In this case the value for Beta is between B=4 and B=5 because it was mentioned above that the value of pressure ratio found from the reference characteristics graph for the original Tay MK-650 was equal to 1.40, by using interpolation a more accurate value for Beta could then be found:

$$\beta = \beta_{\min} + \frac{\frac{P_{13}}{P_1}_{650} - \frac{P_{13}}{P_1}_{\beta_{\min}}}{\frac{P_{13}}{P_1}_{\beta_{\max}} - \frac{P_{13}}{P_1}_{\beta_{\min}}}}$$

The equation above would be represented numerically, in this case;

$$\beta = 4.0 + \frac{1.40 - 1.4087}{1.3924 - 1.4087} = 4.534$$

With every Beta value lies a block of mass flows, pressure ratios and isentropic efficiencies, all corresponding to a specific non-dimensional speed line. Using the Beta values associated with the minimum and maximum non-dimensional speed lines which represented the range of speed lines for the Tay MK-650, the values for mass flows would then be easy to locate. For example the minimum speed line would associate with a Beta value, that Beta value would define the blocks of mass flows,

pressure ratios and efficiencies. After interpolation, the capacity or mass flow scaling factor is calculated by using the following equation :

$$\frac{\dot{m} \sqrt{T_{IN}}}{P_{IN}}_{650} = \frac{\dot{m} \sqrt{T_{IN}}}{P_{IN}}_{610} * C_{41}$$

By using a plot of C_{41} against $N / \sqrt{T_{IN}}_{650}$, it was found that the scaling factors were not constant over the range of engine non-dimensional speed lines.

Alternatively, a minimum and maximum values were taken for the scaling factor, these would represent the values to be used in the equation below in order to give an accurate and definite result to be incorporated in the prediction program for the Tay MK-650 engine.

$$C_{41} = 0.900 - 0.200 * \left\{ \frac{ZNDLPC_{650} - ZNDLPC_{650_{MIN}}}{ZNDLPC_{650_{MAX}} - ZNDLPC_{650_{MIN}}} \right\}$$

$$0.900 = C_{41_{MIN}}$$

$$0.200 = C_{41_{MAX}} - C_{41_{MIN}}$$

Using the efficiency block, the same procedure is applied in order to get the efficiency scaling factor, the former would be calculated as follows:

$$D_{42} = \eta_{650} - \eta_{610}$$

for efficiency calculations of scaling factors, $C_{42} = 1.00$ and for pressure ratio calculations an additional scaling factor is redundant and is defined by $D_{43} = 0.00$.

Finally an average value was taken for all three scaling factors:

Pressure ratio:

$$D_{43} = 0.00 \text{ and } C_{43} = 1.0830$$

Efficiency:

$$C_{42} = 1.00 \text{ and } D_{42} = 5.525 * 10^{-3}$$

Mass flow (capacity) :

C_{41} = variable equation which would be used in the main prediction program for the Tay MK-650.

3.4. IP COMPRESSOR ARRANGEMENTS

In this component, non-dimensional speed needed to be readjusted (scaled). This was due to the intersection point between the original MK-650 mass flow provided by Rolls-Royce data and the equivalent pressure ratio read from the reference MK-610 block of characteristics. When these two values were plotted on the characteristics graph, the position of the intersection was rather offset in comparison to the value of the reference engine non-dimensional speed relative to that mass flow. Hence, the value of that non-dimensional speed had to be scaled down. The method applied in order to scale down the characteristics non-dimensional speeds was by means of projecting a value of the mass flow of the MK-650 engine onto the Rolls-Royce working line for the characteristics graph of mass flow against pressure ratio values. After which, a value for a non-dimensional characteristics speed had to be guessed as accurately as possible. Using the Rolls-Royce MK-650 engine data set of non-dimensional speeds, mass flows, pressure ratios and isentropic efficiencies, each mass flow and its corresponding non-dimensional speed were available. If that non-dimensional speed value did not coincide with the reference speed in the characteristics graph, then some alterations would be in order. The guessed value of non-dimensional speed line was obtained from the reference MK-610 characteristics graph by using a mass flow value of Rolls-Royce MK-650 data sheet. Bearing in mind that each Rolls-Royce mass flow had an equivalent original value of non-dimensional speed line. Because Rolls-Royce had provided a set of data

for fifteen different fuel flow cases, enough intersection points were obtained in order to plot a graph of original MK-650 engine values against reference MK-610 characteristics values for non-dimensional speeds. The former steps allowed the correction of the reference engine characteristics non-dimensional speeds. For example at maximum take-off condition the reference engine non-dimensional speed was equal to 86.50, its corrected value becomes equal to 83.20 and so forth. The scaling factor for pressure ratio was found to be 1.00, this meant that the reference characteristics pressure ratio values need not be scaled down, the reference characteristics mass flows remained unchanged because of the capacity scaling factor being equal to 1.00. Those two scaling factors forced initially as 1.00 do not affect the performance of the MK-650 engine in any way. Finally, the scaling factor of the efficiency was found by applying a similar method as for the Inner Fan.

The final arrangements were given as follows:

Pressure ratio:

$$C_{33} = 1.00$$

Mass flow(capacity):

$$C_{31} = 1.00$$

Efficiency:

$$D_{32} = 0.0187 + 0.0295 * \left\{ \frac{ZNDIPC - ZNDIPC_{MIN}}{ZNDIPC_{MAX} - ZNDIPC_{MIN}} \right\}_{ENG}$$

$$0.0187 = \eta_{650_{optimum}} - \eta_{610_{optimum}}$$

$$0.0295 = \eta_{650_{minimum}} - \eta_{610_{minimum}}$$

$$C_{32} = 1.00$$

The IP Compressor Inlet Guide Vanes will be altered to allow for an increased airflow into the core. The intermediate drive shaft will be constructed from stronger material. The IP Compressor bleed valve system will be deleted.

3.5. HP COMPRESSOR ARRANGEMENTS

In most tests this component is of great importance, the reasons for this statement is that it is very susceptible to surge occurrences. Hence, it is a very delicate part of the engine which requires considerable attention and care. Based on Rolls-Royce research work, (Ref 7), this component suffered surge during application of water ingestion case, thus, very high concentration should be given to this component when scaling from the reference MK-610 engine. Major changes took place in the HP Compressor, including the Inlet Guide Vanes speed schedule, the reference characteristics non-dimensional speeds and Bleeds at 7th stage at entry to the By-pass duct. Based on the reference MK-610 engine characteristics graph of mass flow at inlet to the HP Compressor against the non-dimensional speeds (Fig 3.1), a similar graph was plotted. This graph constituted of the scaled down MK-650 values of mass flows at inlet to the HP Compressor against non-dimensional speed values. These values were available from the data set provided by Rolls-Royce. By projecting characteristics non-dimensional speeds onto the above plot, their corresponding non-dimensional mass flows were found. The method followed to scale down the mass flow values was achieved by using Rolls-Royce working line on the reference characteristics graph (Paragraph 3.3.2). This was similar to the IP Compressor and results were obtained by using the following equation :

$$\frac{\dot{m} \sqrt{T_{IN}}}{P_{IN}}_{650} = \frac{\dot{m} \sqrt{T_{IN}}}{P_{IN}}_{610} * C_7$$

The scaled down values of mass flow still corresponded to the original MK-650 non-dimensional speed values. The sets of values for the MK-610 engine allowed for the revised Air flow characteristics graph of the HP Compressor to be constructed. Both the MK-610 and the MK-650 graphs were then overlaid on one another. It was then possible to correct the reference MK-610 non-dimensional speeds. This was achieved by entering the original MK-650 engine non-dimensional speed values, transferring them onto the reference MK-610 graph, projecting them again onto the original MK-650 graph, and finally, the corresponding true value for non-dimensional speeds was found by re-projecting back to the non-dimensional speed Axis. The original MK-650 graph was created by using Rolls-Royce data sets of non-dimensional speeds, against corrected values of mass flows at entry to HP Compressor. Whereas the reference MK-610 engine graph was constructed using the characteristics data set from the block of values corresponding to the HP Compressor. The difference between the two components for the MK-650 and the MK-610 engines was highly noticeable in the Inlet Guide Vanes turning range. For the 7th stage bleed valve scheduling, the reference values at which the bleed valves opened and closed varied from the new corrected values. This was completed by plotting a fraction equal to the difference between the after overboard bleed and the after handling bleed divided by the air flow at exit from the HP Compressor against the characteristics non-dimensional speeds. The previous values were available from Rolls-Royce data set for the MK-650 Tay engine (Ref 8). The plot gave the range of the 7th stage bleed opening and the magnitude of bleed flow when fully open.

Existing program for reference MK-610 engine uses:

$$\frac{N}{\sqrt{T_{IN}}} \text{ from 0 to 549.4} \qquad \frac{N}{\sqrt{T_{IN}}} \text{ from 568.0 to 1000}$$

$$\text{Magnitude of bleed 0.147} \qquad \text{Magnitude of bleed 00.000}$$

for flow when fully open

The fit for MK-650 is:

$$\frac{N}{\sqrt{T_{IN}}} \text{ from 0 to 503.8} \qquad \frac{N}{\sqrt{T_{IN}}} \text{ from 555.0 to 1000}$$

$$\text{Magnitude of bleed 0.150} \qquad \text{Magnitude of bleed 0.000.}$$

for flow when fully open

The pressure ratio scaling factor was considered next, the method was a standard one and similar to the previous components method. The equation used for pressure ratio scaling factors is given below:

$$C_{22} = \frac{\frac{P_3}{P_{26}} - 1_{650}}{\frac{P_3}{P_{26}} - 1_{610}}$$

The efficiency followed a similar method to that of the inner fan. In order to calculate the corresponding scaling factor D_1 , the following equation was used:

$$D_1 = 0.0356 - 0.0104^* \left\{ \frac{\text{ZNDHPC}_{650} - \text{ZNDHPC}_{650 \text{ MIN}}}{\text{ZNDHPC}_{650 \text{ MAX}} - \text{ZNDHPC}_{650 \text{ MIN}}} \right\}$$

$$0.0356 = (\eta_{650} - \eta_{610})_{\text{MIN}}$$

$$0.0104 = (\eta_{650} - \eta_{610})_{\text{MIN}} - (\eta_{650} - \eta_{610})_{\text{MAX}}$$

With the values having the same significance as the ones defined previously for IP Compressor component. After considering a reasonably accurate average, the final arrangements were found to equal:

Pressure ratio:

$$C_{22} = 1.0410$$

Efficiency:

$$D_1 = \text{variable equation}$$

$$C_1 = 1.000$$

Mass flow(capacity):

$$C_7 = 1.045$$

From an uprate feature of Tay MK-650 using Tay MK-620, it was found that the stages 7-11 discs would be strengthened, there would also be a new stage 12 disc in steel. The spacers would be based on the MK-512 standard including diaphragm spacers on stages 10-11 and 11-12. Spacers 7-8, 8-9, 9-10 and 10-11 are MK-512 components.

3.6. HP TURBINE ARRANGEMENTS

The procedure considered to estimate scaling factors for the HP Turbine is defined similarly to that of the Outer fan illustration. The performance parameters which needed to be scaled down included the Isentropic Efficiency and the Mass Flow, it was not necessary for the pressure ratio to be corrected. The original values of pressure ratio for the Tay MK-650 were kept constant over the engine's original speed range. However, for the mass flow block, an average scaling factor was calculated using the equation below:

$$\frac{\dot{m} \sqrt{T_{IN}}}{P_{IN}}_{650} = \frac{\dot{m} \sqrt{T_{IN}}}{P_{IN}}_{610} * C_3$$

As for the efficiency, the method used was also similar to that of previous

components and led to the following equation:

$$C_2 = \eta_{ENG} - \eta_{CHICS}$$

As a result the average values for both scaling factors of mass flow and efficiency were displayed below:

Efficiency

$$C_2 = 0.9665$$

$$D_2 = 0.000$$

Mass flow (capacity)

$$C_3 = 0.9475$$

The use of original pressure ratios conformed with necessary calculations and plots when using the reference MK-610 characteristics graph. There were no offset positions due to intersections, hence, it was considered practical to keep the original Rolls-Royce MK-650 engine data for pressure ratios. The HP1 Nozzle Guide Vanes - reduced in number from 72 to 50 off, they would be cast in a different material, C1023, using 3D technology for efficient aerodynamic profiling. Borescope access will be provided together with the facility for removal of the HP NGV's from the front as per the Spey MK-512. HP Turbine bearing support in C263 material catering for an HP pre-swirl arrangement based on the RB211-524 to provide an HP cooling air feed to HP1 blades. Provision to be made for a new HP1 brush seal but with a standard labyrinth type seal as a backup. HP1 Turbine blades in MAR-M-002 material of a new design and using DS casting techniques. They are reduced in number from 88 to 72, HP1 rotor disc would be in waspaloy material to suit increased temperatures, the disc would include a drilled rim to feed HP air to the blades. Turbine outer segments and supports are provided with honeycomb seals. A new HP Turbine shaft and bearing sleeve is made to cater for increased hub thickness of HP1 disc. HP2 Nozzle Guide Vanes

would be reduced in number from 84 to 78 off, they would be cast in MAR-M-002 material, using 3D technology for aerodynamic profiling. The corresponding turbine blades are of a new design and cast using single crystal material, the HP2 Turbine rotor disc is in waspaloy to suit increased disc rim temperatures. HP/LP seal panels and triple seal arrangement is different but similar to existing parts. Finally the HP Turbine module clearance is to be set independent of LP Turbine module.

3.7. LP TURBINE ARRANGEMENTS

Exactly the same illustration was considered for the LP Turbine. There was no need to alter or correct the pressure ratio values of the original Tay MK-650 engine. The two performance parameters scaled were the efficiency and the mass flow values. The average scaling factors were found to equal the following:

Efficiency:

$$C_{10} = 1.0051$$

$$D_{10} = 0.000$$

Mass flow (capacity):

$$C_{11} = 0.4785$$

Based on the "uprate" features of the Tay MK-650 from the Tay MK-620, the additional information is given. There would be a requirement for a 2% reduction in the capacity of the LP Turbine. This would be achieved by the introduction of a new LP1 Nozzle Guide Vane, similar to the basic Tay Component but with a new inner foot location to suit the repositioned HP1 disc outer seal. The LP2 NGV will incorporate a new aerofoil shape to complete the 2% capacity reduction. There would also be a new LP1 NGV inner seal support, cast in N80 material, which would incorporate a honeycomb seal.

Paragraphs 3.8-3.12 are all based on the Tay MK-650 "UPRATE"

Features using the original Tay MK-620 engine. See Figs (3.2 - 3.9) for the uprate version features of the Tay MK-650 using the Tay MK-620.

3.8. COMBUSTION CHAMBER

The transply combustion liners incorporate a graded airflow transply head and a thermal barrier coating. A new transply discharge nozzle to match the new HP Turbine annulus will include effusion cooled end frames. A combustion casing of increased thickness and with provision for single borescope access to the HP Turbine and borescope access to all combustion liners. The intermediate by-pass duct would have facility for access.

3.9. FUEL SYSTEM

It is anticipated that by employing the Spey MK-512 gearing, with a machining change to the gearbox housing, except for the HP Tachometer Drive, the gearbox ratio change would be attainable. This in return would allow for the increased capacity of the HP fuel pump to be accommodated. A new internal fuel manifold system as well as a new fuel burner of the Parker Hannifin type are required.

3.10. EXHAUST MIXER

The total nozzle area would remain unchanged. However, a new exhaust mixer would be employed incorporating approximately 18% reduction of the hot mixer area and 10% increase in the cold mixer area.

3.11. BY-PASS DUCT BLOCKAGE

Various additional core fairings are employed in order to reduce duct losses.

3.12. AUTOMATIC RESTORATION OF THRUST SYSTEM (A.R.T.S.)

To enable greater use of flexible take off procedures, A.R.T.S. will be deleted from the TAY MK-650.

3.13. SUMMARY OF ARRANGEMENTS

The fact that hand calculations were used, the above results of scaling factors required high concentration in order to allow for practical and sensible values to be introduced. Scaling factors which were used in a variable equation form, were included in the main prediction program. The prediction program constituted of different components, for every component the necessary scaling factor was included in order to allow for the required correction to take place. Other scaling factors which were represented by a constant value, were added to a data set which was used each time the main program was executed. These scaling factors were all tabulated, so that to give a better general presentation (Tables 3.1, 3.2). A graphical representation comparing the differences in characteristics between the reference MK-610 and the MK-650 engines, is displayed in figs 3.10-3.13. It can be seen from fig 3.12 that there are no significant differences in the IP component but there are differences in the other components.

CHAPTER IV

INTRODUCTION OF WATER THERMODYNAMIC EFFECTS INTO THE PREDICTION PROGRAM FOR TAY MK650 ENGINE

4.1. INTRODUCTION

In order to study the effects of water thermodynamics on the performance of the Tay MK-650, some important alterations had to be made in the prediction program. This program which can be used for both transient and steady state predictions, was formerly used for the reference engine Tay MK-610.

With the introduction of all the necessary scaling factors as described in chapter III, the performance of the Tay MK-650 engine, using the intercomponent volume method, can be predicted. The program used is called TICVWAT. The computational procedure for a single-spool engine is described in Appendix E. The procedure for a two-spool engine would be similar only with extra iterative loops, this is shown diagrammatically in Fig 2.4. The method is briefly described in the following paragraph.

4.2. PERFORMANCE PREDICTION OF THE TAY MK650 USING THE ICV METHOD "DRY AIR CASE"

The prediction program is written in FORTRAN 77 which was initially run on a digital computer mainframe ICL 2988, using the VME system. As a result of continuously developing technology, the former facility is now available on the IBM 3080, with the CMS system. This was the system used in the present work. This facility is used at Glasgow University Department Of Mechanical Engineering. The computational procedure used is mainly based on the characteristics of each component

in the engine. For Inner and Outer Fans and IP, HP Compressors and Turbines, these characteristics are listed as tables of a number of non-dimensional speed lines, each line is made of a number of points, and for each point value of non-dimensional speed, corresponding values of pressure ratio, non-dimensional mass flow, and isentropic efficiency are tabulated.

The method of dealing with the flows in the Inner and Outer Fans will first be explained. The method used allows for interchange of flow between the Inner and the Outer fans. Initially, the characteristics had been based on frontal area split of a ratio of 1 to 3 between Inner and Outer fan sections. The corresponding parameter for this quantity is called GEOM. This represents the fraction of the total frontal area corresponding to the Inner section and was assumed to equal 0.25. In order to allow for interchange of flow between inner and outer sections, the axial component of velocity for air into the fan is assumed constant over the whole annular area at any given instant, and that the fraction of this area which represents the Inner fan is not necessarily equal to GEOM but is equal to some fraction of it. This fraction is referred to as the fraction of split FCSP and may vary from one engine condition to another. The program calculates this fraction at each engine condition. In order to begin the digital simulation of the two-spool gas turbine, initial conditions have to be met. These conditions represent the selection of initial shaft speeds together with fuel flow, ambient pressure, flight Mach number, and ambient temperature (Chapter II). Initially, pressure values corresponding to the different volumes are guessed. Engine stagnation conditions at entry are calculated from the previously given flight Mach number, static temperature and pressure. A pressure recovery factor of 0.999 is used to account for any diffusion losses in the Intake, Appendix A. During the initialising period, typically 0.2 to 0.5 second, shaft speeds and fuel flow are held constant and the program quickly calculates the correct pressure distribution in the engine. For the case of the

investigation of a transient response, once this pressure distribution has stabilised, the transient can be started. For the determination of a steady-running condition at a given fuel flow, this fuel flow is held constant and the shaft speeds are released and allowed to move to the appropriate stable value.

4.2.1. FAN

As explained above, the fan is treated as two separate sections, the inner fan and the outer fan. The split between the two sections is allowed to vary from one engine condition to another.

4.2.1.1. OUTER FAN

Since the inlet factors mentioned above are all known, the parameters GEOM and FCSP are used to correct the actual value of the non-dimensional mass flow rate which in return allows for the calculation of the isentropic exit temperature and the isentropic efficiency, from which the actual exit temperature could be found, see Appendix B.

4.2.1.2. INNER FAN

As the inlet values for pressure, temperature and non-dimensional speed are known as well as the mass flow through the outer fan, the mass flow through the Inner fan would be calculated by means of both GEOM and FCSP and by assuming constant and uniform inlet velocity. Once the mass flow rate is determined, the corresponding pressure ratio and isentropic efficiency would be found by use of interpolation if necessary.

4.2.2. IP COMPRESSOR

This is dealt with in a way similar to the Outer fan. Knowing the inlet pressure, temperature, non-dimensional speed and pressure ratio, by use of interpolation, the non-dimensional mass flow rate and isentropic

efficiency are determined, and then the outlet temperature for the IP Compressor is found.

4.2.3. HP COMPRESSOR

The inlet parameters are known which helps determine the mass flow rate and exit temperature, Appendix A. This component is handled in the same way exactly as the IP Compressor.

4.2.4. HP TURBINE

Initially, a value for the non-dimensional mass flow rate into the combustion chamber is guessed, the former is achieved from the known fuel flow and the known mass flow (Paragraph 4.2.3) at exit from the HP Compressor. The mass flow out of the combustion chamber as well as an initial guess for the Turbine efficiency are used as starting values. The known pressure ratio and the guessed Isentropic efficiency across the turbine allow the temperature at exit from the HP Turbine to be found. Since both temperatures at inlet and outlet from the turbine are now available, a corresponding work factor could be calculated. A new isentropic efficiency for the turbine is now found, this would be compared to the initially guessed one. An iterative method takes place until convergence is obtained for the turbine outlet temperature. The known value of inlet temperature and pressure to the turbine help to determine a value for the gas mass flow rate into this component. A second iterative loop enables the original air mass flow rate before the combustion to be revised. This procedure is repeated, until convergence for the gas mass flow rate into the HP Turbine is achieved. Accurate values for the turbine inlet and outlet temperatures are found in this calculation.

4.2.5. LP TURBINE

The temperature at inlet to the LP Turbine is taken to be that of the gases leaving the HP Turbine. A guess is taken for the isentropic efficiency of the LP Turbine. Since the pressure ratio across this component is known, the temperature at exit from the LP Turbine could be calculated. Given both temperatures at inlet and outlet from the component, an estimated value for the work factor could be found. The new isentropic efficiency would now be easy to find. A quick check is then made by comparing the new value and the original guessed one for the isentropic efficiency. If the two values do not match, which they rarely do at first, an iterative procedure is then used until convergence in the Turbine outlet temperature is achieved. Once this is done, the accurate value for the isentropic efficiency is established. The value of gas mass flow rate entering the LP Turbine is then calculated from the turbine's capacity characteristics.

4.3. PERFORMANCE OF THE ENGINES "WATER INGESTION CASE"

The performance of the engine is based upon the performance characteristics of each component. This investigation is based on the MK-650 characteristics. The Tay MK-650 was considered by Rolls-Royce as suitable for tests with water ingestion.

In this Thesis, these water ingestion tests have been simulated by introducing a number of developments in the prediction program for this engine (dry air case). These developments are models of the effects of the introduction of quantities of water/water vapor into the air or gas flow in the various components. The prediction program is built on models of the flow through the various engine components. The introduction of the water is simulated by effects such as evaporation which occurs along the engine at various planes. Another important effect accounted for is the

braking torque on the rotating shafts due to the water droplets being struck by blades and given angular momentum.

Under normal circumstances, water would be ingested through the engine inlet in front of the Fan. In this research, water ingestion would be represented by subsequent evaporation of water which is assumed to occur at a series of possible locations. Three major engine locations had been considered - evaporation in plane between IP Compressor and HP Compressor, plane between HP Compressor and Combustor and finally for the water which passes through the Bypass duct, plane between Mixer and Nozzle. It is assumed that there will be little evaporation in the regions between the Fan and the next component as the temperature rise given to the air in the Fan is quite modest. Drags or rotating torques due to the water droplets hitting the blades were also taken into consideration. These drags were assumed to occur at three locations Fan, IP Compressor and HP Compressor. Another important effect was the influence on both C_p and R (Gas constant) of the working fluid. Both properties were initially being used for dry air only. However, since the prediction program should allow for both cases of dry air and water ingestion to occur, it was necessary to develop the corresponding equations to allow for both cases.

The procedure followed in allowing evaporation to take place at these various engine locations is now explained. Firstly, the plane between the IP and HP Compressor was considered. A separate flow of air and water would enter the IP Compressor component both at specific temperatures, this flow having been separated from the Bypass flow. At exit from the IP Compressor, a combined flow of air and water vapour would manifest itself. As stated before some water evaporation would take place in the IP component, hence, at inlet to the HP Compressor there would be a mixture of air and water vapor plus possibly water, all at a specific temperature. In the present work this has been simulated by having all the evaporation which occurs within the IP Compressor take

place in the space between the IP and HP compressors. An equation of conservation of energy based on the mass flows, temperatures and enthalpies of the air and water at outlet from the IP Compressor would then be used in order to find the temperature of air/water vapour mixture at inlet to the HP Compressor. Initially several numerical approximations were used for the temperature drop at inlet to the HP Compressor component. Once an energy balance was established, a generalised form of the above temperature drop was found. The derivation of the generalised analysis is given in Appendix C. The generalised equation was found using the engine parameters described above and is a function of the air and water/vapour mass flow rates. The equation was then included in the simulation program. By using the equation above, it was possible to obtain reasonably accurate values for temperature calculation at inlet to HP Compressor. In addition to this equation, allowances had to be made for the increase in the final mass flow of air plus vapour at exit from the IP Compressor. Hence a fraction of mass flow of water vapour was added to the total mass flow going into the HP Compressor component.

Secondly, the facility was provided to have water evaporation in the plane between the HP Compressor and the Combustor. The method followed was similar to the one explained above, the temperature at entry to the Combustor for the mixture being a function of air/water vapour mass flow rate at inlet to that same component. The final mass flow at entry to the Combustor had to be increased to allow for the presence of the water vapour. The former would be represented by the mass of air flow out of the HP Compressor component plus the mass of water vapour at inlet to the Combustion Chamber. The final possible water evaporation was to occur in the plane between the Mixer and the final Nozzle. This was to evaporate the water which entered the bypass flow, and would not evaporate until it went through the Mixer. The same method was considered to get the final temperature for the mixture of hot gases/water vapour at the plane at entry to the final Nozzle. Before applying the

generalised form of equation for all the assumptions of water evaporation at different locations, simple numerical tests were tried in order to test the sensitivity and accuracy of the results in question. Only when satisfying results were achieved that a general method was introduced.

Next, the effect of braking torque or drag caused by the impingement of water droplets on the blades is described. Based on the assumptions above, drags would be likely to occur in the components affected by water ingestion. Hence there would be a Fan Drag, IP compressor Drag and finally an HP compressor Drag. These Drags or Power absorption effects are all evaluated in the same manner. Firstly, it is known that the Torque is a function of water droplet mass flow, blade velocity and the mean radius of that specific component. The blade velocity is a function of rotational shaft speed and the mean radius. The Power absorbed is equal to the Torque times the angular velocity. Therefore the final equation would be a function of either the LP/HP shaft speed, the mass flow of water droplets multiplied by the number of Fan/IP/HP compressor stages where the impingement occurs, and the different radii values. Drag is proportional to the shaft speed and the mass flow of water in a way that if both or one value is increased, the value for Drag would increase accordingly.

The generalised equations for Drags were introduced as statements in the performance simulation program. These parameters would play an important role in altering the value of the acceleration power, when studying transients, in both LP and HP shafts. This would in return affect the acceleration Torque, the shaft acceleration and last but not least the final shaft speed when the engine has stabilised.

As a result of mixed flows at the different evaporation locations in the engine, new gas properties had to be evaluated. Normally, the prediction program only uses R and C_p for dry air. However, in this research a method is found to allow for new R and C_p to be used. This method is described in Appendix D. The gas constant for the mixture of

air and water vapour or gas and water vapour would be in terms of gas constants for air and steam and air/water percentage. The new gas constant R for the mixture would be a function of the Universal gas constant, molecular weights of air and steam and a mass fraction of air/water. The previous is illustrated in Appendix D and Table 4.1. The specific heat at constant pressure, Cp, for the mixture was originally a fourth order equation function of inlet Temperatures. However, this would create erroneous results during iteration processes in the engine simulation tests. In order to avoid this problem, Cp for mixture was simplified to a first order equation in function of temperature. Both fourth order equations for air and steam were plotted over a range of inlet temperatures Fig 4.1. A corresponding tangent to each curve was found, that allowed for the gradient of the first order equation to be calculated. Hence both Cp for air and steam were reduced from a fourth order to a first order function. These functions were then incorporated into the simulation program to allow for reasonably accurate gas properties for the corresponding mixture to be used.

Based on dimensional analysis, Appendix F, it was known that the pressure ratio across a compressor or turbine generally, was a function of non-dimensional speed and non-dimensional mass flow rate. For many applications the gas constant R and the linear dimension D do not change, and the full non-dimensional groups can be simplified to:

$$\frac{\dot{m}\sqrt{T_0}}{P_0}, \frac{N}{\sqrt{T_0}}$$

However for the present work the gas constant R will vary, so the more complete non-dimensional groups, incorporating R, would be used. This is explained in Appendix D. Having estimated new values for R, these were then used in the non-dimensional mass flow and speed for the components concerned in the performance simulation program. The value of non-dimensional speed and mass flow rate would now allow for a

multiplying factor of R for air over R for mixture to be included, this would apply in the component in question as well as the components downstream from it, Appendix D. When the HP Compressor is under study, the HP Turbine and LP Turbine would have a satisfactory non-dimensional speed and mass flow groups.

4.3.1. HP COMPRESSOR

In order for this component to satisfy both performance with water conditions and normal dry air conditions, an important statement was introduced in the performance simulation program. The engine performance relies on a set of data input. This data set contains all the necessary coefficients which allow the execution of steady running or transient performance for the engine. A new coefficient referred to as AWTH represents a constant which defines whether the simulation program would be executed for a water ingested engine or a normal dry case. If AWTH was equal to any other value apart from zero, a chain reaction would be triggered to allow for water evaporation to take place in the plane between the IP and HP Compressor, hence, permitting all the necessary equations and coefficients to change so that water effects could take place. However, a zero value would allow the simulation program to be executed with dry air only. From a general point of view, the quantities which were expected to alter would be:

- a) Temperature at entry to the HP Compressor
- b) Mass flow through the HP Compressor
- c) Non-dimensional speed across the HP Compressor
- d) Non-dimensional mass flow across the HP Compressor
- e) Gas constant R and C_p for mixture of air/water vapour.

4.3.2. COMBUSTION CHAMBER

In the Combustion Chamber, a non zero value for the corresponding

coefficient BWTH would allow for water thermodynamic effects to take place. If on the other hand BWTH was equal to zero, then, there would be no water effects taking place and the only medium undergoing combustion would be dry air. It is very important to ensure that in the case of water evaporation in the combustion chamber the same expected changes would take place downstream from that component, in other words new R , C_p , non-dimensional speed and mass flow rate in the HP Turbine, LP Turbine, and final Nozzle.

4.3.3. BYPASS DUCT

Similarly to the HP Compressor and the Combustion Chamber, effects of water precipitation through the frontal area of the engine have to be accounted for. During the flight of an aircraft through heavy rainstorms it would be expected that water would infiltrate the frontal area of the engine. A fraction of that water would flow through the engine core and the rest through the bypass duct. It could be said that most of the water would flow into the bypass duct because of the reaction of Fan blades on water droplets. A first estimate of the distribution would be based on the assumption of 75% water through the Bypass Duct and 25% water through the engine core, this being the approximate split of the air flows. However, in order to account for a more realistic division, as explained above, a split of 90% and 10% respectively, was adopted. This assumption was regarded as sensible when compared to Rolls-Royce observation results in Table 4.2. Rolls-Royce experimental tests showed that over a range of engine condition (LP shaft speed) about 90-100% of water aimed at core would be centrifuged into the engine Bypass duct. Having already discussed the effects water would have on the HP Compressor and the Combustion Chamber, it would be of interest now to study the presence of water in the bypass duct and how it would affect the engine as a whole.

It is quite reasonable to assume that water would in fact cause little or no damage at all in the bypass duct before it reaches the Mixer and also little of it will evaporate, due to the modest temperature rise of the air. Once the water flows into the Mixer, it would mix with the hot gases coming from the LP Turbine exit and present in the Mixer. The resulting evaporation effects would be represented by the reduction of flow temperature and the increase of mass flow quantity in the specific plane of evaporation between the Mixer and the final Nozzle. The coefficient DWTH would determine whether the simulation program for the engine would run under normal dry air conditions or water ingestion conditions. If given a non zero value, the prediction program would allow for water effects to take place in the Mixer and downstream from the Mixer, however, a zero value would allow for a normal performance.

4.4. DERIVATION OF BASELINE

Firstly, based on the previous assumptions of water evaporation locations, calculations were performed on each evaporation plane at a time. A steady running state run for a clean engine (water free) was performed for a set of fuel flows. Similar runs with the same constant fuel flows were then executed individually for reference evaporation at plane between IP and HP Compressors, at plane between HP Compressor and Combustion Chamber and at plane between Mixer and final Nozzle. Steady state performances were also executed to investigate Inlet Fan Drag, First stage IP Drag, Three Stages IP Drag and finally First Stage HP Drag. Each steady state performance provided final readings for LP and HP shaft speeds as well as various temperatures and pressures across the engine and at different locations for evaporation. These tests provided a baseline for the effects of water evaporation and droplet impingement drags at the various engine locations.

CHAPTER V

MATCHING OF PREDICTIONS TO TEST DATA FROM TAY MK650 ENGINE

5.1. ENGINE TEST CONDITIONS

Rolls-Royce had carried out tests using a Tay MK-650 Engine in which water was injected directly into the front face of the IP Compressor, Refs 7, 8. Thus no water entered the Bypass flow. The reason for injecting the water directly into the core, as compared with in front of the fan, was to avoid the uncertainty of what fraction of water entering the fan will be centrifuged out into the Bypass duct (see Section 4.3.3). In these engine tests, observations made by Rolls-Royce, for full throttle setting, were changes in HP shaft speed, LP shaft speed, HP Turbine exit temperature and fuel flow for a range of water injection rates up to surge. The results obtained from Rolls-Royce investigations, are shown in Figs 5.1 and 5.2. The curves corresponding to the three main engine parameters stated above, initially behaved in a linear manner as the water flow increased (Fig 5.1). When the water flow increased beyond 1.008 kg/s which is about 2.2% of the core airflow, the subsequent changes in shaft speeds and LP Turbine Entry Temperature are seen to become non-linear and a further increase in water flow of 75% causes the HP Compressor to surge.

The condition of water flow of 1.008 kg/s, ie the end of the linear behaviour, is taken in this research as the one for which to match the modelling predictions to Rolls-Royce observations. Once this matching is achieved, the performances of the HP Compressor and other components in the engine are investigated.

5.2. ENGINE CORE PREDICTIONS

This research was based on individual evaluations of engine parameters. After each engine simulated performance, each component would have an output of inlet and outlet parameters (Temperatures, pressures, mass flows.....etc).

Before finding the above match, each evaporation plane was considered on its own. Each case provided a set of results from which the match was going to be located. These cases included evaporation at plane between IP and HP Compressors, evaporation at plane between HP Compressor and Combustion Chamber, one stage IP drag, three stage IP drag and finally one stage HP drag. Individual cases were analysed on their own over a range of fuel flows.

5.2.1. WATER EVAPORATION AT PLANE BETWEEN IP AND HP COMPRESSORS

In order to provide a reasonable explanation for the case of water evaporation at this location, it was necessary to compare its results which correspond to the steady state performance with the clean engine one. Such procedure would enable both a study of these results, hence, an attempt to explain the differences which occurred between the two cases. A general analysis of the effects corresponding to the ingestion and evaporation of water would then follow. It was considered valuable to test the engine program simulation over a wide range of fuel flows, in order to check the consistency of the performance. The results are shown in tables 5.1, 5.2 and 5.3.

One important observation was that, at lower fuel flows of 0.84 kg/s, the change of HP shaft speed between reference evaporation and clean engine was rather high, that difference however, kept diminishing when the fuel flow was being increased. Initially at a fuel flow of 0.84 kg/s, N_H for water evaporation had dropped by 3.17% from the original value for

clean engine, ie $\Delta N_H = -3.17\%$. At $\dot{f} = 0.86$ kg/s, ΔN_H was equal to -2.90% and finally to $\Delta N_H = -1.47\%$, at a fuel flow of 0.97 kg/s. It could thus be said that at lower fuel flows the water ingestion effects were substantial and so effective as to reduce the HP shaft speed by a high margin from its corresponding clean state value, on the other hand the more the fuel flow increases, the narrower the difference in N_H , see Fig 5.3.

The following is an explanation to this phenomena. Due to the cooling effects of water ingestion and its evaporation at that specific location, the temperature at entry to HP Compressor was forced to drop by approximately fifty degrees Kelvin. Hence, the non-dimensional speed was bound to increase. In general, be it for transient or steady running behaviour, the rate of change in thrust with respect to non-dimensional shaft speed for any engine, is more substantial at lower speeds than higher ones. This is due to the fact that even though the shaft speed has reached its maximum value, the thrust can still increase, see fig 5.4. Since in this case there is an increase in non-dimensional speed, the change in thrust is comparatively small, hence there would be a drop in HP shaft speed at lower fuel flows and the opposite at higher fuel flows. At normal capacity of the IP-HP Intercomponent Volume, (Volume 26) , the mass flow at outlet from HP Compressor was initially very high because of the very high non-dimensional speed due to the compulsory reduction in temperature caused. As a result of the capacity of Volume 26, the mismatch between the mass flow out of the HP Compressor and that at exit from the HP Turbine was apparent. While Volume 26 was emptying Volume 3, which represents the HP Compressor-Combustion chamber Intercomponent Volume, was filling up. Hence, the HP shaft speed would decelerate gradually. This deceleration was forced to be less marked at higher fuel flows. As a test, Volume 26 was reduced and similar performance runs were performed. It was observed that the mismatch between the two previous mass flows had reduced allowing for a less obviously marked deceleration of HP shaft speed to take place.

From a graph of air flow characteristics of HP Compressor, in which mass flow at inlet to the component was plotted against non-dimensional speed, see Chapter III, Fig 3.1. It was found that at higher fuel flows and consequently higher non-dimensional speeds, the shape of that curve, which increases continually, starts to level out. That change in shape was due to the high Mach numbers of the flows in the HP Compressor. Thus, when operating at the lower fuel flow of 0.84 kg/s, an increase in HP Compressor non-dimensional speed of 6%-7% gives a greater increase in non-dimensional air flow through the compressor than when operating at the higher fuel flow of 0.97 kg/s. This eventually causes, at the lower fuel flows, a greater reduction in HP shaft speed.

From the above explanation It would be quite reasonable to say that the effects of water evaporation in this area on a turbo-fan engine are less harmful at higher fuel flows and non-dimensional speeds. Another important parameter to observe is the steady running line in the HP Compressor. The steady running line of the clean engine and of the engine with water evaporation at the plane prior to inlet to the HP Compressor are shown. It is seen that there is little movement when comparing the two lines. This is because the mass flow through the Turbines, although it contains water vapour, is also, apart from various bleeds, the mass flow through the HP Compressor. The same working medium was flowing through both the HP Compressor and Turbine, which means that the surge margin is not significantly altered.

5.2.2. WATER EVAPORATION AT PLANE BETWEEN HP COMPRESSOR AND COMBUSTION CHAMBER

Quite differently from the previous case, this case predicts a continuous rise in the change of HP shaft speed between reference water evaporation at that specific location and the one corresponding to the clean engine.

At a fuel flow of 0.84 kg/s, ΔN_H was equal to -2.03%. In other words the

HP shaft speed N_{H1} for the reference evaporation had dropped by 2.03% compared to the reference clean engine. At a fuel flow of 0.86 kg/s, the drop had increased to $\Delta N_{H1} = -2.08\%$ and finally a drop of $\Delta N_{H1} = -2.40\%$ was registered when the test was performed at a fuel flow of 0.97 kg/s.

An attempt to explain the above follows. From the simulated test runs where each was performed at a constant fuel flow, it was noticed that both T_4 and T_5 drop, these temperatures represent temperatures at inlet to and exit from the HP turbine. T_4 drops by approximately 5.3% whereas T_5 reduces by 5%. As a result of that temperature drop, the power per unit mass of the total gases would drop by approximately 5%. The power per unit mass of air at the engine core would drop too, except that it does so after eliminating the 1% mass of water quantity to be evaporated. The former would mean a total reduction of 4% ie (5%-1%). The power per unit mass of total gases drops by 5% and the power per unit mass of air drops by 4%. This reduction represents an imbalance of power in itself, and because of this difference, the HP shaft speed would automatically reduce in order to counterbalance the reduction in power per unit mass of air through the core, see Tables 5.1, 5.2 and 5.3.

It should be noted that the range of fuel flows initially varied from 0.84 to 0.97 kg/s. However this range was later increased (0.10 kg/s-0.98 kg/s) in order to get a more satisfying view in every component of the steady running line in comparison to the surge line.

As mentioned previously, it is important to observe the steady running line in the HP Compressor for evaporation prior to the Combustion Chamber. The Beta values mentioned in Chapter III, correspond to how far or how close the steady running line of any component is to the surge line. A surge situation would be equivalent to a value of Beta equal to unity. Since the mass flow at inlet to the Combustion Chamber was being increased by 2.1% to allow for a water quantity of 1.008 kg/s to be evaporated, the same increase would manifest itself in the LP Turbine. The mass flow through the HP Compressor

component would differ in state to the one through the HP Turbine. Thus, while prior to the HP Compressor there was no water and/or water vapour present, the opposite was found after the Combustion Chamber. This created an imbalance which forced the steady running line of the HP Compressor closer to the surge line. This was observed from the reduction in the Beta value of the HP Compressor component. The surge margin would, unlike the case of water evaporation at plane between the IP and HP Compressor, be altered significantly in this case of evaporation at plane between the HP Compressor and the Combustion Chamber.

In order to achieve a reasonably accurate explanation of this movement towards surge for the HP Compressor steady running line, an alternative test was considered. The test consisted of reducing the capacity of the HP Turbine and performing similar steady running performances for a clean engine at fuel flows equal to 0.84, 0.86, and 0.97 kg/s. A comparison in the output data between the original clean engine with the full HP Turbine capacity to that with the reduced one would then become appropriate. Reducing the HP turbine capacity by 1% with the LP Turbine capacity being unaltered, increased the turbine work per unit mass by approximately 1%, hence, work done per unit mass for the HP Compressor would also increase by nearly 1%. Reducing the HP turbine capacity does not alter the mass flow at entry to that same component, this being constrained by the LP shaft compression which is only slightly affected. The high pressure ratio across the HP Compressor causes the temperature leaving the compressor to be increased by about 2.5 Kelvin. Thus the temperature at the HP Turbine inlet will be increased by a similar amount, at the same fuel flow. Since the non-dimensional mass flow group at entry to the HP Turbine has to drop by 1%, then P_4 has to rise by about 1.1%. This indeed was the case.

$$\frac{\dot{m}_4 \sqrt{T_4}}{P_4} \text{ drops by } 1\%$$

Another important factor would be the effects on the mass flow through the HP compressor as a result of reducing the HP turbine capacity,

$$\frac{\dot{m}_{26} \sqrt{T_{26}}}{P_{26}}$$

The capacity of the HP turbine was previously reduced by means of allowing a factor C_3 , which represents a multiplying factor on the HP Turbine Capacity, to be made smaller. As a consequence, The split of power between the HP and LP shafts would move the HP shaft speed up and the LP shaft speed down. This would in return cause pressure ratios to change,

$$\frac{P_4}{P_5} \text{ would increase, however, } \frac{P_5}{P_6} \text{ would decrease.}$$

From the above observations in this case, the HP shaft speed would be expected to rise even faster than the LP shaft speed. The LP shaft speed only increased by 2 rpm, which represents a very negligible amount unlike the rise observed for the HP shaft speed. It was discovered from the performance outputs in Tables 5.4, 5.5 and 5.6, that the previous statement was accurate. Based on that statement, the non-dimensional speed for HP compressor was bound to rise.

$$\frac{N_H}{\sqrt{T_{26}}} \text{ is expected to rise}$$

Since the mass flow at entry to the HP Compressor \dot{m} had moved up, it would therefore allow for the rise in the non-dimensional mass flow group for the HP compressor.

$$\frac{\dot{m}_{26} \sqrt{T_{26}}}{P_{26}} \text{ would also rise}$$

Hence, justifying the small movement in the HP Compressor mass flow which happens in this particular evaporation plane.

The reduction in HP Turbine capacity allowed for the determination of the direction of the Beta values for the HP Compressor. This was found to be satisfactory as the Beta value had dropped reasonably compared to the one for clean engine. This means that the danger occurs in this plane of evaporation rather than the plane between the IP and HP Compressors.

5.3. MATCHING OF PREDICTIONS TO ROLLS-ROYCE ENGINE TESTS

Since Rolls-Royce's study was related to water injection into the engine core only, it was necessary to follow the same procedure by investigating water ingestion and evaporation at different possible core locations. As described before and as far as the engine core is concerned the two main evaporation locations were between the IP and HP Compressors and between the HP Compressor and the Combustion Chamber. Since water was to be ingested in front of the IP Compressor, it was important to investigate, separately, evaporation of the water at both previously mentioned locations. Using previous engine simulations, the changes of shaft speeds and temperatures, NL, NH and T5M (LP Turbine entry temperature), between clean engine and water ingested engine, were calculated, see Tables 5.1, 5.2 and 5.3. The temperature would be rather high across the Combustion Chamber, hence, all the water would evaporate prior to the entry to that component. A suitable combination of water evaporation distributions was sought in order that a

reasonable matching of results could be attained. Several estimates of water evaporation distribution and rotational drag occurrence were attempted over a range of high fuel flows, approaching those used in the Rolls-Royce engine. After numerous attempts, Tables 5.6-5.15, it was found that the best matched evaluation to Rolls-Royce's observations through the engine core, involved a 10% evaporation at the plane between IP and HP Compressors and 90% evaporation at the plane between HP Compressor-Combustion Chamber. The best match also required 3 stages of IP drag caused by reactions of compressor blades on the quantities of water ingested, however, no HP Compressor drag was involved, Table 5.15. The procedure which was followed in achieving this match is now described.

The Rolls-Royce results, at a water ingestion rate of 1.008 kg/s, were $\Delta NL = -40$, $\Delta NH = -25$ and $\Delta T5M = -34$, with an increase in $\Delta \dot{f} = +1.7\%$ between clean engine and water evaporation states, see Figures 5.1, 5.2. As seen from Tables 5.1 to 5.3, considering evaporation on its own, the predicted shaft speed reductions are substantially greater, even with the increase in speeds associated with the fuel flow raised by 1.7%. The instrumentation recording the shaft speeds and T5M is considered to be reliable. It was therefore assumed that the fuel flow recordings were in error. Therefore, in attempting to achieve a match on ΔNL , ΔNH and $\Delta T5M$, it was assumed that the fuel flow rose by an amount to align the predicted ΔNL with the observed ΔNL of -40 (rpm). The effects of fuel flow change on ΔNL , ΔNH and $\Delta T5M$, were found by running the "clean engine" simulation program over a range of fuel flows. With this assumption and the divisions of evaporation and drag described above, the corresponding ΔNH (predicted) virtually coincided with the experimental change and the predicted $\Delta T5M$ was -23 Celsius compared with the experimental change of -34 Celsius. The $\Delta \dot{f}$ required was +7.9%. These changes, and changes for other combinations of evaporation and drag, are shown in Tables 5.4, 5.5 and 5.6. In each of the cases, the fuel flow was

adjusted to align ΔNL with the observed change of -40 (rpm). However even in this case there were some differences between prediction and observation. All other distributions examined gave predictions which were significantly different from the Rolls-Royce engine tests.

5.4. USE OF MATCHED MODEL TO PREDICT SURGE

As far as Rolls-Royce results were concerned, the above quantity of water was by no means the limit at which surge occurred, in the contrary, surge did not occur until a much higher mass flow of water was being ingested through the core, see Paragraph 5.1. Water was being introduced into the engine gradually, starting from a minimum value of 0.252 kg/s to a maximum value of 1.764 kg/s. It was noted in Fig 5.1 that the behaviour of the three parameters NH, NL and T5M, once the quantity of water exceeded 1.008 kg/s, became non-linear. Thus a water mass flow of 1.008 kg/s (the limit of the linear behaviour) was applied in the simulation program. This would allow for the investigation of any differences in the effects of water ingestion prior to surge, between Rolls-Royce's experimental observations and the simulation program used in this research.

Components were considered individually. For the Inner Fan prediction (conditions-sea level, Mach 0.2), little difference was noticed in the movement of the steady running line in Figure 5.5. The reason behind this was the introduction of water directly through the IP Compressor using the simulation program. Even if water had been ingested at the front of the engine, later investigations (Chapter VI) predicts little effect in the Inner fan. This is due to the low temperatures found at that level.

Since there is only water ingestion in the core, no water would be present in the Outer Fan Component. By comparison, Fig 5.6 shows that the steady running line was seen not to be altered in anyway.

For the IP Compressor, the 10% evaporation at 26 causes a significant lowering of the IP Compressor working line, due to the higher $(N_H / \sqrt{T_{26}})$ of the HP component. But the 90% evaporation at 3 causes the working line to be raised, this being due to the HP shaft dropping more in speed and associated air breathing capacity, than the LP shaft and IP compressor drop (at a constant fuel flow). The droplet impingement drag in the IP Compressor lowered the working line, due to the LP shaft speed dropping whereas the HP shaft speed increased. The combined effect is to give a slight lowering of the working line in the IP Compressor, as seen Figs 5.7.

Finally and most importantly from Fig 5.8, the HP Compressor steady running line was observed to rise significantly in comparison to the clean engine steady running line. This is due mainly to the combination of increase in total mass flow through the HP Turbine Nozzle Guide Vanes. It is known that the non-dimensional mass flow of the HP Turbine rises with increased work factor, however, the HP Turbines nozzle guide vanes become choked at a relative non-dimensional speed. This effect forces the non-dimensional mass flow to remain constant over the speed range, and because of the aerodynamic coupling with the HP Compressor, the mass flow and pressure ratio through this component increase accordingly, the latter more than the former. These effects reduced the safety margin by approximately 40%. It is important to realise that evaporations at 3 and 26 were 90% and 10% respectively because ΔNL , ΔNH and $\Delta T5M$ best fitted Rolls-Royce results. Hence, evaporation at 3 would cause more damage to the HP Compressor surge line than evaporation at 26, that was found when comparing Beta values in both performances, Tables 5.4, 5.5 and 5.6.

The previous assumptions were consistent in relation with Rolls-Royce observations in a way that the HP Compressor was more prone to surge. Hence, it would be the component most likely to suffer serious damage than any other component in the engine.

CHAPTER VI

APPLICATION TO PREDICTION OF PERFORMANCE OF ENGINE IN RAINSTORM

6.1. INTRODUCTION

By using the previous chapters, a general description of all the necessary changes which were applied to the prediction program, in order to allow for water ingestion could now be revealed. Originally this research was based on the study of the effects of water and/or water vapour through the engine core. However due to the importance of such experience a broader outlook was adapted in order to investigate the effects mentioned above on the whole engine performance. The reason behind this investigation would be to provide a reasonable study of a problem corresponding to real life experience. An aircraft flying through a severe rainstorm would fall into this category. It could be said that this research was initially based on core evaporation in order to compare the results to Rolls-Royce's own observations. Secondly, it was deemed relevant to investigate any other possible locations of water/water vapour evaporation starting from the main entrance for the engine. Before the changes of both predictions are described, a wider study of Rainstorms would be valuable in order to analyse how an amount of rainwater would become so dangerous over a period of time to the extent of putting the aircraft's engine(s) at risk.

6.2. RAINSTORM DATA

With the increased frequency of commercial carrier flights employing turbofan engines and the extension of such air service into the more remote places of the earth, there exists increasing possibility that these aircraft will encounter heavy rainstorms during flight.

Normally the flight would be diverted around the storm, but a particular condition such as landing or take-off might require operation through the rainstorm. Operation in heavy rainfall and the ingestion of large quantities of water into the engine even for a short period of time could influence the engine service life in addition to affecting the immediate performance output.

An estimate of the probable maximum moisture content for a range of altitudes has been made for the following assumed weather conditions, Ref 2:

- (1) Tropical cumulus cloud; maximum cloud water, no precipitation.
- (2) Moderate continuous rain; rainfall rate, 7.62 mm (0.3 in) per hour.
- (3) Heavy continuous rain; rainfall rate, 25.4 mm (1.0 in) per hour.
- (4) Heavy shower; rainfall rate, 50.8 mm (2.0 in) per hour.
- (5) Practical maximum rainfall; rainfall rate, 314.96 mm (12.4 in) per hour.

Curves showing the estimated free water-air ratio as a function of altitude for each of these conditions are shown in Fig 6.1. The practical maximum rainfall rate of 314.96 mm per hour is the greatest water-air ratio considered herein and is a statistically estimated maximum rate such that, if a location is chosen at random in the United States east of the Rocky Mountains and the rainfall is observed for a period of one year, the probability is 1:1000 that the rainfall rate will exceed 12.4 inch per hour for a period of five minutes. The probability of encountering values much in excess of those shown in Fig 6.1 is extremely small.

Cloud droplets diameters can range from a few micrometers to about 100 micrometers, occasionally some twice as large. Raindrops usually vary between 500 micrometers to 5000 micrometers, with a rate of raindrop reaching 100 drops per m^3 . At collision with a smooth surface the raindrop leaves a spot which diameter is seven times larger than the original one. Thunderstorms extend to altitudes of about 10 km.

A project airplane flying through a storm at an elevation of about 5 km measured an updraft of about 25 m/s. Drops with 1 mm in diameter fall

twice as fast, those with diameters over 4.5 mm have a speed of about 8.0 metres per second.

Rainstorm records are :

12.55 inches in 24 hours (Harrisburg USA, 1962)

7.66 inches in 24 hours (USA, 1889)

19.0 inches in 24 hours (Central America, 1934).

6.3. APPLICATION OF RAINSTORM TO TAY ENGINE

When an aircraft is flying, the air intake sweeps out a volume that is proportional to the front area of the inlet, and the quantity of water ingested is dependent on the flight Mach Number of the airplane and the inertia effects of the rain droplets. It can be assumed that the moisture content is homogeneously distributed throughout the volume swept by the inlet. Data for a typical subsonic inlet are shown in Fig 6.2 and demonstrate that the engine would ingest about 100% of the free water content at a flight Mach Number of 0.6. Considerably less water would be ingested at lower flight Mach Numbers, and as much as 144% would be taken in at a flight Mach Number of 0.8. Therefore, the maximum free water-air ratios likely to be encountered at the engine inlet during subsonic flight are of the order of 1.44 times 0.016 or about 0.023 lb of water per lb of air at an altitude of 20,000 ft, this means that at these corresponding flight conditions 2.3% of the total flow intake would be water. The maximum water-air ratio to be ingested during high subsonic speed near sea level would be of the order of 0.7 times 0.016 or about 0.012, Ref 2.

The quantity of Water to be ingested through the frontal area of the Tay MK-650 engine would be based on the principle above. Initially a performance of steady running behaviour would be completed for a clean engine state at ISA conditions, altitude of 20,000 ft and Mach 0.8 for a fuel flow range between 0.10-0.60 kg/s. This would help determine the total quantity of air going through the frontal area of the engine.

Once this is achieved, 2.3% by mass of that air flow would be made to carry water properties. After completion of various steady state performance predictions of water ingested engine, results would then be discussed.

6.3.1. WATER DISTRIBUTION IN FAN/FRONTAL AREA

Under normal circumstances for the Tay Engine, the air flow split between Inner and Outer Fan would be equal to 25% and 75% respectively. The first estimate of water distribution was based on the split of air flows, with 10% of that 25% being evaporated at plane between IP and HP Compressors and 90% of 25% being evaporated at plane between HP Compressor and Combustion Chamber. It was discovered from the components Beta values that the HP Compressor steady running line had moved dangerously closer to the surge line. However, for a more realistic and sensible division, justified by the fact that most of the rain water would be forced by the centrifuging reaction of Fan blades on water droplets to flow into the Bypass duct, only a small proportion of water would make its way to the engine core. That division would be more reasonably associated with a 90% water through the Bypass duct and 10% water through the engine core. The results from this assumption showed that the HP Compressor surge margin was seriously eroded. These previous evaporation assumptions proved very important in knowing the water trajectory and whether water is to remain in the engine core or move out to the Bypass (Evaporation at 7) where there was little effect on the HP Compressor working line. Thus, to avoid serious problems, it would be crucial to reduce the fraction of water which remains in the core. This could be achieved by increasing the distance between the trailing edge of Fan blades and the splitter.

Since most water would flow through the Bypass duct, it would be of interest to study its effects on engine performance once it reaches the Mixer. This is described next.

6.3.2. WATER EVAPORATION EFFECTS AT PLANE BETWEEN MIXER AND FINAL NOZZLE

The most hazardous aspect of rain water ingestion during flight is that it could affect engine performance. Based on previous studies Refs (1-6), engine behaviour is likely to be affected during take off, landing and at different altitudes due to the direction of rain water droplets. The engine during these situations has to continue to operate normally. However, due to the angle of attack, it becomes liable to ingest large quantities of water when flying through severe rainstorms. Water would be expected to enter the whole inlet front area of the engine. Hence, water ingestion would be divided between the engine core and the bypass duct. It would now be of interest to make an attempt at studying the effects of water through the bypass duct.

It is reasonable to say that the water while within the bypass duct would have no serious effects on the engine core due to the considerably low temperatures found in the Bypass duct of the engine. Hence, only a small fraction of the water will evaporate. However, once the water reaches the mixer, the situation is bound to change. As the water now mixes with a hot gas stream, various engine parameters such as temperatures, mass flows, pressure ratios, non-dimensional speeds would most definitely tend to vary.

The conditions chosen in this case corresponded to an altitude of 20.000 ft, Mach number of 0.8, this selection being explained in Paragraph 6.3 above. Based on a similar principle of water ingestion, allowances were made in the simulation program for a 100% water evaporation to take place between the Mixer and final Nozzle plane. Following similar methods as in Chapter III, it was realised that a drop in temperature and an increase in the final mass flow at inlet to that component (Mixer), would represent the initial water ingestion effects on the engine performance defined by the generalised equations added to the simulation program.

An initial value of 0.32 kg/s of fuel flow was tried, after allowing for the engine to stabilise, values for N_H , N_L , and T_{5M} were registered. With respect to the clean engine case, the differences in shaft speeds and temperature at exit from the LP Turbine were calculated and found to be, $\Delta N_H = +17.94$, $\Delta N_L = +136.03$, and $\Delta T_{5M} = +2.62$. These values were repeated for fuel flows of 0.20 kg/s and 0.12 kg/s. Generally speaking, ΔN_L was found to be decreasing, as the average value for ΔN_L was equal to +200. An average value for ΔN_H was equal to +42. ΔT_{5M} did not suffer any serious changes, its average value was always within plus 5K. This is considered to be a relatively small difference.

For a range of fuel flows varying between 0.10-0.32 kg/s, N_L for water evaporation case increases when compared to the clean engine. That would mainly be due to the mixed air-water/water vapour flow going through the fixed Nozzle area. The cooling effects on temperatures and the increase in mass flows at entry to the Mixer causes the exit temperature of outcoming gases from the LP Turbine to be distorted. Since the mixed flows into the final Nozzle are expected to have a reasonably high temperature, the fact that this is reduced increases the density of the flow, the velocity of the flow slows down as a result. However the main idea is that the temperature drop causes the volume of the flow to reduce hence, increasing the flow density. As a result, more flow area would be allocated to the mixed flow at entry to the final Nozzle. Since the final nozzle has a bigger area, by means of gas dynamics balance, more Fan speed would be noticed. This is the reason for the LP shaft speed increase. As the LP shaft speed increased, more air mass flow would enter the IP Compressor. The HP shaft speed suffered a slight increase, this is due to the fact that the HP Compressor is operating at choked turbine conditions and most importantly that the final nozzle can handle more kgs per second of core gases which pushes the HP shaft speed slightly higher. The behaviour of both the LP and HP shaft speeds was observed by predicting the performance of a clean engine with a 2%

increase in the Final Nozzle area over a range of fuel flows. The output confirmed the rise in both shaft speeds when compared to the original clean engine prediction. This test enforces the previous argument in a way that if more area is allocated to the flow in the Final Nozzle, both LP and HP shaft speeds would tend to increase the former more than the latter.

The effects of the water evaporation between the Mixer and Final Nozzle on the running lines of the engine components is now explained. Characteristic graphs were put together for every component and then compared to those of clean engine state. Fig 6.3 shows steady running lines for clean engine and water evaporation at entry to Mixer. It was found that the steady running line had dropped by a very small amount, approximately 0.5%. This is due to the increase in total gas mass flow through the Mixer which causes the LP shaft speed to increase in order to maintain the energy balance in the LP shaft. Thus, since the inlet temperature had not changed, the non-dimensional speed would increase, sucking more air into the Inner Fan. The pressure across the component rose by 2.75%, however, the non-dimensional mass flow at inlet to the component rose by 5.86%. The slight lowering of the steady-running line gives a very slightly increased surged margin. To summarise, it could be said that no serious effects had taken place in the Inner Fan Component. The steady running lines for the Outer Fan are shown in Fig 6.4. In this component changes are bound to happen due to the increase in mass flow intake, the steady running line had dropped by a very small percentage which is mainly due to the temperature drop caused by water prior to the Final Nozzle. This effectively increases the flow area at the Final Nozzle available for the Bypass air. This slightly increases the surge margin in this component. The IP Compressor behaved in an opposite manner, in a way that steady running line shifted towards surge by a very small percentage. This is due to the higher mass flow initiated by the increase in the LP shaft speed but with only a small increase in HP shaft speed. The increase in mass flow caused the pressure ratio to rise moving the steady

running line upwards and reducing consequently the surge margin by nearly 10%, which is by no means a drastic rise, Fig 6.5. Finally and most importantly, the effects on the HP Compressor were observed from Fig 6.6. Even though the HP shaft speed had slightly dropped, the steady running line neither rose nor fell, the reason for this is that the HP Compressor operates ahead of choked turbine conditions. Hence, it could be concluded from the above investigation that serious effects may only be anticipated if water is present in the engine core. This necessitates the water to be distributed between Bypass and core. The evaporation takes place simultaneously at different stages of the engine.

6.3.4. PREDICTED PERFORMANCE IN RAINSTORM

An attempt is now made to predict the performance of an engine flying in the realistic rainstorm (Paragraph 6.3). All the effects analysed in Chapter V and in Section 6.3.2 above are included in the final prediction. Due to the uncertainties of water centrifuging, it was important to investigate water evaporation at different engine locations. An appropriate distribution of water between the Bypass duct and the engine Core is necessary. Various tests provided a better insight toward finding a suitable combination of locations for water evaporation involving both core and Bypass duct ie the whole engine.

This case predicts the simulated evaporation of 2.3% of the total engine inlet mass flow which represents water. The necessary change of properties would allow that percentage to behave as water. The water quantity was divided between the engine Bypass where 90% of water evaporation takes place at Mixer-Nozzle plane once it mixes with the outcoming hot gases from the LP Turbine, and 10% through the core, see Paragraph 6.3.1. The quantity of water through the core is itself divided between a 1% and 9% evaporation at IP-HP Compressors and HP Compressor-Combustion Chamber planes respectively, see Chapter V. Due to centrifugal reactions of compressor and fan blades on the water, a

three stage IP Drag and a fan Drag were considered. A comparison of steady running lines between clean engine and water evaporation was in order. Firstly the Inner fan was considered, Fig 6.3. By superimposing one graph on the other, it was realised that the steady running line suffered little change. The reason being that even though water was going through this component, water evaporation developments on the simulation program were only taking place at a later stage in the engine. Hence, no drastic changes would occur between both performance predictions. The steady running line dropped by about 3.2% on pressure ratio, both pressure and non-dimensional mass flow decreasing across the Inner Fan component. This causes a drop in both LP and HP shaft speeds. Fig 6.4 show the Outer fan lines for both cases. Here the steady running line for the evaporation case has moved away from the surge line by approximately 10% on pressure ratio. This was largely due to the reduction in specific volume of the bypass flow between the Mixer and the Final Nozzle. The specific volume change was interpreted as a drop in the effective non dimensional mass flow of air through the Final Nozzle, which caused the pressure ratios across the Final Nozzle to drop. The changes in the IP Compressor Component were hardly significant. The steady running lines in Fig 6.5 more or less coincided, though a very negligible move, away from surge, was noticed. The steady running line shifted downwards by approximately 1% on pressure ratio. The reduction in the LP shaft speed being more marked than the reduction in the HP shaft speed, this resulting from the droplet impingement drags in the Fan and IP Compressor components, see Tables 6.1, 6.2 and 6.3. The HP Compressor is sucking in more mass flow than the IP Compressor is able to provide. In order to enforce this explanation an alternative test was undertaken, the steady running performance was simulated for a clean engine with an effective three stage IP Drag and a Fan Drag. These Drags would normally be caused by a 2.3% water ingested and evaporated through the engine. It was noticed that both the LP and HP shaft speeds

dropped, the former more substantially than the latter, resulting in an even more significant reduction in the IP steady running line. The presence of these Drags causes both pressure ratios and non-dimensional mass flows through the IP Compressor to fall. Last but not least the HP Compressor is investigated. As a reminder the mass flow of water ingested is equal to 2.3% of the total air mass flow. This value is by no means the maximum value which can be encountered by an engine. This assumption was based on the fact that the quantity of water is dependent on the flight Mach Number of the airplane and the inertia effects of the rain droplets. It can be assumed that the moisture content is homogeneously distributed throughout the volume swept by the inlet. Using Fig 6.6, it was discovered that the steady running line had definitely shifted upwards towards the surge line, making the engine liable to suffer damaging consequences throughout the defined range of fuel flows. The movement towards surge for the steady running line, was largely caused by water evaporation at plane between HP Compressor and Combustion Chamber, see Chapter V. The steady running performance covered a range of fuel flows which started from a minimum of 0.10 kg/s to a maximum of 0.60 kg/s. The rise towards surge was approximated to 25% at lower fuel flows and as much as 75% at higher fuel flows. The dominant cause of this rise towards surge is due to water evaporation in the combustion chamber, as explained in Paragraph 5.3. It should be repeated here that the magnitude of the movement towards surge will depend on the fraction of the entry rainwater which actually continues into the core. As stated above, in the present work this fraction has been assumed to be 10% (as compared with the air fraction of about 25%). The restoration of the power balance in the HP shaft as well as the volume increase caused by the reduction in flow density between Mixer and Final Nozzle allows for this behaviour of rise towards surge.

As a result, pressure ratios tended to rise and non-dimensional mass flows rose by a negligible amount. It has already been said that because 90% of water was being evaporated at the Mixer-Nozzle plane, more Nozzle area

would be required because of density reduction. This would normally force the LP shaft speed up. Although, the Temperature into the HP Compressor was lowered due to water evaporation, the HP shaft speed drops more which gives a lower non-dimensional speed and a lower pressure ratio. These lower values would cause a drop in the non-dimensional mass flow across the HP Compressor. Less mass flow would get sucked through both the IP and the HP Compressors. Hence, both the LP and HP shaft speeds would fall and this is what effectively was found in the performance prediction outputs. The reasonable increase in pressure ratios through the HP Compressor would automatically push the steady running line nearer the surge line.

The effects of fan and three stage IP compressor drags were minimal on both LP and HP shaft speeds. The reason behind this was that, the prediction program was run for equivalent values of drags but no water ingestion, it was noticed that neither shaft speeds was drastically altered.

Even though the steady running line had not crossed the surge line, it did get dangerously close to it. This reduction in the safety margin is very significant and would put limitations on a real engine to operate over a very sensitive and hazardous area. In the long run that could have serious consequences over the performance and the life of an engine.

CHAPTER VII

CONCLUSION AND SUGGESTIONS FOR FURTHER WORK

7.1. CONCLUSION

The prediction program written by MACCALLUM and described in Ref 27, served as a modelling procedure for the simulation of the performance of a two-spool turbofan aircraft engine. By means of a slight but important modification of the above simulation program, the prediction of the performance of a water laden reference turbofan was made possible.

This developed simulation was tested against experimental results and observations of Rolls-Royce in which water was injected directly into the engine core ie at inlet to the IP Compressor. For best alignment of the predicted changes of the LP and HP shaft speeds and the HP Turbine inlet temperature with the experimental observations, it was concluded that 90% of the water passed through the IP and HP Compressors before evaporating in the Combustors. The remaining 10% of water was likely to evaporate between the IP and HP Compressors. The alignment indicated that Drag due to droplet impingement would be experienced in all three stages of the IP Compressor. However there appeared to be negligible droplet impingement Drag in the HP Compressor.

With these alignments, the simulation predicted no change in the steady-running line for the Fan, a significant lowering of the running line in the IP Compressor (due to droplet Drag) and a significant raising of the running line in the HP Compressor (mainly due to evaporation between the HP Compressor and Combustors). It is noteworthy that in the Rolls-Royce Engine Test, injection of water at a rate of 4% of the core

air flow caused the HP Compressor to surge. 50% of this rate of injection in the simulation led to a predicted reduction of 40% of remaining surge margin.

Having aligned the simulation, it was then used to predict the performance of engine when flying at 6000 metres (20,000 ft), Mach Number 0.8 in extreme rain conditions. These conditions correspond to a water to air mass ratio of 0.023. It was assumed that the water would distribute itself 90% to the bypass flow and 10% to the core flow. With this assumption, the predicted engine effects were -

- (i) Lowering of steady-running line in Fan
- (ii) Lowering of steady-running line in IP Compressor
- (iii) Significant raising of steady-running line in HP Compressor, reducing the remaining surge margin at high speed conditions to 25% of original surge margin.

7.1.1. Comment on above Conclusions :

In the above prediction for the rainstorm case, a distribution had to be assumed to be 90% to Bypass and 10% to core.

In view of the presence of rotating blades and the whirl component of velocity of the mixture of water vapour and air, the redistribution of water and vapour due to centrifugal action is an extremely important factor. Centrifugal action would more or less divert water towards the tip region and water vapor towards the hub region. The performance of a compressor stage is affected by the presence of water as well as by the presence of water vapor, although by entirely different mechanisms - the water droplets cause an adverse effect due to impingement Drag, while water vapour changes the properties of the flow.

In a multistage compressor, the changes in the performance parameters of any stage and in the intensity of the various processes depend upon the entry conditions to that stage.

In any case, the equilibrium running line of the engine and the available surge margin may be affected due to the following changes in the engine components:

1) Changes at inlet to the compressor in :

- (a) Mass flow, (b) Temperature,
- (c) Pressure, (d) Uniformity of flow conditions.

2) Changes at the compressor exit in :

- (a) Mass flow, (b) Temperature,
- (c) Pressure, (d) Variation of flow properties spanwise and circumferentially.

The overall performance parameters are adversely affected by the ingestion of water both by a reduction in the gas phase mass flow and also in the work input absorbed by the mixture. The effects of water ingestion are more severe at higher non-dimensional speeds and larger water mass flows.

7.2. RECOMMENDATIONS

The development of measurement techniques is of the greatest urgency in droplet-laden flows. Heat exchange between the working fluid and the components was not accounted for, due to the lack of incorporation of such complicated models describing heat transfer effects in water ingested gas turbine engines. At entry to the engine, more care and study should be given to the distribution of water/water vapor between the engine core and the Bypass duct. That could have major consequences on the HP Compressor and the engine performance during rainstorms. This could be an interesting topic to investigate.

An analysis of the following processes would therefore prove useful to investigate:

- 1) Aerodynamic performance changes with two phase flows, including effects of fluid composition and blade-flow interactions.
- 2) Centrifugal action on droplets and water vapor.
- 3) Interphase heat and mass transfer processes.
- 4) Droplet-size adjustment.
- 5) Droplet impact and rebound from the blades.
- 6) Film formation on the blades.
- 7) Reingestion of water into the wakes.

Further,

- 8) The analysis of the phenomenology of compressor processes with water ingestion in three possible regimes:
 - i) Prior to setting in of boiling of water.
 - ii) Following the commencement of boiling of water.
 - iii) Completion of phase change of liquid to vapor everywhere.
- 9) A compressor, whatever the working fluid or the number of stages, suffers two critical conditions at each speed of operation, namely:
 - i) Surging and,
 - ii) Choking.

Detailed experimental and analytical studies are required to understand and to quantify the physical processes underlying the phenomena occurring under the conditions of water ingestion.

REFERENCES

- 1) MURTHY, S.N.B, et al
"Water ingestion into axial flow compressors." August 1976.
- 2) USELLER, J.W., LEWIS, W. AND ZETTLE, E.V.
"Effect of heavy rainfall on turbojet aircraft operation."
Lewis flight propulsion laboratory, NACA, 1955.
- 3) TSUCHIYA, T.AND MURTHY, S.N.B.
"Effect of water ingestion into axial flow compressors."
Technical report AFWAL-TR-80-2090, Air force systems command,
Wright-Patterson Air force base.
Part I : Analysis and Predictions, Oct 1980
Part II : Computer Program, Dec 1980
Part III : Experimental Results and Discussion, July 1980.
- 4) MURTHY, S.N.B, EHRESMAN, C.M, AND HAYKIN, T.
"Direct and system effects of water ingestion into jet engine
compressors."
AIAA/ ASME paper, Internal symposium of turbomachinery
performance deterioration, 1986.
- 5) HAYKIN, T.
"Jet engine simulation with water ingestion in compressors."
M.S.M.E Thesis, Purdue University, West Lafayette, May 1986.
- 6) RUSSELL, R.E. AND VICTOR, I.W.,
"Evaluation and correction of the adverse effects of
i) Inlet turbulence and
ii) Rain ingestion on high bypass engines."
AIAA Paper 84-1984, 1984.

7) ROLLS-ROYCE, plc.

"Performance tests on water ingestion in Tay MK-650 engine "

Unpublished work, July 1989.

8) ROLLS-ROYCE, plc.

"Aligned performance of Tay MK-650 engine "

Unpublished performance output, 1990.

9) MACCALLUM, N.R.L.

" Lecture notes Dimensional analysis."

University of Glasgow, 1989.

10) BENNET, H.W.

" Aero engine development for the future."

Proc Inst Mech Engrs Vol 197A, IMechE 1983.

11) FAWKE, A.J. AND SARAVANAMUTTOO, H.I.H.

"Digital computer methods for prediction of gas turbine dynamic response."

SAE Paper 710550, 1971.

12) MACCALLUM, N.R.L

"Comparison of CMF and ICV methods for predicting gas turbine transient response."

Glasgow University, Department of Mechanical Engineering. August 1989.

13) MACCALLUM, N.R.L. and QI, O.F.

"The transient behaviour of aircraft gas turbines."

University of Glasgow, 15 September 1989

I.Mech.E.Seminar London, November 1989.

14) PILIDIS,P. and MACCALLUM, N.R.L.

"The effects of heat transfer on gas turbine transients."

A.S.M.E. Paper 86-GT-275, 1986.

15) FAWKE, A.J.

"Digital computer simulation of gas turbine behaviour."

Phd Thesis, bristol university, 1970.

16) PILIDIS, P.and MACCALLUM, N.R.L.

"A study of the prediction of tip and seal clearances and their effects on gas turbine transients."

A.S.M.E. Paper 84-GT-245, 1984.

17) MACCALLUM, N.R.L.

"Axial compressor characteristics during transients."

AGARD Conf Proc No 324, Paper 22, 1982.

18) LARJOLA, J.

"Simulation of surge margin changes due to heat transfer effects in gas turbine transients."

A.S.M.E. Paper 84-GT-129, 1984.

19) MACCALLUM, N.R.L. and CHIA, B.H.

"Thermal modelling of an aero-gas turbine combustor."

Glasgow University, Department of Mechanical Engineering Report.
August 1989.

20) MACCALLUM, N.R.L.

"Effect of bulk heat transfer in aircraft gas turbines on compressor surge margins."

Heat and fluid flow in steam and Gas turbine plant,
I.Mech.Engrs; London, 1974, 94-100.

21) MACCALLUM, N.R.L. and GRANT, A.D.

"The effect of boundary layer changes due to transient heat transfer on the performance of an axial-flow air compressor."

S.A.E. Trans, March 4, 1977, 86, 770284.

22) GRANT, A.D.

"The effect of heat transfer on boundary layer stability in axial flow compressors." IBID, 252-258.

23) MACCALLUM, N.R.L.

"Thermal influences in gas turbine transients - effects of changes in compressor characteristics." A.S.M.E. Paper 79-GT-143, 1979.

24) MACCALLUM, N.R.L. and PILIDIS, P.

"The prediction of surge margins during gas turbine transients."

A.S.M.E. Paper 85-GT-208, 1985.

25) PILIDIS, P.

"Digital simulation of gas turbine performance."

PhD Thesis, 1983, Glasgow University.

26) LAKSHMINARAYANA, B.

"Methods of predicting the tip clearance effect in axial flow turbomachines." J. Basic Engng, 1970, 92, 467-480.

27).SARAVANAMUTTO, H.I.H, FAWKE, A.J. and HOLMES, M.

"Experimental verification of a digital computer simulation method for predicting gas turbine dynamic behaviour."

I.Mech.Engrs. Proceedings 1972, Vol 186 27/72.

APPENDIX A

ENGINE EFFICIENCY

1. GAS TURBINE PROPULSION

By exhausting gas at high velocity from the nozzle, the engine provides an unbalanced force giving an increase in momentum to the air flowing past the aircraft, the gas turbine engine works ideally to the Joule or Brayton cycle, involving compression and expansion at constant entropy (isentropic) and heat addition and rejection at constant pressure. Based on a Brayton cycle the thrust is produced by partial expansion of the high temperature, high pressure combustion gases in the turbine, which in turn are expanded in a nozzle to give high velocity gases. Assuming isentropic expansion in the nozzle an observer sits on the engine, relative to this observer the air enters the intake to the engine with a velocity V_i equal and opposite to the speed of the aircraft and leaves the engine with the jet relative velocity V_j . Assuming that the mass flow m is constant, then the net thrust X_n represents the rate of change of momentum which by assuming full expansion is :

$$X_n = (\text{momentum flux of flow at a plane behind the engine}) - (\text{momentum flux of flow in front of engine})$$

$$X_n = mV_j - mV_i$$

$$X_n = m * (V_j - V_i) \quad (1)$$

mV_j is called the Gross Momentum thrust.

mV_i is called the intake momentum drag.

The way to impart this increase in momentum is by using a 'heat engine'. As stated earlier gas turbine cycles are based on an approximation to the

Brayton cycle, working gas is compressed from point 1` to point 2`. Then heat is added at a constant pressure from point 2` to point 3`. Then expanded from point 3` to point 4` ideally returning to the initial pressure. Finally the gas is cooled at constant pressure to the initial temperature point 5`.

Due to inefficiencies in the various components of the engine the actual cycle departs from the ideal Brayton cycle. At inlet to the compressor the pressure and temperature do not equal the corresponding atmospheric values due to the ram compression at intake of the engine, when the aircraft is not stationary. Then the fluid is compressed from 1a to 2 or from 1 to 2, depending whether the aircraft was moving or stationary. 1 is a point of lower pressure due to intake losses. Heat is then added on from 2 to 3, accounting for a loss in pressure due to friction and losses associated with the combustion process. that causes the turbine inlet pressure to be slightly lower from ideal compressor delivery pressure point 3`. Gases are then expanded to point 4. The required work to drive the compressor is represented by the expansion from 3 to C which takes place in the turbine. Expansion then continues from C to 5 in the nozzle, which produces the useful work output. From the former analysis it can be understood that, in the ideal cycle turbine and compressor work are the same, whereas in the real cycle the turbine has to produce a larger work to account for inefficiencies and losses, see Figure of Brayton cycle. The useful work is is in the form of an increase in kinetic energy of the working medium. Increase in kinetic energy per unit time is equal to :

$$\frac{mV_j^2}{2} - \frac{mV_i^2}{2} \quad (2)$$

Thrust power is the product of the net thrust and the aircraft speed.

$$\text{Thrust power} = mV_i (V_j - V_i)$$

The propulsive efficiency is given as :

$$\frac{\text{THRUST POWER}}{\text{RATE OF SUPPLY OF MECHANICAL ENERGY TO PROPULSIVE SYSTEM}}$$

$$\eta_p = \frac{mV_i * (V_j - V_i)}{m \left\{ (V_j - V_i) + \frac{(V_j - V_i)^2}{2} \right\}}$$

$$\eta_p = \frac{2}{(1 + (V_j / V_i))} \quad (3)$$

Thermal efficiency is the efficiency of energy conversion within the plant, and is given as:

Thermal Efficiency = Rate of useful work output / Rate of consumption of thermal energy.

$$\eta_t = \frac{\left(\frac{mV_j^2}{2} - \frac{mV_i^2}{2} \right)}{f * CV} \quad (4)$$

or ;

$$\eta_t = 1 - \left(\frac{1}{R^{\gamma / \gamma - 1}} \right) \quad (4a)$$

Where R represents the overall pressure ratio of the engine thermodynamic cycle. f is the fuel flow rate, and (C.V.) is the calorific value of the fuel.

The overall efficiency is the ratio of thrust power to the rate of consumption of thermal energy:

$$\eta_o = mV_i * (V_j - V_i) / f * CV \quad (5)$$

from equation (3),(4) and (5) it is clear that:

$$\eta_o = \eta_t * \eta_p \quad (6)$$

This analysis has been done in order to clarify that to achieve a high

overall efficiency it is in order to maximize both the Thermal Efficiency and the Propulsive Efficiency. The first is maximized by increasing the pressure ratio while the other is maximized by decreasing the jet velocity, that can be seen from equations (4a) and (3).

APPENDIX B

ENGINE SIMULATION

1. INLET CALCULATIONS

Since the initial conditions parameters of Flight Mach and Ambient pressure are known, the inlet stagnation temperature and pressure can be evaluated as follows :

$$T = T_{AMB} * (1 + 0.2M^2)$$

$$P = \text{Recovery Factor} * P_{AMB} * \left(\frac{T_1}{T_{AMB}}\right)^{3.5}$$

The recovery factor for pressure is equal to 0.995 in order to account for non-isentropic diffusion losses.

2. OUTER FAN

Known parameters

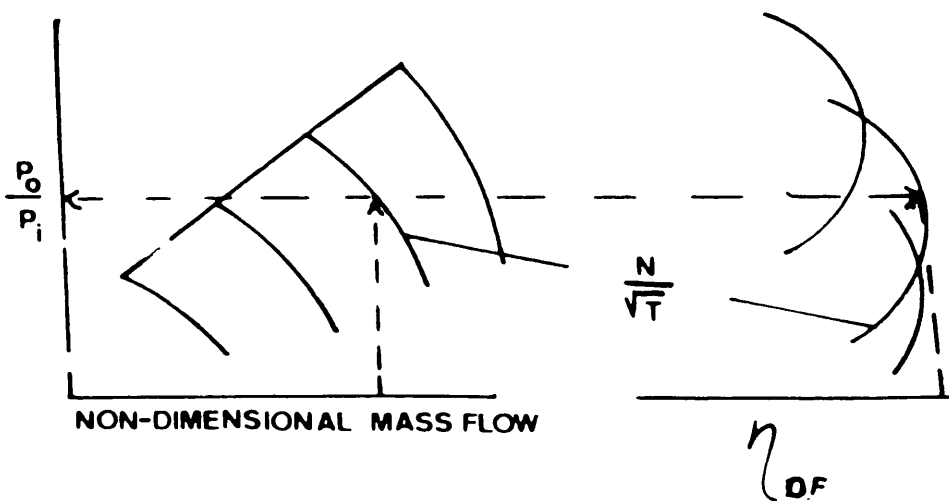
Pi, Ti, FCSP and GEOM

Gussed parameters

Po

Wanted parameters

\dot{m} and To



In order to calculate \dot{m} (capacity) the following steps are taken:

A) Calculate pressure ratio and non-dimensional speed

B) Linear interpolation in characteristics tables determines the value for the capacity

C) The actual capacity is defined by the equation below:

$$\left(\frac{\dot{m} \sqrt{T_1}}{P_1}\right)_{ACT} = \left(\frac{1 - GEOM * FCSP}{1 - GEOM}\right) * \left(\frac{\dot{m} \sqrt{T_1}}{P_1}\right)_{CHICS}$$

D) A final value for m is found.

Temperature at exit is found as follows.

A) Initial Cp is equal to 1.00

B) Gamma is found from

$$\gamma = \frac{C_p}{C_p - R}$$

C) The isentropic exit temperature T_o is determined from

$$T_o - T_1 = T_1 * \left\{ \left(\frac{P_o}{P_1}\right)^{\frac{\gamma-1}{\gamma}} - 1 \right\}$$

D) Linear interpolation in characteristics tables gives the overall efficiency

E) T_o is calculated from

$$\eta_{OVERALL} = \frac{T_o - T_1}{T_o - T_1}$$

F) A more accurate value for Cp is determined from

$$C_p = 0.944 + 0.00019 * \left(\frac{T_o - T_1}{T_o - T_1}\right)$$

G) This follows a do loop process until actual value of T_o is found.

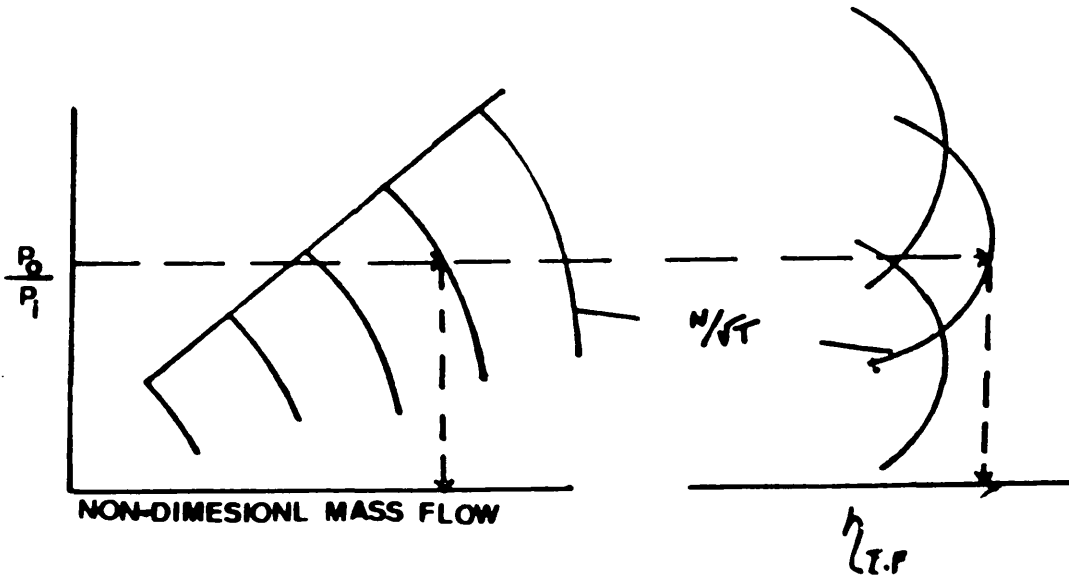
3. INNER FAN

Known parameters are

$P_i, T_i, N, FCSP$ and GEOM

Wanted parameters are

\dot{m}, T_o, P_o



In order to calculate \dot{m} (capacity) the following steps are taken:

A) The inner fan mass flow rate is calculated by means of outer fan mass flow rate, FCSP and GEOM.

$$\dot{m}_{INF} = \dot{m}_{OUF} * \left(\frac{FCSP * GEOM}{1 - FCSP * GEOM} \right)$$

B) Calculate actual capacity

C) Equivalent characteristics capacity is calculated by using FCSP in the equation below

$$\left(\frac{\dot{m} \sqrt{T_i}}{P_i} \right)_{CHICS} = \frac{1}{FCSP} * \left(\frac{\dot{m} \sqrt{T_i}}{P_i} \right)_{ACT}$$

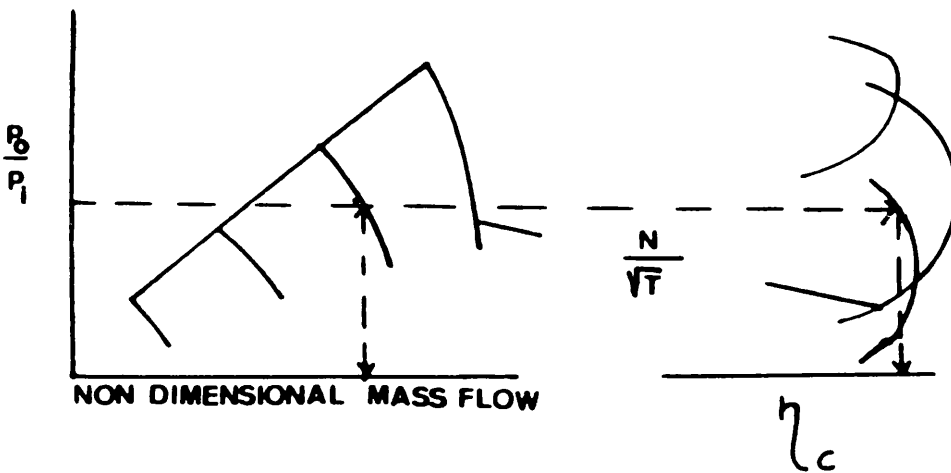
D) Linear interpolation in characteristics allows the calculation of the pressure ratio

E) Finally, P_o is found.

Temperature at exit is found in exactly the same method as for the Inner fan.

4. IP AND HP COMPRESSOR SIMULATION

Known parameters	P_i, T_i and N
Guessed parameters	P_o
Wanted parameters	\dot{m}, T_o



In order to calculate \dot{m} (capacity) the following steps are taken:

- A) Pressure ratio and non-dimensional speed are calculated
- B) Mass flow defined by use of linear interpolation on characteristics tables
- C) Finally, the mass flow actual is found

Temperature at exit is found as follows.

- A) Initially $C_p=1.00$
- B) Gamma is found by using

$$\gamma = \frac{C_p}{C_p - R}$$

C) The isentropic exit temperature, T_o^* is found from

$$T_o^* - T_i = \eta_{IPC} * T_i * \left\{ \left(\frac{P_o}{P_i} \right)^{\frac{\gamma-1}{\gamma}} - 1 \right\}$$

D) The isentropic efficiency is defined by linear interpolation in characteristics tables

E) T_o^* is found from

$$\eta_c = \frac{T_o - T_i}{T_o^* - T_i}$$

F) Calculate a better value for C_p from

$$C_p = 0.944 + 0.00019 * \left(\frac{T_o + T_i}{2} \right)$$

G) This follows a do loop process until actual value of T_o is found.

5. TURBINE SIMULATION

Known parameters

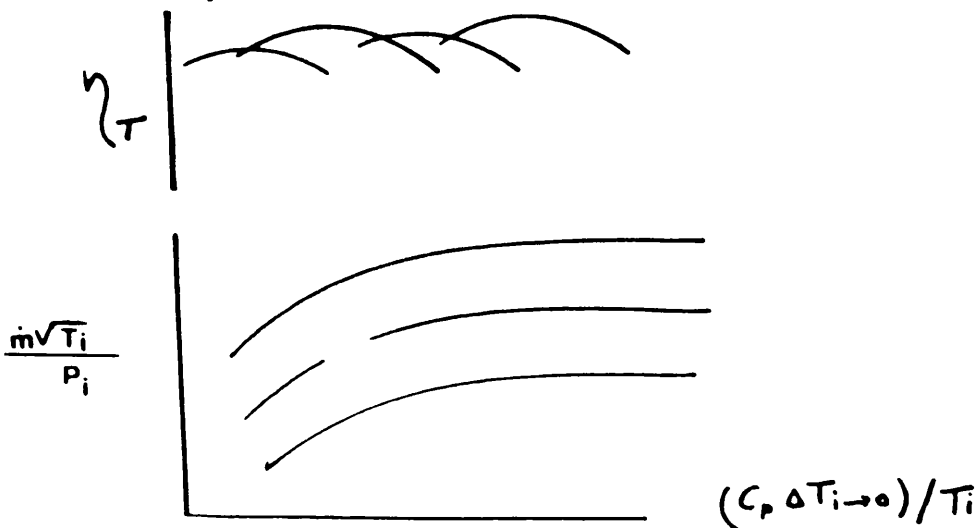
P_i, T_i and N

Guessed parameters

P_o , Turbine Efficiency

Wanted parameters

\dot{m} , T_o



A) C_p and \dot{m} from the outlet conditions of the previous component are considered

B) Gamma is calculated as before

C) The isentropic exit temperature is calculated from

$$T_i - T_o = T_i * \left\{ 1 - \left(\frac{P_o}{P_i} \right)^{\frac{\gamma-1}{\gamma}} \right\}$$

D) A value for T_o is determined from

$$T_i - T_o = \eta_{TUR} * (T_i - T_o')$$

E) Work factor is found,

$$\left(\frac{C_p \Delta T_{i-o}}{T_i} \right)$$

F) Linear interpolation in characteristics table gives a better value for turbine efficiency

G) A better value of C_p is determined from

$$C_p = 0.944 + 0.00019 * \left(\frac{T_o + T_i}{2} \right)$$

This C_p would be modified for fuel/air ratio of products

H) The above process follows a do loop for a better value of C_p , then linear interpolation in characteristics tables is used to define a value for \dot{m}

I) Estimated and calculated mass flows are compared

J) Estimated mass flow is revised

K) The above process is repeated until both values reasonably agree

L) Given a correct mass flow would enable the calculation of actual T_o , which is calculated in the final estimation.

6. BY-PASS DUCT AND MIXER SIMULATION

Both by-pass duct and nozzle represent intercomponent volumes. Therefore the mismatch of mass flow rate entering and leaving the two

volumes should be determined. The mass flow rate entering the by-pass duct is equal to the mass flow leaving the outer fan. The mass flow entering the nozzle is equal to the mass flow leaving the LP turbine. The mass flow rate is defined by using the following gas dynamics equation

$$\dot{m} = \frac{P * A}{\sqrt{T}} * \left[\frac{2\gamma}{(\gamma - 1) * R} \left(\frac{P_s}{P} \right)^{\frac{\gamma-1}{\gamma}} \right]$$

The areas used above represent the core gas and by-pass air flow areas at the mixer chutes. The exit temperature and mass flow are corrected in the case of the by-pass duct due to the bleeds flows from the engine core. The core gas duct assumes an isentropic flow, however the by-pass duct suffers pressure losses which are corrected by means of a pressure loss factor.

7. FINAL NOZZLE CALCULATION

Both core gas and by-pass air are assumed isentropic, however even if treated separately in an identical manner to one another these two flows do not mix.

Initially, it is determined whether the flow is choked or not by using the basic gas dynamics equation:

$$\frac{P}{P_s} = \left(1 + \frac{\gamma - 1}{2} M^2 \right)^{\frac{\gamma-1}{\gamma}}$$

If choked, Mach number is made equal to 1, hence

$$\frac{P}{P_s} = \left(\frac{1 + \gamma}{2} \right)^{\frac{\gamma}{\gamma-1}}$$

The flow is choked when :

$$\frac{P}{P_{atm}} > 0r = \left(\frac{1 + \gamma}{2} \right)^{\frac{\gamma}{\gamma-1}}$$

The mass flow rates entering the volume defined from the mixer to the throat of the final nozzle are equal to the flows leaving the mixer which represents a mixture of core gases and by-pass air. The exit areas are determined by using the gas dynamic equation below:

$$\frac{\dot{m} \sqrt{T}}{P \dot{A}} = M \sqrt{\frac{\gamma}{R}} \left(1 + \frac{\gamma - 1}{2} M^2\right)^{\frac{\gamma + 1}{2(1 - \gamma)}}$$

If flow is choked, the equation reduces to

$$\frac{\dot{m} \sqrt{T}}{P \dot{A}} = \sqrt{\frac{\gamma}{R}} \left(\frac{1 + \gamma}{2}\right)^{\frac{\gamma + 1}{2(1 - \gamma)}}$$

The total exit area is equal to the sum of the two calculated areas, this final area is then adjusted by means of a coefficient of discharge. It is only when steady state running is completed that the required area would equal the actual nozzle exit area.

The ration of required to actual exit areas, in addition to the mass flow rates entering the final nozzle help calculate the actual mass flow rates at exit from the final nozzle.

8. FRACTION OF SPLIT

The factor of split differs from steady running state to transient state. For the former, it is initially assumed to be unity, and then evaluated at each time interval. For the latter case, a guessed value is considered, that guess is estimated by performing a steady state run at the same starting fuel flow of the transient state. Once the value is stabilised, it could be used as the guessed value for the transient.

FCSP is calculated using the following equation :

$$FCSP_{NEW} = FCSP * A$$

$$A = \left\{ 1 + 0.1 * \left(\frac{\dot{m} \text{ AT EXIT FROM VOL24} - \dot{m} \text{ AT ENTRY INTO VOL24}}{\dot{m} \text{ THROUGH INNER FAN}} \right) \right\}$$

APPENDIX C

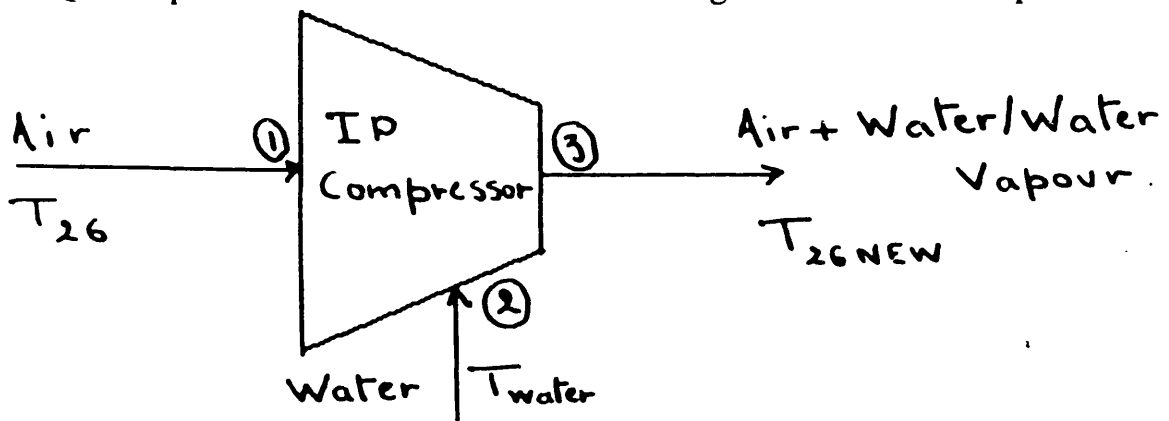
WATER THERMODYNAMICS CALCULATION

1. AT ENTRY TO THE HP COMPRESSOR

The temperature at entry to the compressor T_{26} should always be a function of the mixture of air mass flow rate and water flow rate. Therefore the initial mass entering the above component would be equal to

$$AIMS_{26} = AIMS_{26} + AWQTN$$

AWQTN represents the mass of water to be ingested into the compressor.



From the above representation, the equation for conservation of energy would be equal to:

$$H_1 + H_2 = H_3$$

$$H_1 = \dot{m}_a * C_{p_{air}} * T_{26}$$

$$H_2 = \dot{m}_w * C_{p_w} * T_w$$

$$H_3 = \dot{m}_a * C_{p_a} * T_{26} + \dot{m}_w * H_{SS \text{ AT } T_{26}}$$

$$C_{p_a} = 0.944 + 0.00019 * T_{26}$$

Under set conditions and for a specific value of $T_{26} = 390.780 \text{ K}$, C_{p_a} was found to equal 1.0182 (kJ/kg.k) . H_w is equal to $(C_{p_w} * T_w)$, which from steam tables was found to equal 62.9 kJ/kg.k . By using the

assumption of ($T_{26} = T_{26} - A * 10$ Celsius), where A represents a multiplying factor, the value for H_{SS} is calculated for each and every value of T_{26} . The factor (A) is taken between an interval of 1 to 6. The former assumption was considered due to the reduction which water would cause on temperature of dry air entering the HP Compressor. It was considered reasonable to start from a small reduction of ten degrees celsius and then increase this factor until an enthalpy balance between the mixture of flows going in and the ones going out is reached.

T_{26} (Celsius)	H_{SS} (kj/kg.k)
107.63	2702.65
97.63	2683.54
87.63	2664.74
77.63	2645.94
67.63	2627.14
57.63	2608.34

By using the above information, both sides of the conservation of energy equation are quantified, and the outcome compared until a satisfactory result is reached. The case where A is equal to 5 seem to give a very reasonable match, hence using case 5 an interpolation is completed for T_{26} and gave $T_{26} = 67.8256$ Celsius (340.8 Kelvin). From the former it could be stated that if T_{26} is greater or equal to 50.Celsius, evaporation would take place.

One way to predict a reasonable assumption is to proceed as follows:

From steam tables and simulation output examples, it is known that

$$P_{SAT VAP} = 28.0 \text{ kn} / \text{m}^2$$

$$P_{TOTAL AT 26} = 240.27 \text{ kn} / \text{m}^2$$

$$\dot{m}_s = 50.56 \text{ kg} / \text{sec}, \dot{m}_v = 1.008 \text{ kg} / \text{sec}$$

$$SPECIFIC VOLUME OF AIR = R * T / P,$$

$$VOLUME\ OCCUPIED\ BY\ AIR = \dot{m}_a * R_a * T / (P_{total} - P_{vap})$$

$$VOLUME\ OCCUPIED\ BY\ WATER = \dot{m}_w * R_w * T / (P_{vap})$$

Both volumes should be equal to one another;

$$\dot{m}_a * R_a * T / (P_{total} - P_{vap}) = \dot{m}_w * R_w * T / (P_{vap})$$

after substituting the above given parameters P_{vap} is found to equal 7.47 kn/m^2 which is less than $P_{saturated}$ at $T = 340\ K$, in other words the above assumptions are permissible as long as T_{26} is greater or equal to 50 Celsius.

From conservation of energy equation, it is known that:

$$H_1 + H_2 = H_3$$

$$\dot{m}_a * C_{p,air} * T_{26} + \dot{m}_w * C_{p,w} * T_w = \dot{m}_a * C_{p,air} * T_{26}' + H_{SS\ AT\ T_{26}'}$$

$$\dot{m}_a * C_{p,air} * T_{26} - \dot{m}_a * C_{p,air} * T_{26}' = \dot{m}_w * C_{p,w} * T_w - m_w * H_{SS\ AT\ T_{26}'}$$

$$\dot{m}_a * C_{p,air} * (T_{26}' - T_{26}) = m_w * (H_w - H_{SS\ AT\ T_{26}'})$$

$$T_{26}' - T_{26} = \left(\frac{\dot{m}_w}{\dot{m}_a * C_{p,air}} \right) * (H_w - H_{SS\ AT\ T_{26}'})$$

this leads to the final equation which is equal to:

$$T_{26}' - T_{26} = \left(\frac{AWQTN}{AIMS_{26} * C_{p,air}} \right) * (62.9 - H_{SS\ AT\ T_{26}'})$$

$$AWQTN = Const$$

$$AIMS_{26} = Const$$

$$C_{p,air} = const = 0.944 + 0.00019 * T_{26}$$

A graph of T_{26} gotten from the steady state output as a function of H_{SS} at T_{26} , calculated from steam tables, shows that both of these parameters are represented by a linear equation of the first order,

$$H_{SS\ AT\ T_{26}} = A + B * T$$

The above graph was constructed by means of water thermodynamics induced engine performances during steady running and at three different fuel flows. Each of the former runs gave a value for T_{26} for which a corresponding value of enthalpy had to be interpolated from steam tables. Finally from the previous calculated values of temperature and enthalpy, a graph was constructed, linear interpolation lead to the relationship below.

$$H_{SS \text{ AT } T_{26}} = A + B * T_{26}$$

$$A = 1974.6$$

$$B = 1.9117$$

In other words, the corresponding enthalpy was found to be:

$$H_{SS} = 1974.6 + 1.9117 * T_{26}$$

From this equation, the reduction of temperature due to water ingestion at entry to HP Compressor can be quantified as follows:

$$T_{26} - T_{26} = \left(\frac{AWQTN}{AIMS\ 26 * C_{p\ air}} \right) * (62.9 - H_{SS \text{ AT } T_{26}})$$

$$T_{26} - T_{26} = \left(\frac{AWQTN}{C_{p\ air} * AIMS\ 26} \right) * (62.9 - 1974.6 - 1.9117 * T_{26})$$

C_{p_a} was found to be equal to 1.0067 KJ/KG.K.

Finally the temperature at entry to the HP Compressor was determined as:

$T_{26} = T_{26ACH}$ (actual value of T_{26})

$$T_{26ACH} = \left\{ \frac{(AIMS\ 26 * T_{26} - (1898.97 * AWQTN))}{(AIMS\ 26 + 1.8989 * AWQTN)} \right\}$$

2. AT ENTRY TO THE COMBUSTION CHAMBER

At entry to the above mentioned component the same equation was used with the corresponding terms for inlet mass flow rate and the quantity of water to be evaporated. The equation in question was defined as follows:

$T^3 = T_{3ACTH}$ (actual value for T^3)

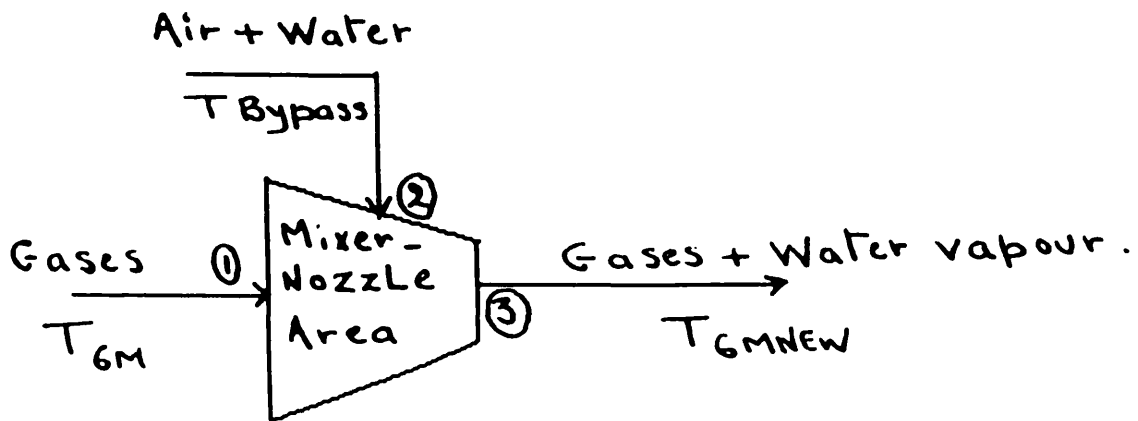
$$T_{3ACTH} = \left\{ \frac{((AIMS\ 3 * T_{3ACTH}) - (1898.97 * QWTICC))}{(AIMS\ 3 + 1.8989 * QWTICC)} \right\}$$

3. AT ENTRY TO MIXER

The principle was used at entry to this component. A quantity of water was ingested through the bypass duct with its effects on mass flow and temperature taking place once it reaches the Mixer.

An equation for energy balance was needed to find the relationship which would link the temperature and the mass flow considered.

$$H_{IN} = H_{OUT}$$



A similar procedure was used to quantify both sides of the equation, the only difference was the notations which included ;

<i>GASMS 7</i>	<i>MASS FLOW THROUGH MIXER</i>
<i>CPGAS 7</i>	<i>SPECIFIC HEAT THROUGH MIXER</i>
T_{6M}	<i>TEMPERATURE BEFORE EVAPORATION</i>
T_{6MNEW}	<i>TEMPERATURE AFTER EVAPORATION</i>
<i>QWIBP</i>	<i>QUANTITY OF WATER IN BYPASS</i>

A graph of enthalpy of superheated steam against different values of temperatures (T_{6M}), enabled the linearisation of H_{SS} against T_{6m} . Three values were obtained from steady running performances of the engine under the effect of water through and from the bypass and into the mixer. The final equation was found to equal:

$$H_{SS} = 1896.30 + 2.006 * T_{6MNEW}$$

After following the same steps as the ones for the HP Compressor a general formula was found, this formula related the new mixing temperature to the new mass flow of mixtures through the Mixer and into the Nozzle.

$$T_{6MNEW} = \left\{ \frac{((GASMS\ 7 * T_{6M}) - (2087.377 * QWTIBP))}{(GASMS\ 7 + 1.7946 * QWTIBP)} \right\}$$

IP, HP AND FAN DRAG FACTORS

Due to the centrifuging reaction of the blades due to the ingestion of water in order to deviate most of it away from the core and into the bypass and engine casings, some kind of resistance would be present. This resistance is referred to as drag. The drags in question are mainly a function of the water quantity ingested as well as the number of stages taken into account. The HP, IP and Fan Drags are generalised as follows :

Torque = mass flow rate * (blade mean radius)² * rotational speed

$$TORQUE = \dot{m} * r^2 * \omega$$

Power absorbed = mass flow rate * (blade mean radius)² * (rotational speed)²

$$POWER\ ABSORBED = \dot{m} * r^2 * \omega^2$$

DRCIP = drag produced in IP shaft

$$DWQTNI = 0.252 * ZNIPS * DRGCOF$$

0.252 kg/sec = minimum quantity of water to be ingested

ZNIPS = number of IP stages

DRGCOF = coefficient of drag

$$DRCIP = DWQTNI * SHSPL * r_{ip}^2 * (2 * \pi / 60)$$

$$POWER\ ABSORBED\ IN\ IP\ SHAFT = DWQTNI * SHSPL * 1.55671 * 0.000001$$

DRCHP = drag produced in HP shaft

$$DWQTNH = 0.252 * ZNHPS * DRGCOF$$

0.252 = minimum quantity of water to be ingested

ZNHPS = number of HP stages

DRGCOF = coefficient of drag

$$DRCHP = DWQTNH * SHSPH * r_{hp}^2 * (2 * \pi / 60)$$

$$POWER\ ABSORBED = DWQTNH * SHSPH * 1.03325 * 0.000001$$

IN HP SHAFT

The radiee for both IP and HP blades were taken from a configuration of the TAY MK-650 Engine and were equal to :

$$r_{ip} = 0.2827\text{ m}$$

$$r_{hp} = 0.2466\text{ m}$$

The two equations above would have a direct effect on the acceleration power, the acceleration torque and the new shaft speed after the engine had stabilised. These effects would be based on the same amount of water

$$r_{ip} = 0.2827 \text{ m}$$

$$r_{hp} = 0.2466 \text{ m}$$

The two equations above would have a direct effect on the acceleration power, the acceleration torque and the new shaft speed after the engine had stabilised. These effects would be based on the same amount of water to be vaporised, in other words the drag coefficient would act as a multiplying factor on the minimum amount of water which is 0.252, to give the accurate value corresponding to water ingested, either at entry to HP Compressor or Combustion Chamber. For example if AWQTN was equal to 1.008 kg/s, then DRGCOF would be equal to 4 as (4×0.252) would equal 1.008 kg/s. The effects would have a relative impact on the engine's shaft speeds since they would be based on the same quantity of water ingested.

The Fan drag was only applied for extreme weather conditions when flying at an altitude of 20,000 ft. This means that the whole frontal area of the engine would be subjected to water ingestion. Instead of the constant water quantity applied in core water evaporation, a percentage equal to 2.3% of the total flow into the engine was made to behave as water. Drags considered, unlike the two previous situations, would be a function of that percentage and the corresponding number of stages.

$$DWQTFN = 0.023 * (AIMS1F + AIMS1E) * ZNFNS * DRGCOF$$

AIMS1F = Mass flow through Outer Fan

AIMS1E = Mass flow through Inner Fan

$(AIMS1F + AIMS1E)$ = Total mass flow into the engine

ZNFNS = Number of stages

DRGCOF = Drag coefficient.

APPENDIX D

GAS CONSTANTS AND SPECIFIC HEATS CALCULATION

INTRODUCTION

In the case of a clean engine, both values for C_p and R are considered to have Air properties throughout the whole engine. These two values are defined as follows in the simulation program:

$$C_p = 0.944 + 0.00019 * T \text{ kj/kg.k}$$

T is the mean value of the actual temperature for the next component in addition to the actual temperature of the component in question.

$$R = 0.2871 \text{ kj/kg.k}$$

However in the case of mixed flows, both of the above values change due to the different properties of both flows.

The general equation defining C_p for any substance is defined as follows:

$$C_p = R_u * (A + B * T + C * T^2 + D * T^3 + E * T^4)$$

$$R_u \text{ (Molar Universal gas constant)} = 8.3144 \text{ kj/kmol.k}$$

The temperature in this case, would be represented by the values included in the interval (400 to 1400 Kelvin). Coefficients A, B, C, D, E for both air and steam are defined in a table, as well as the Molecular weight, Gas constant and Specific heat ratio. In order to find C_p for steam, a straight forward application follows; since all the coefficients are given , all that was needed was to substitute them into the general equation and get a C_p in terms of temperatures. The same was applied to C_p for air. A range of

temperatures was chosen, and for every temperature, a value for C_p was found. Finally a general equation for C_p steam was found, C_p air was already given. Both these equations were set under the condition that they both followed a similar and linear curve in the previously given range of temperatures. The final equations were given as follows :

$$C_{P \text{ AIR}} = 0.944 + 0.00019 * T \text{ kj/kg.k}$$

$$C_{P \text{ STEAM}} = 1.6179 + 0.00066 * T \text{ kj/kg.k}$$

The above was completed in order to avoid using a forth order equation in the simulation program which might lead to erroneous results when determining C_p values.

For a mixture of flows both values for C_p and R have to be found, and these were determined using the equations below:

$$C_{P \text{ MIXTURE}} = (1 - X) * C_{P \text{ AIR}} + X * C_{P \text{ STEAM}}$$

$$R_{\text{MIXTURE}} = R_U * \left\{ \left(\frac{1 - X}{\text{MOLECULAR WEIGHT FOR AIR}} \right) + \left(\frac{X}{\text{MOLECULAR WEIGHT FOR STEAM}} \right) \right\}$$

X = mass of water evaporated (steam) / (mass of air + mass of steam),

or

X = mass of steam / total inlet mass

In each component, changes had to take place in order to allow for both clean engine running state and water evaporation. Since evaporation was only introduced at front of either HP compressor, Combustion chamber, or through the bypass leading to the Mixing Chamber, Inner fan and Outer fan were unchanged as far as C_p and R were concerned because only air properties were being used.

HP COMPRESSOR

In this component, allowances for both air and mixture properties were catered for. By taking conditions of one or the other, engine simulation was able to take place in a satisfactory manner. These two conditions were defined as follows;

If water is present then calculate mass fraction,

$$X = \frac{AWQTN}{AWQTN + AIMS\ 26}$$

calculate new gas constant R mixture

calculate new non-dimensional HP speed

$$ZNDHPC = \frac{SHSPH}{\sqrt{T_{26ACH}}} * \sqrt{\frac{R_{AIR}}{R_{MIXTURE}}}$$

calculate mean temperature T

calculate Cp air, Cp steam, and final Cp mixture

A do loop is followed in order to give a better value for Cp mixture

Else if clean engine then:

AWQTN = 0.00 ,hence X = 0.00

R goes back to 0.2871 air properties, which is equal to R air

$$ZNDHPC = \left(\frac{SHSPH}{\sqrt{T_{26ACH}}} \right)$$

$$C_{P\ AIR} = 0.944 + 0.00019 * T \text{ kj/kg.k}$$

In the case when there is water evaporation, changes should also take place downstream from the HP Compressor, in other words HP turbine, LP turbine, Mixer and nozzle. The conditions in these components are defined below:

COMBUSTION CHAMBER

This component follows similar calculations to allow for both conditions

Mean temperature is calculated

If water is present then:

calculate mass fraction

$$Y = \frac{QWTICC}{QWTICC + AIMS\ 32}$$

calculate R mixture

calculate fuel to air ratio FARCC

$$A = \frac{FARCC}{(98.0 + (FARCC + 1.0))}$$
$$B = \frac{92.51}{FARCC + 255.83}$$
$$C = \frac{0.01862}{FARCC + 0.05228}$$
$$C_{P\ AIR} = A * (B + C * T)$$
$$C_{P\ STEAM} = 1.617996 + 0.00066 * T$$

first calculation for Cp mixture follows:

$$C_{P\ MIXTURE} = (1 - Y) * C_{P\ AIR} + Y * C_{P\ STEAM}$$

Mass flow is calculated in the same manner as the non-dimensional speed, in other words multiplied by a factor of (Rair / R mixture)

Else if clean engine then

$$QWTICC = 0.00, Y = 0.00$$

$$Cp\ mixture = Cp\ air$$

Similarly to the previous component for water evaporation, changes should also take place downstream from the combustion chamber, in

other words HP turbine, LP turbine Mixer and nozzle. The conditions in these components are defined as follows:

HP TURBINE

If water is present in HP Compressor or Combustion chamber then mass fraction is

$$WVHPT = \frac{CWTH}{CWTH + GASMS 4}$$

calculate new R mixture

evaluate new non-dimensional HP turbine speed:

$$ZNDHPT = \left(\frac{SHSPH}{\sqrt{T_4}} \right) * \sqrt{\frac{R_{AIR}}{R_{MIXTURE}}}$$

calculate mean value for

$$T = \frac{T_{4ACTH} + T_{5INIT}}{2.0}$$

calculate fuel to air ratio in HP turbine:

$$FARTH = \frac{FUEL}{GASMS 4 - FUEL}$$

$$CPTAIR = 0.944 + 0.00019 * T$$

$$CPTRFF = 0.9702 + 0.0001954 * T$$

calculate Cp steam

calculate Cp mixture as follows:

$$Cp_{air} = CPTAIR + (FARTH/0/0160) * (CPTRFF - CPTAIR)$$

$$C_{P_{MIXTURE}} = \{(1 - Z) * C_{P_{AIR}} + Z * C_{P_{STEAM}}\}$$

A do loop is followed in order to give a better value for Cp mixture.

Mass flow is calculated in the same manner as the non-dimensional speed, in other words multiplied by a factor of ($R_{air} / R_{mixture}$).

Else if clean engine then: $CWTH = 0.00$, $Z = 0.00$, $Cp_{mixture} = Cp_{air}$

LP TURBINE

The method of calculation in this component was exactly the same as in the HP Turbine component.

MIXER

After following the same procedure as in the above components, Gamma is given a new value whenever evaporation takes place, otherwise it would be equal to Gamma for air.

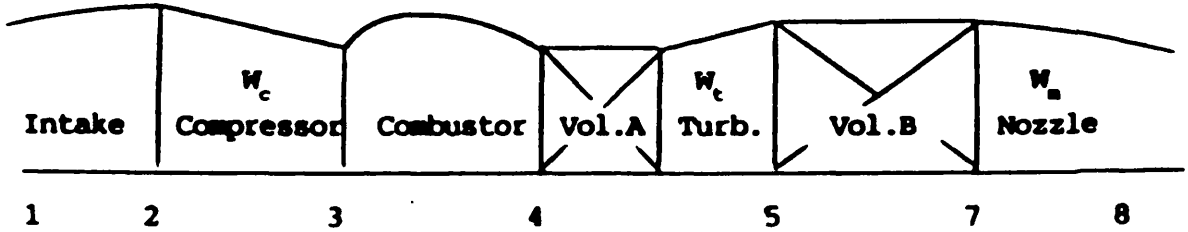
CONCLUSION

To make sure that the above changes took place, output values for the case of clean engine were compared to that of water evaporation.

APPENDIX E

INTERCOMPONENT VOLUME METHOD ICV METHOD

1. SINGLE-SPOOL ENGINE



This case of single-spool engine is illustrated above. Consider two Inter-Component Volumes :

Volume A, which represents half the volume of the compressor plus the volume of the combustion chambers plus half the volume of the turbine.

Volume B, which represents half the volume of the turbine plus the volume of the jet pipe, up to nozzle throat.

1.1. CALCULATION PROCEDURE

1). At the starting instant, N , T_1 , P_1 and fuel flow (from power lever angle position or from schedule of fuel control unit) will be known.

2). Initial values of P_3 and P_5 are selected - from previous experience running program at a range of steady fuel flows. Best results are achieved

if the program is written so that it assesses this previous data set and interpolates for P_3 , P_5 appropriate to the particular P_1 and $N / \sqrt{T_1}$ assuming non-dimensional engine. It is possible to have a short initializing time, e.g. from -0.2 s to 0.0 s, in which speed is held constant but gas pressure is allowed to adjust itself from the initial guesses.

3). Using compressor characteristics, enter with known $N / \sqrt{T_1}$ and expected P_3 / P_2 to get T_3 (using efficiency data) and w'_c .

4). In the Combustion chamber, by using the now known w'_3 and initially known WFE, T_4 could be found. ΔP_{34} could also be found from combustor pressure loss relationships, thus P_4 could be found.

5). In the Turbine, from now known (or forecast) P_4 / P_5 and $N / \sqrt{T_4}$, the mass flow of turbine could be found $w'_4 \sqrt{T_4} / P_4$, hence w'_4 .

6). In the Nozzle, from now known (or forecast) P_5 / P_8 and the nozzle effective area A_8 , T_8 and w'_8 could be obtained.

New masses, temperatures and pressures in Volumes A and B could now be calculated :

$$m_{i+\Delta t} = m_i + (w'_i - w'_j) * \Delta t \quad (\text{mass balance})$$

$$T_{i+\Delta t} = \frac{(w' c_p \Delta T)_i + (m_v - w'_j \Delta t) c_p T_v}{(w' c_p \Delta T)_i + m_v c_p - w'_j \Delta t c_p} \quad (\text{enthalpy balance})$$

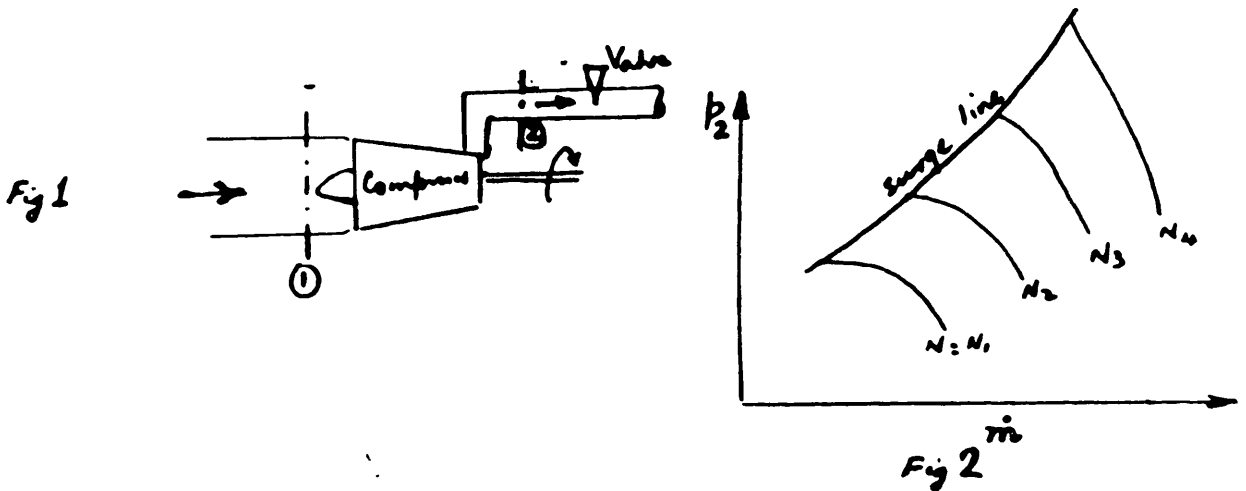
$$P_{i+\Delta t} = \frac{R T_{i+\Delta t} w'_{i+\Delta t}}{V} \quad (\text{characteristics equation})$$

Where i and j are the components before and after the volume in consideration.

APPENDIX F

THE USE OF DIMENSIONAL ANALYSIS IN REPRESENTING THE CHARACTERISTICS OF TURBOMACHINES

If it is assumed that for a test carried out on an air compressor, the inlet conditions were T_1 and P_1 . Results for delivery pressure P_2 would be found from Fig 2.



If inlet conditions in service are different from the values in the test, it would be useless to use the results of the test. However, by applying methods of dimensional analysis, the delivery pressure P_2 would be a function of inlet conditions $(P_1, \rho_1, N, \dot{m}, D)$.

P_1	pressure at inlet conditions
ρ_1	air density at inlet conditions
N	shaft rotational speed
\dot{m}	mass flow rate through the compressor
D	characteristic linear dimension of compressor.

$$P_2 = fn(P_1, \rho_1, N, \dot{m}, D) \quad (1)$$

or

$$P_2 = \epsilon \text{ const } (P_1)^a (\rho_1)^b (N)^c (\dot{m})^d (D)^e \quad (\text{II})$$

now dimensionally :

$$\frac{M}{LT^2} : \left(\frac{M}{LT^2}\right)^a \left(\frac{M}{L^3}\right)^b \left(\frac{1}{T}\right)^c \left(\frac{M}{T}\right)^d (L)^e$$

Equating indices of mass \dot{M} : $+1 = +a + b + d$ (i)

length L : $-1 = -a - 3b + e$ (ii)

time T : $-2 = -2a - c - d$ (iii)

Since \dot{m} and N are the the principle independant variables used in the plotting of the test results in Fig 2, the indices associated with these variables would be selected. There are five unknowns, indices (a, b, c, d and e) and three equations. Three of these indices would be expressed in terms of the two principle variables indices. The two principle variables will appear only once in the right hand side of the final relationship.

From (iii)

$$2a = 2 - c - d$$

Substituting in (i)

$$b = \frac{c}{2} - \frac{d}{2}$$

Substituting in (ii)

$$e = c - 2d$$

So

$$P_2 = \epsilon \text{ Const } (P_1)^{1 - \frac{c}{2} - \frac{d}{2}} (\rho_1)^{\frac{c}{2} - \frac{d}{2}} (N)^c (\dot{m})^d (D)^{c - 2d} \quad (\text{III})$$

But since

$$\rho_1 = \frac{P_1}{RT_1}$$

then

$$P_2 = \epsilon \text{ Const } (P_1)^{1 - \frac{c}{2} - \frac{d}{2}} \left(\frac{P_1}{RT_1}\right)^{\frac{c}{2} - \frac{d}{2}} N^c \dot{m}^d D^{c - 2d}$$

By grouping terms to indices c and d :

$$P_2 = \epsilon \text{Const} (P_1) \left(\frac{ND}{\sqrt{RT_1}} \right)^c \left(\frac{\dot{m} \sqrt{RT_1}}{P_1 D^2} \right)^d$$

in other words ;

$$\frac{P_2}{P_1} = \epsilon \text{Const} \left(\frac{ND}{\sqrt{RT_1}} \right)^c \left(\frac{\dot{m} \sqrt{RT_1}}{P_1 D^2} \right)^d$$

or

$$\frac{P_2}{P_1} = \text{function} \left(\frac{ND}{\sqrt{RT_1}}, \frac{\dot{m} \sqrt{RT_1}}{P_1 D^2} \right) \quad (\text{IV})$$

R is constant if air or similarly gas is used. If only one size of compressor is considered D would be constant. Thus,

$$\left(\frac{P_2}{P_1} \right) = f_n \left(\frac{N}{\sqrt{T_1}}, \frac{\dot{m} \sqrt{T_1}}{P_1} \right) \quad (\text{V})$$

The original test results can therefore be plotted in terms of :

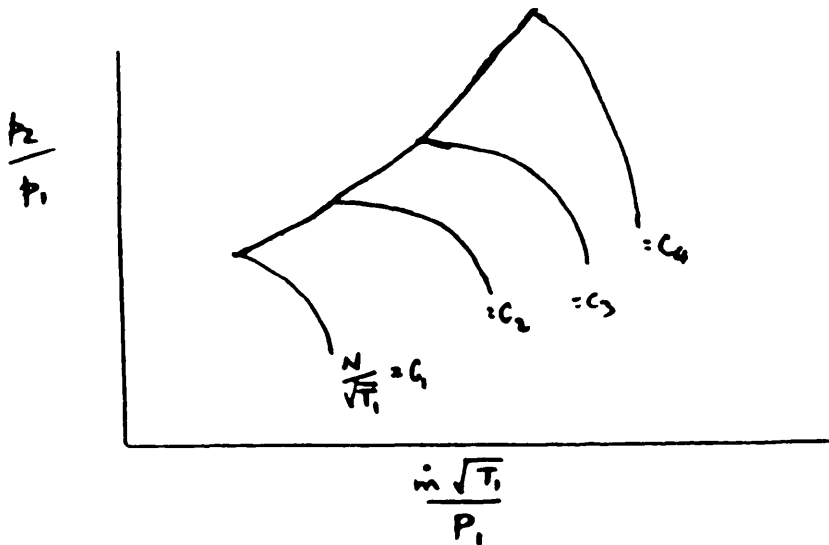


Fig 3

The relationships of Fig 3 are valid for any inlet conditions of T_1 and P_1 . This is the description of the characteristics is handled in general. The only exception arises when flying at low Reynolds Numbers for example

when at high altitudes. The characteristics then become slightly dependant on Reynold Numbers. In this case, the Reynold Number variable should be included in the right hand side of equation I, and will therefore appear as a final addition to right hand side of equation (V).

Similarly to the pressure ratio, both compressor efficiency and mass flow could be handled in exactly the same way for single gas and compressor size.

REQUIRED ENGINE CHARACTERISTICS

Safe power output

Low fuel consumption

Stable and flexible operation

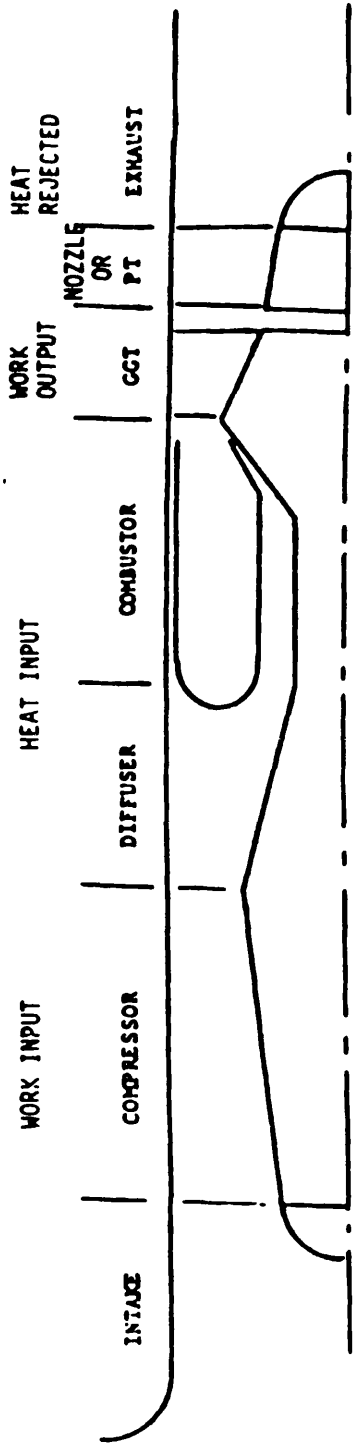
Reliability, durability and ease of maintenance

Minimum size/weight

Inexpensive development and production

Low noise and emissions

Suitable matching of output at different conditions



GGT - GAS GENERATOR TURBINE

PT - POWER TURBINE

SCHEMATIC OF A GAS TURBINE

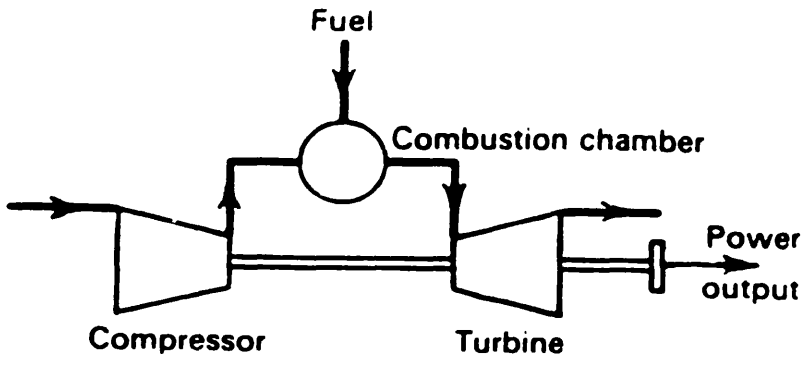


FIG 1.1 Simple gas turbine system.

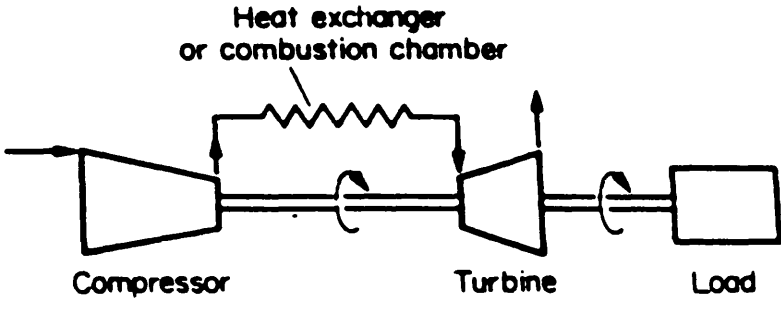
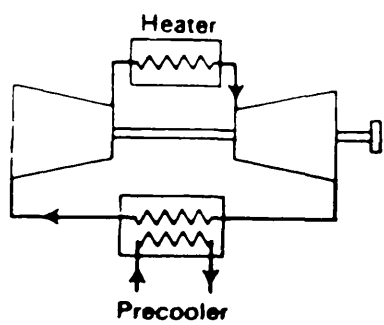
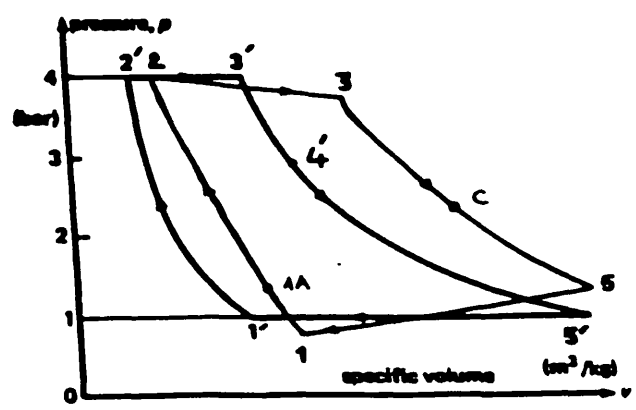


FIG 1.2 Single-shaft arrangement.



Simple closed cycle.

FIG 1.3



Brayton cycle.

FIG 1.3(a)

THE BRAYTON OR JOULE CYCLE

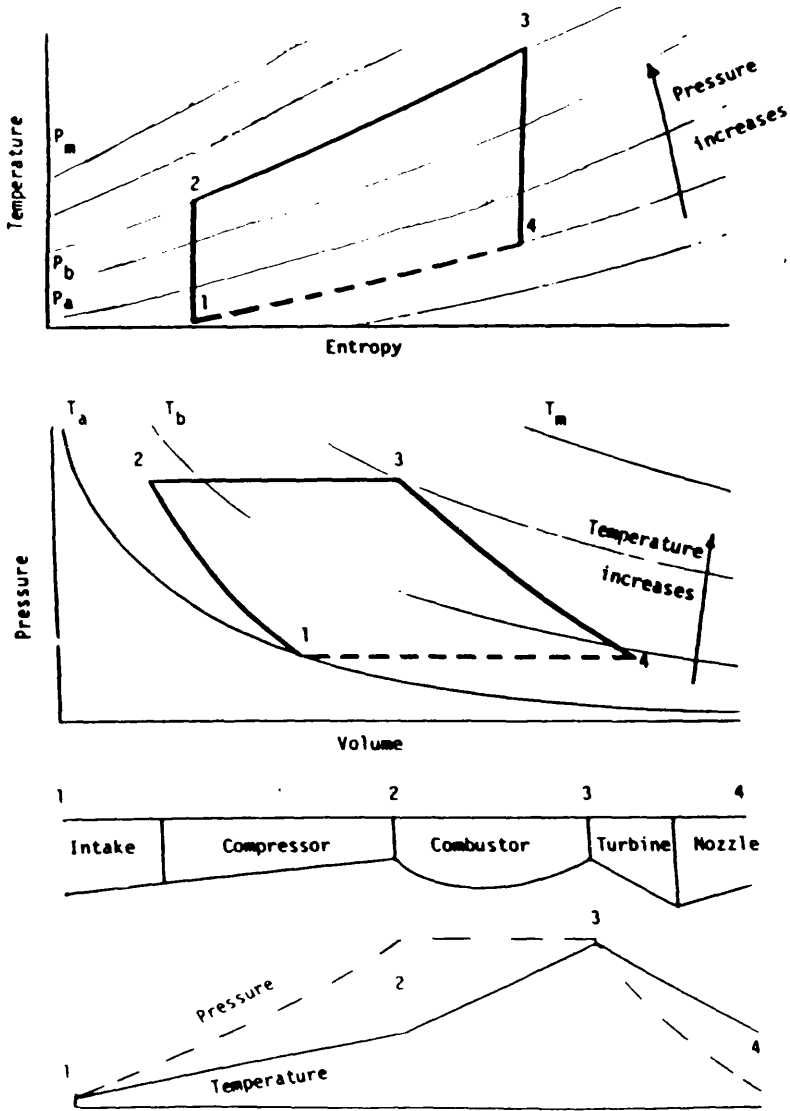
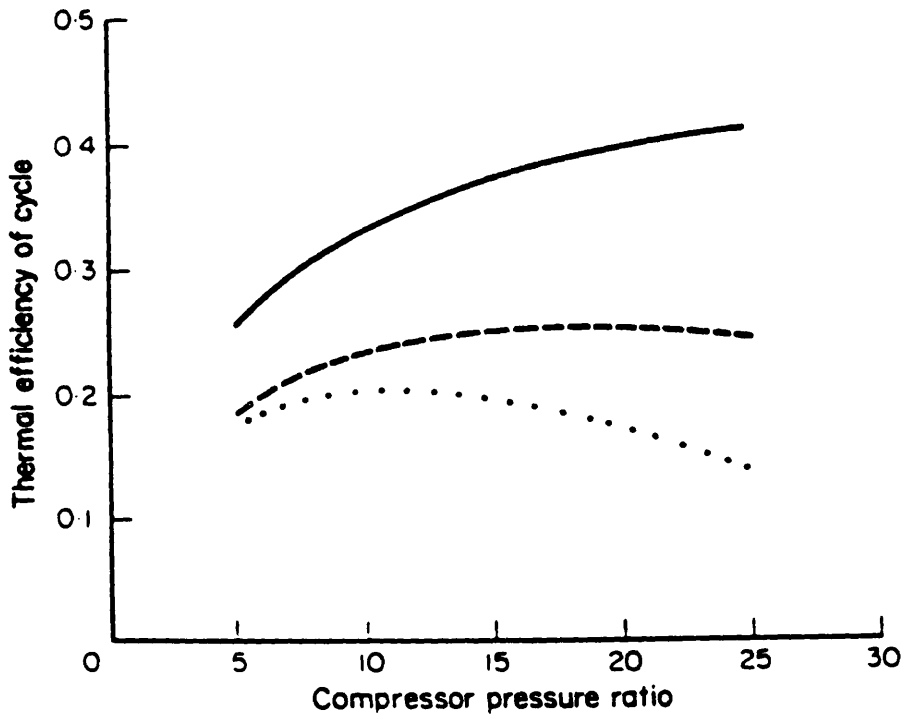
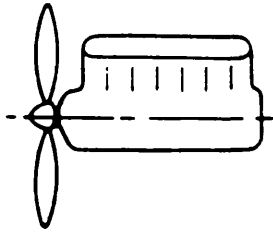


FIG 1.3(b)

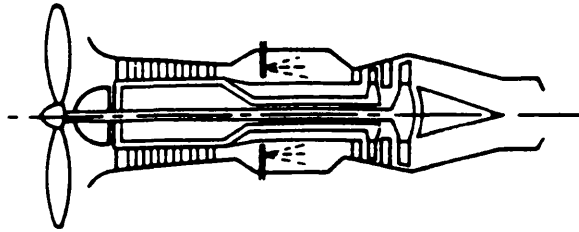


Cycle thermal efficiency as a function of other factors: —, $\eta = 0.9, T_1 = 1400 \text{ K}$; ---, $\eta = 0.8, T_1 = 1400 \text{ K}$; . . . , $\eta = 0.8, T_1 = 1200 \text{ K}$ (η is compressor and turbine efficiency, T_1 is turbine inlet temperature)

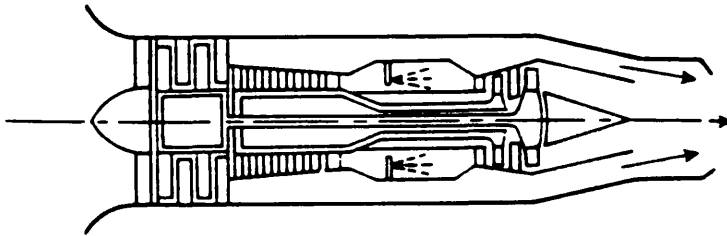
FIG 1.4



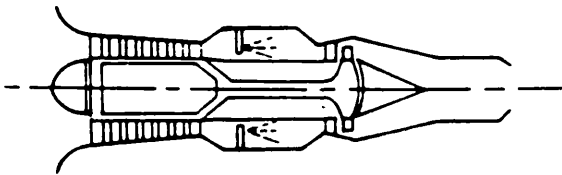
(a) Piston engine



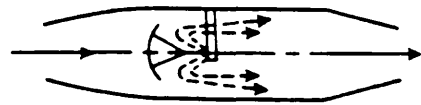
(b) Turboprop engine



(c) Turbofan engine



(d) Turbojet engine



(e) Ramjet engine

FIG 1.5 Propulsion engines.

GAS TURBINES FOR PROPULSION

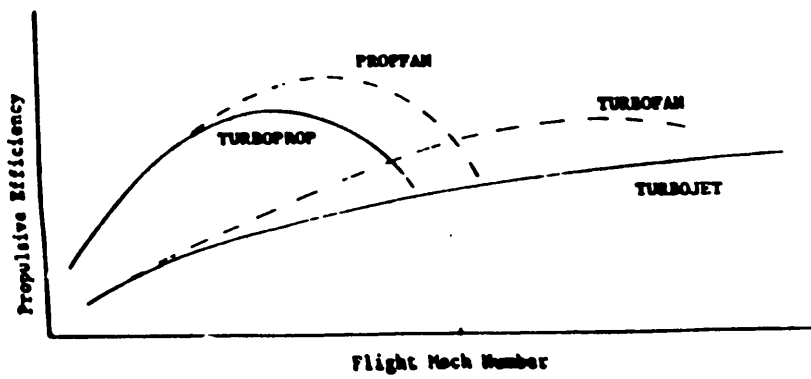
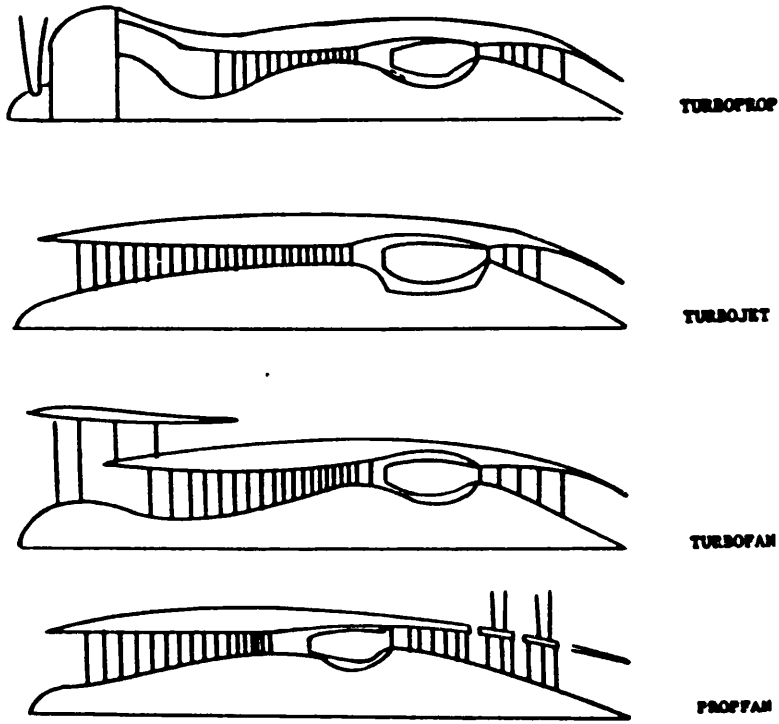


FIG 1.6

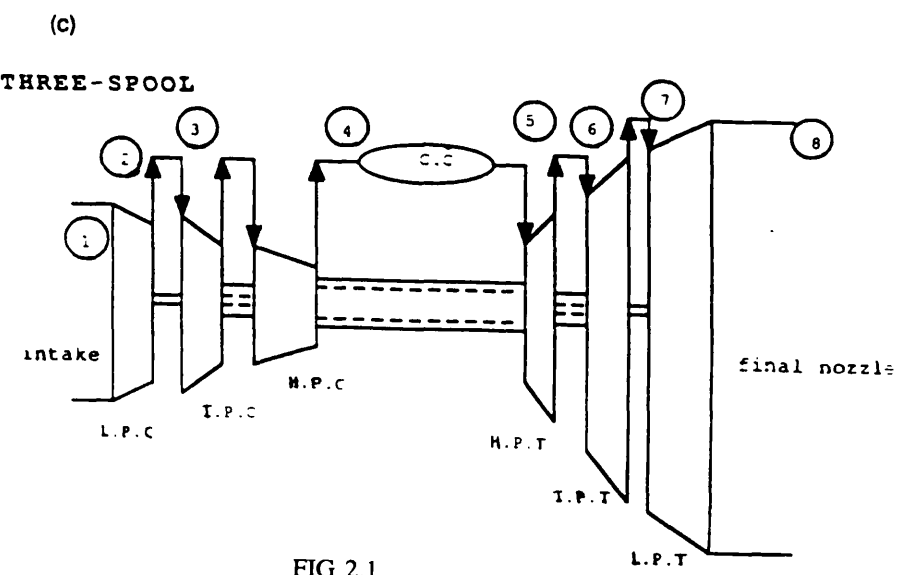
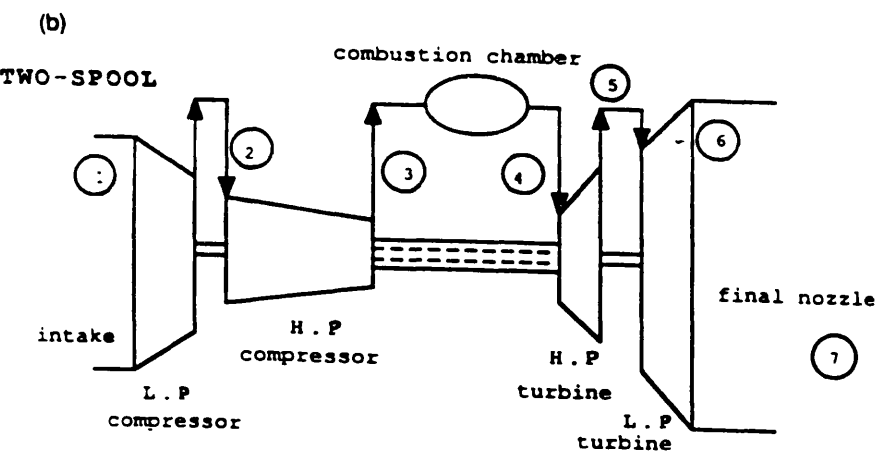
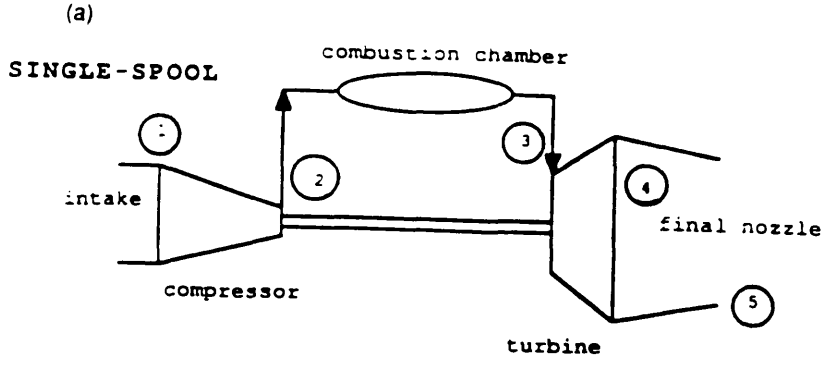
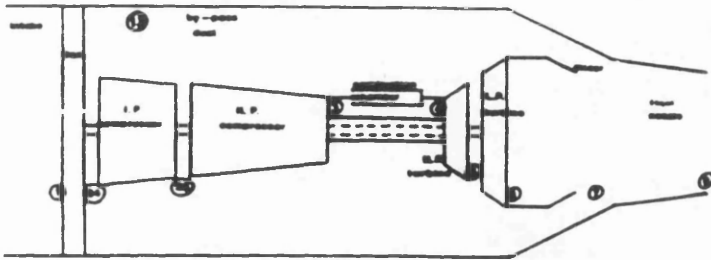
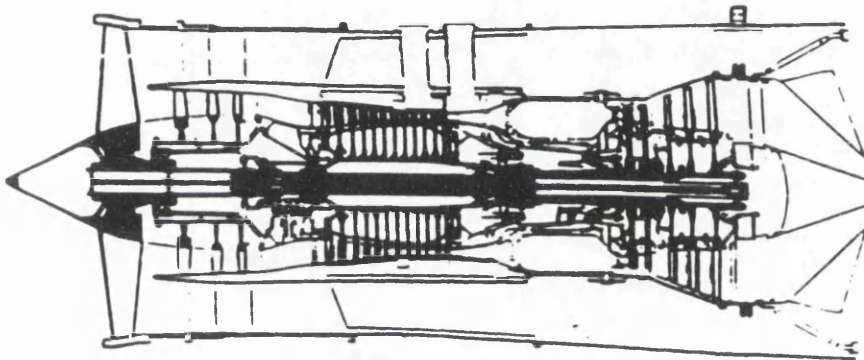


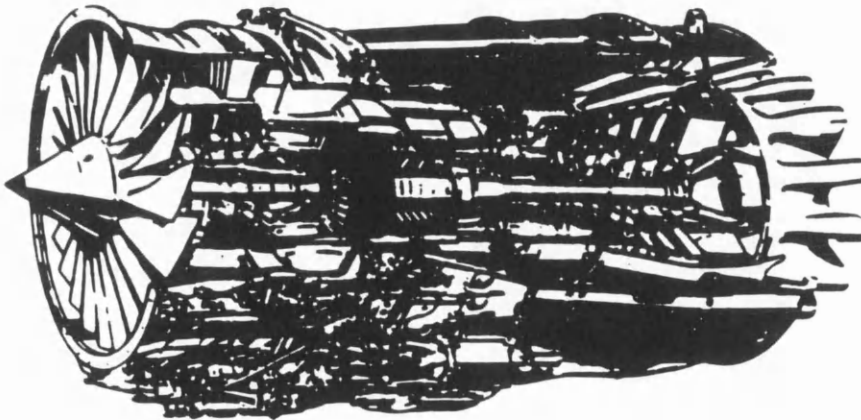
FIG 2.1



Tay turbofan engine station arrangements



Cross-section of Rolls-Royce Tay turbofan

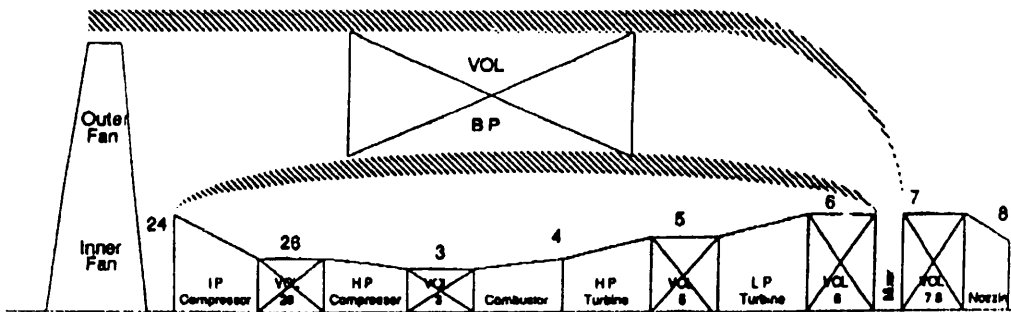


Cutaway drawing of the Rolls-Royce Tay turbofan

FIG 2.2 TAY TURBOFAN ENGINE

Analysis of a More Complex Engine by ICV method

Two-spool Turbofan with Mixed Exhausts



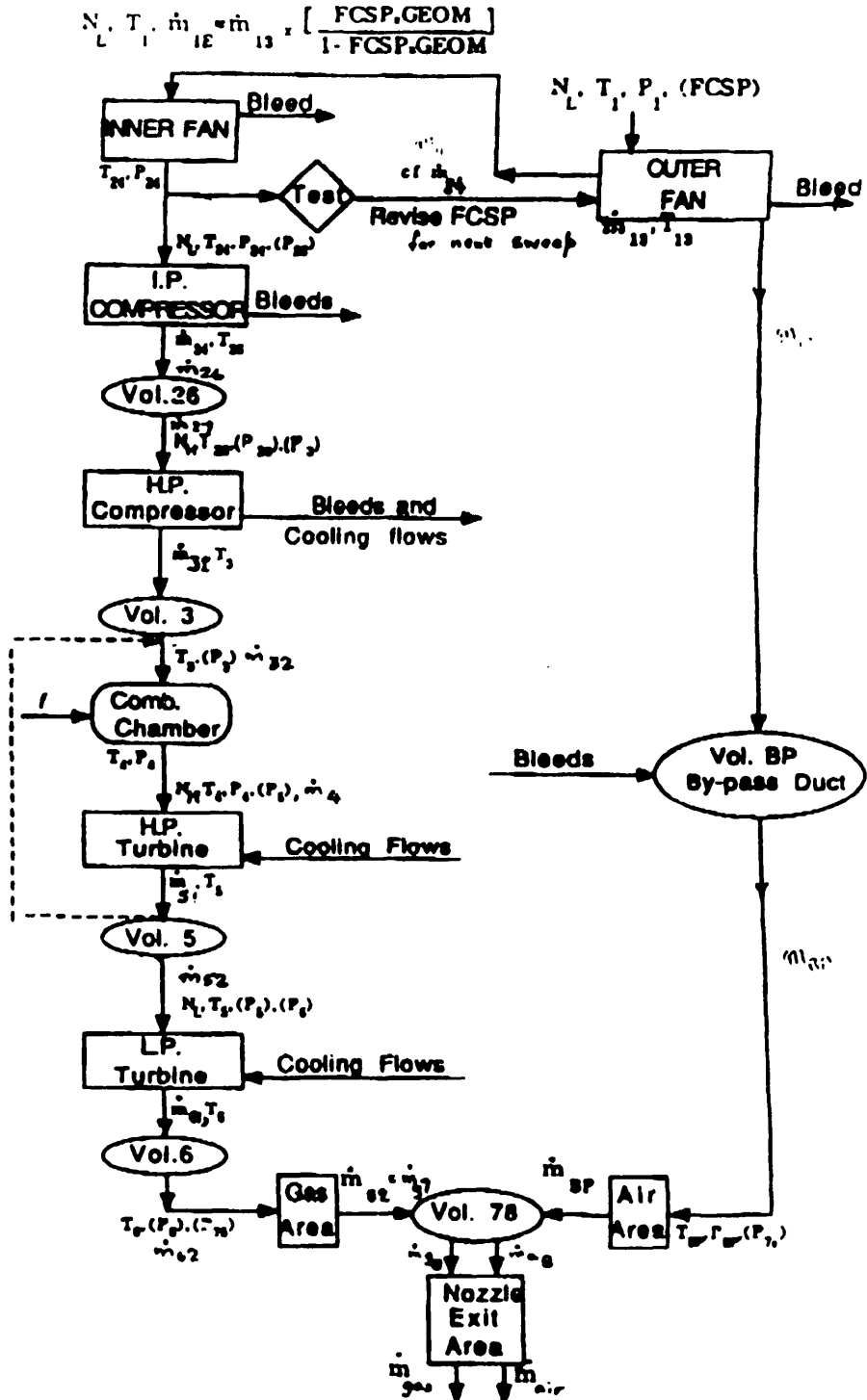
Calculation procedure is as indicated on the next sheet.

The computation requires to use double precision, due to the very short ~~time~~ increments which are necessary to avoid oscillations.

FIG 2.3

Analysis of a More Complex Engine by ICV method

Two-spool Turbofan with Mixed Exhausts



Calculate new pressures and Accelerations

FIG 2.4

Comparison of Predictions from the Two Methods

For single-spool engine it is reported that

- Both methods yield very similar results except during the first few instants of the transient.
- Acceleration rates and trajectories obtained from both methods are very similar.
- The difference is due to mass storage in the engine. This effect is perceptible during the first instants of the transient but is small afterwards.

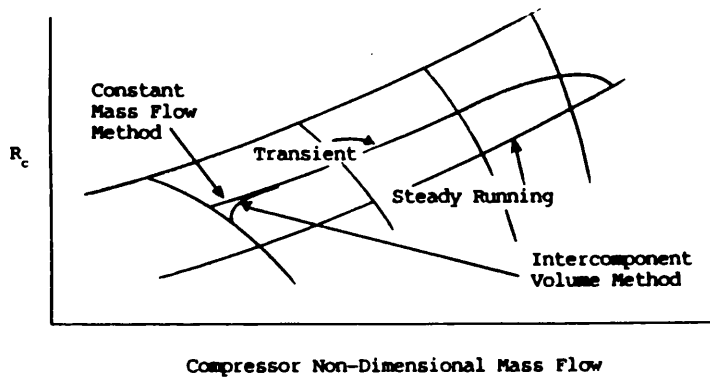


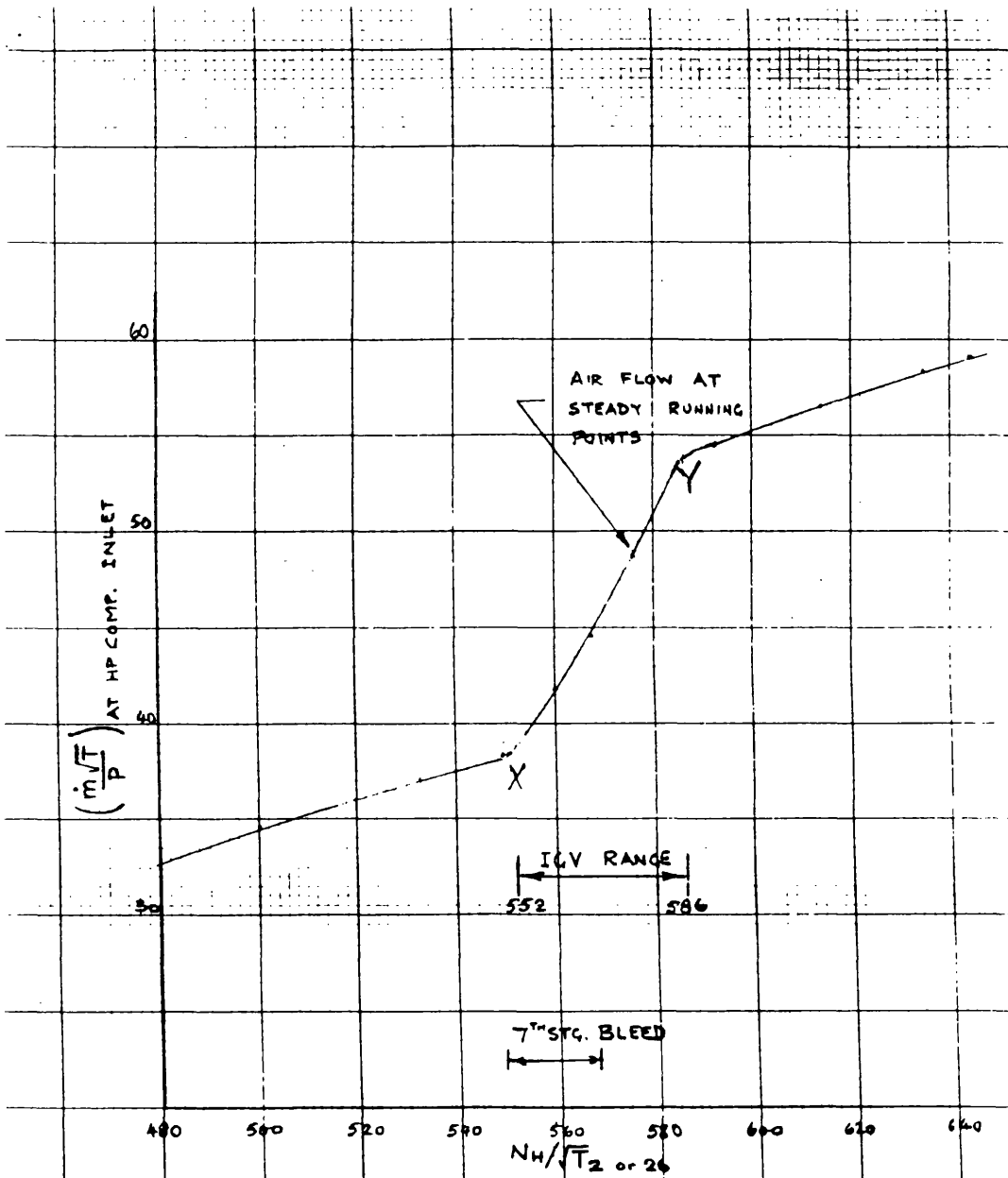
FIG 2.5

PERFORMANCE PARAMETERS	RELATIONSHIP	INNER FAN	OUTER FAN	IP COMPRESSOR	IIP COMPRESSOR	IIP TURBINE	I.P. TURBINE
CAPACITY	$MF650 = MF610 * FACTOR$	C18	C41	C31	C7	C3	C11
EFFICIENCY	$EFF650 = EFF610 + FACTOR$	D9	D42	D32	D1	C2	C10
PRESSURE RATIO	$(PR - 1)650 = (PR - 1)610 * FACTOR$	C21	C43	C33	C22		
NON-DIMENSIONAL SPEED	$NDS650 = NDS610 * FACTOR$	C23	C44	C34	C24		
VARIABLE EXPRESSIONS	INNER FAN						
	$D9=0.1405-0.1064*(ZNDIPC-194.696)/(437.656-194.696)$						
	OUTER FAN						
	$C41=0.90+0.20*(ZNDIPC-220.0)/(470.0-220.0)$						
	IP COMPRESSOR						
	$D32=0.0187+0.0295*(ZNDIPC-191.827)/(408.657-191.827)$						
	IIP COMPRESSOR						
	$D1=0.0355-0.0104*(ZNDIPC-530.494)/(613.584-530.494)$						

TABLE 3.1

PERFORMANCE PARAMETERS	FACTORS	TAY MK610	TAY MK650
CAPACITY	C31	1.0156	1
NON-DIMENSIONAL	C34	1	1
PRESSURE	C33	1.0081	1
	D33	0	0
EFFICIENCY	C32	1	1
	D32	0.0023	VARIABLE EXPRESSION
CAPACITY	C7	1.0136	1.045
NON-DIMENSIONAL	C24	1.00034	1.00034
PRESSURE	C22	1.006	1.041
	D22	0.0115	0
EFFICIENCY	C1	1	1
	D1	-0.0077	VARIABLE EXPRESSION

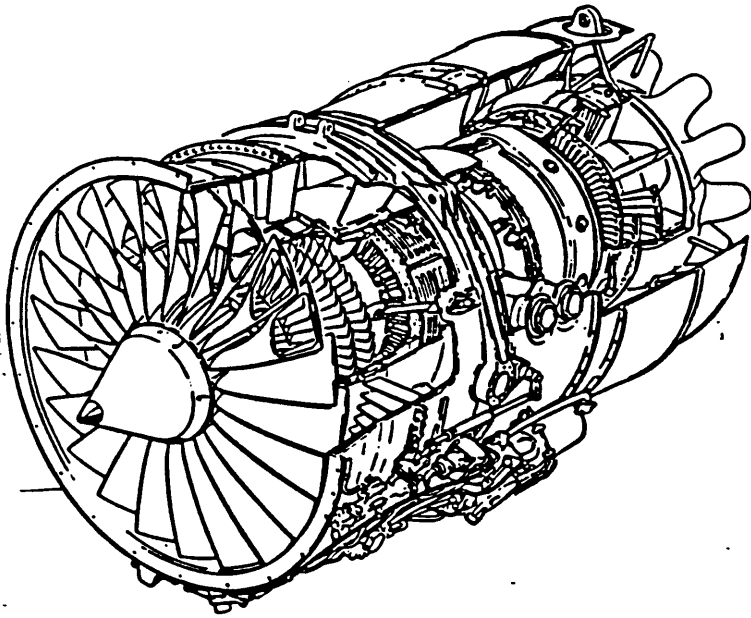
TABLE 3.2 b



AIR FLOW CHARACTERISTICS OF H.P. COMPRESSOR
 SPEY RB183-02 3 TAY RB 183-03

FIG 3.1

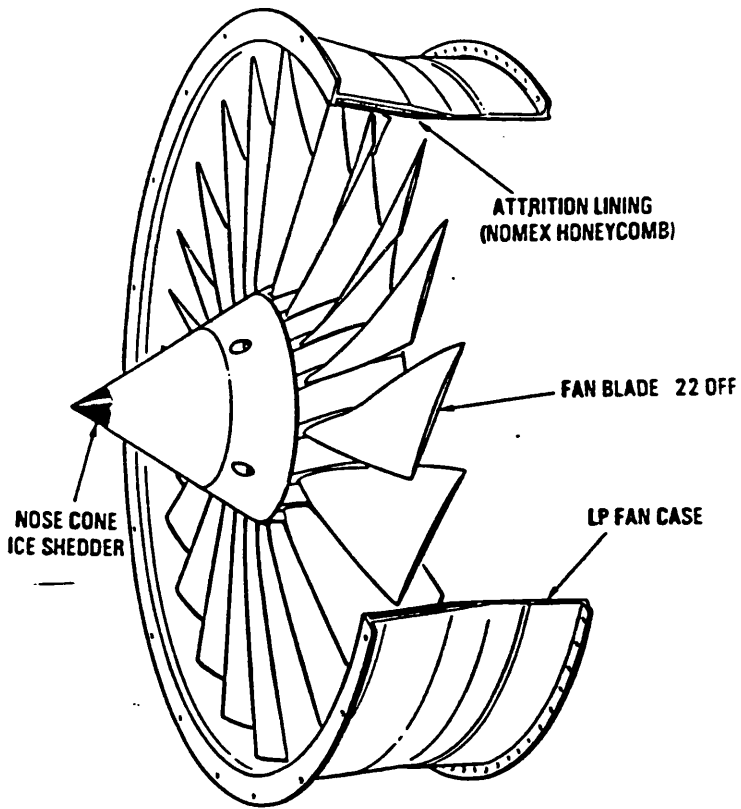
TAY
620-15



ROLLS-ROYCE TAY

FIG 3.2

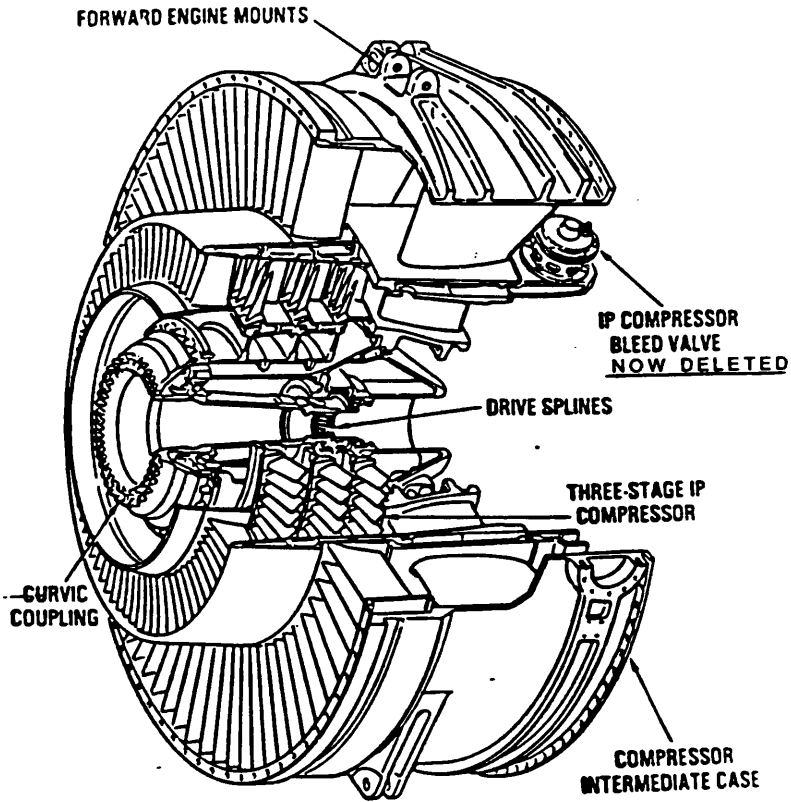
TAY
620-15



TAY LP FAN ASSEMBLY AND CASE

FIG 3.3

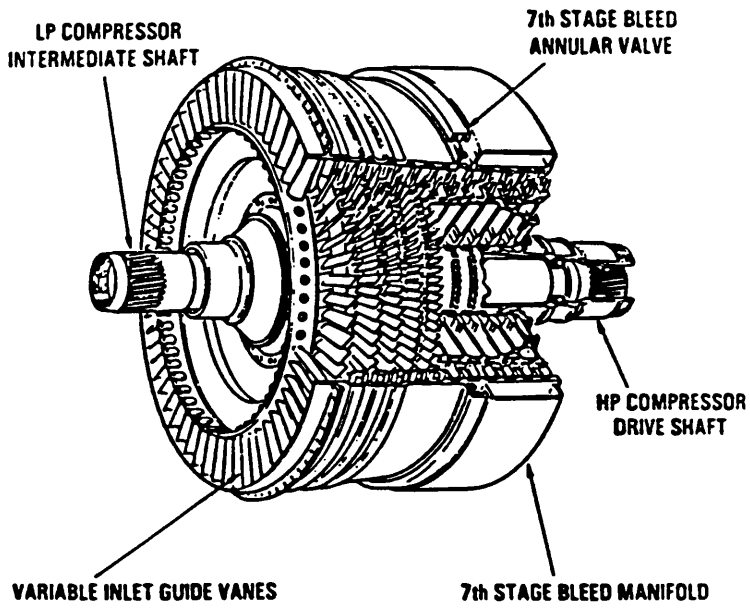
TAY
620-115



TAY IP COMPRESSOR SYSTEM

FIG 3.4

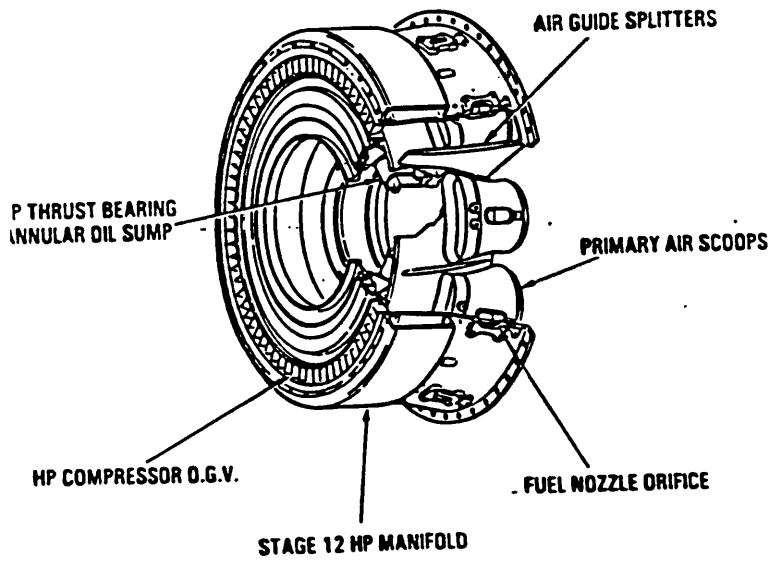
TAY
620-15



TAY HP COMPRESSOR SYSTEM

FIG 3.5

TAY
620-15

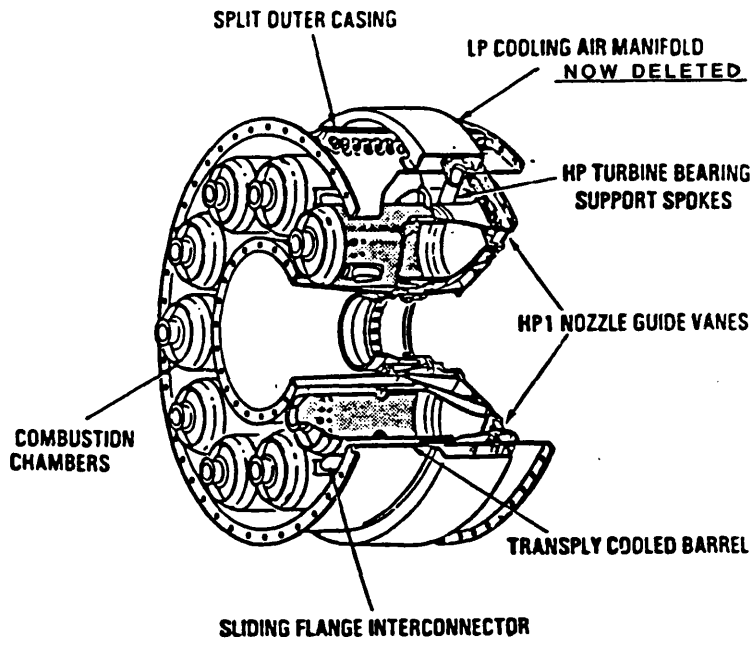


TAY DIFFUSER CASE

FIG 3.6

TAY

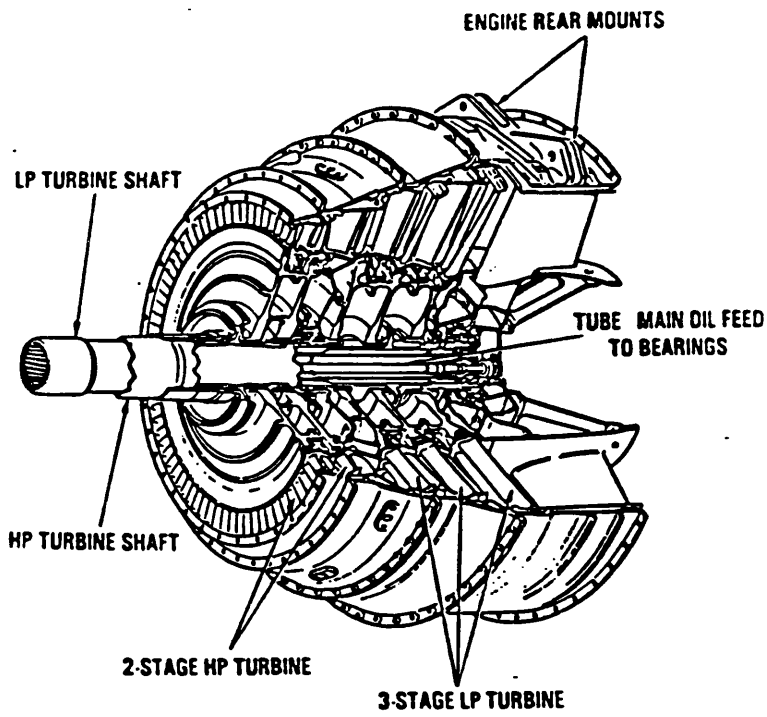
620-15



TAY COMBUSTION SYSTEM

FIG 3.7

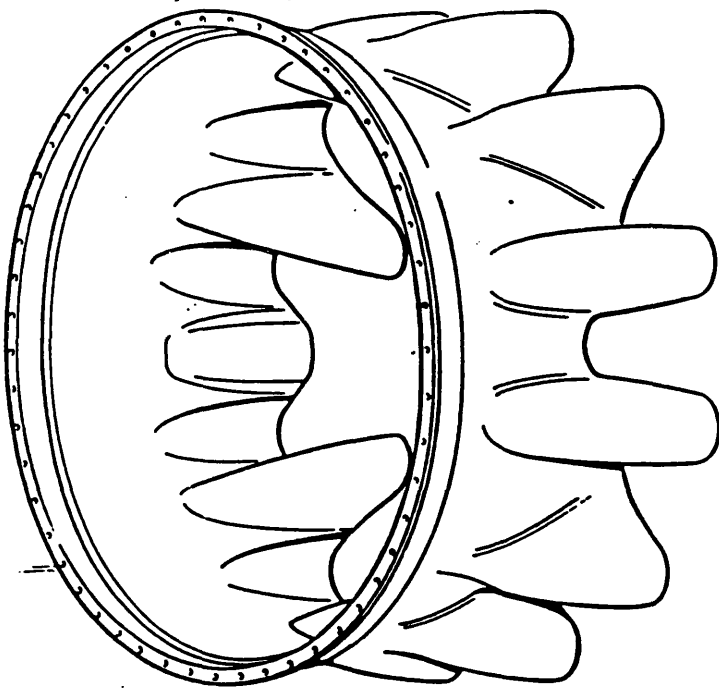
TAY
620-15



TAY TURBINE SYSTEM (HP & LP)

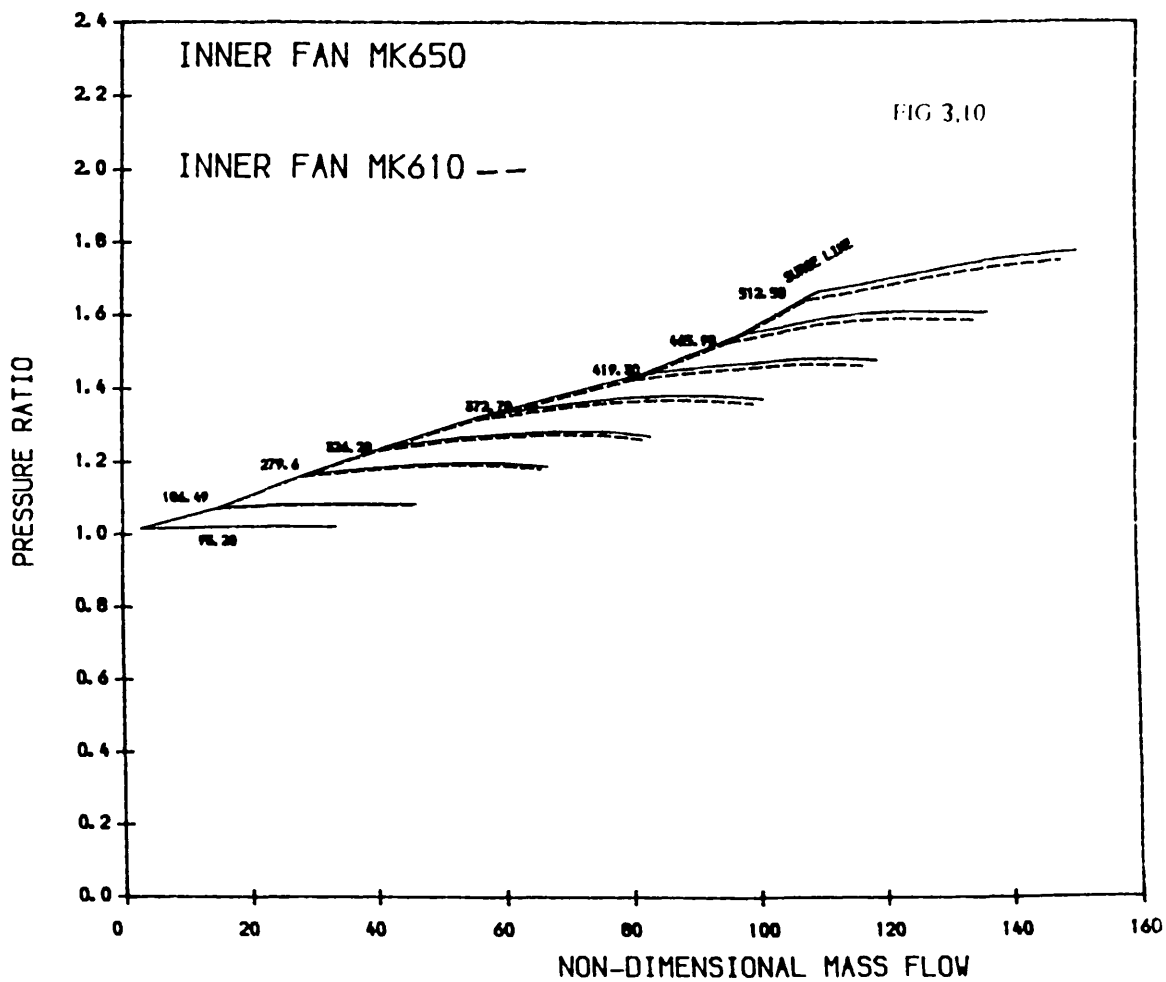
FIG 3.8

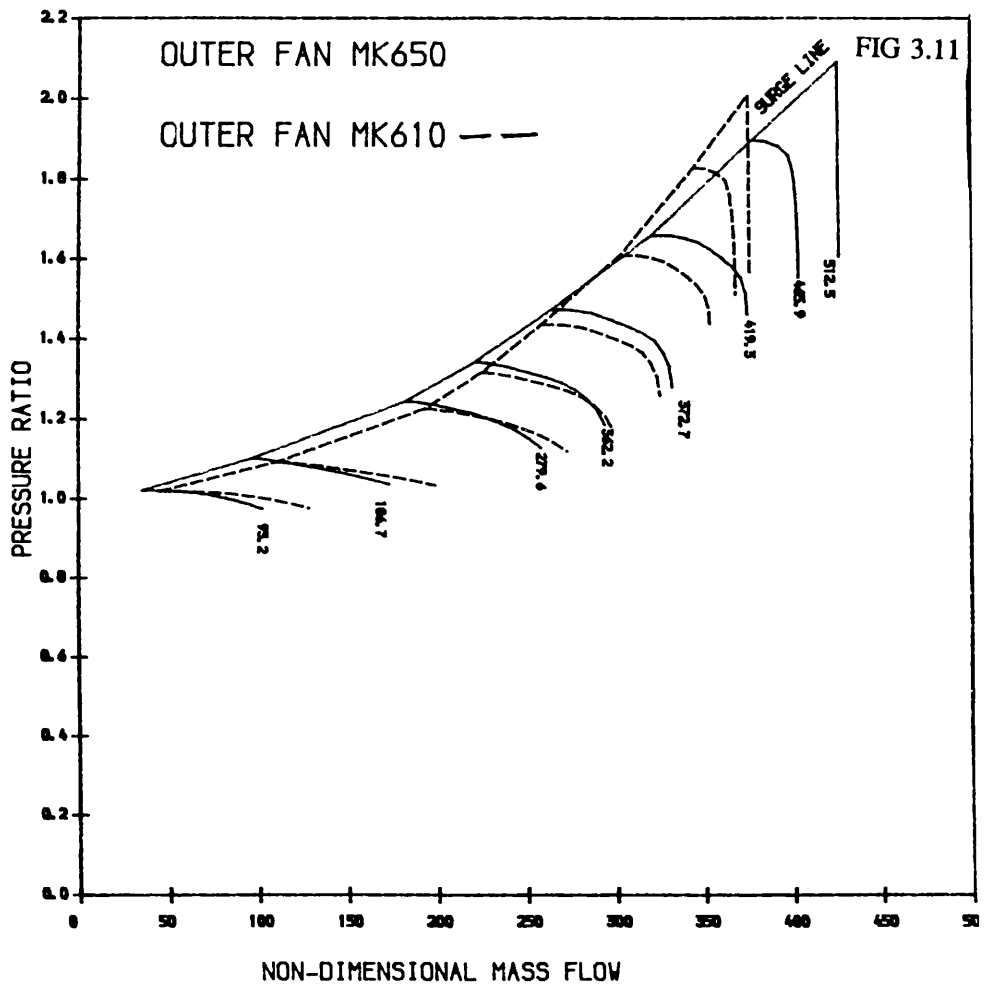
TAY
620-15

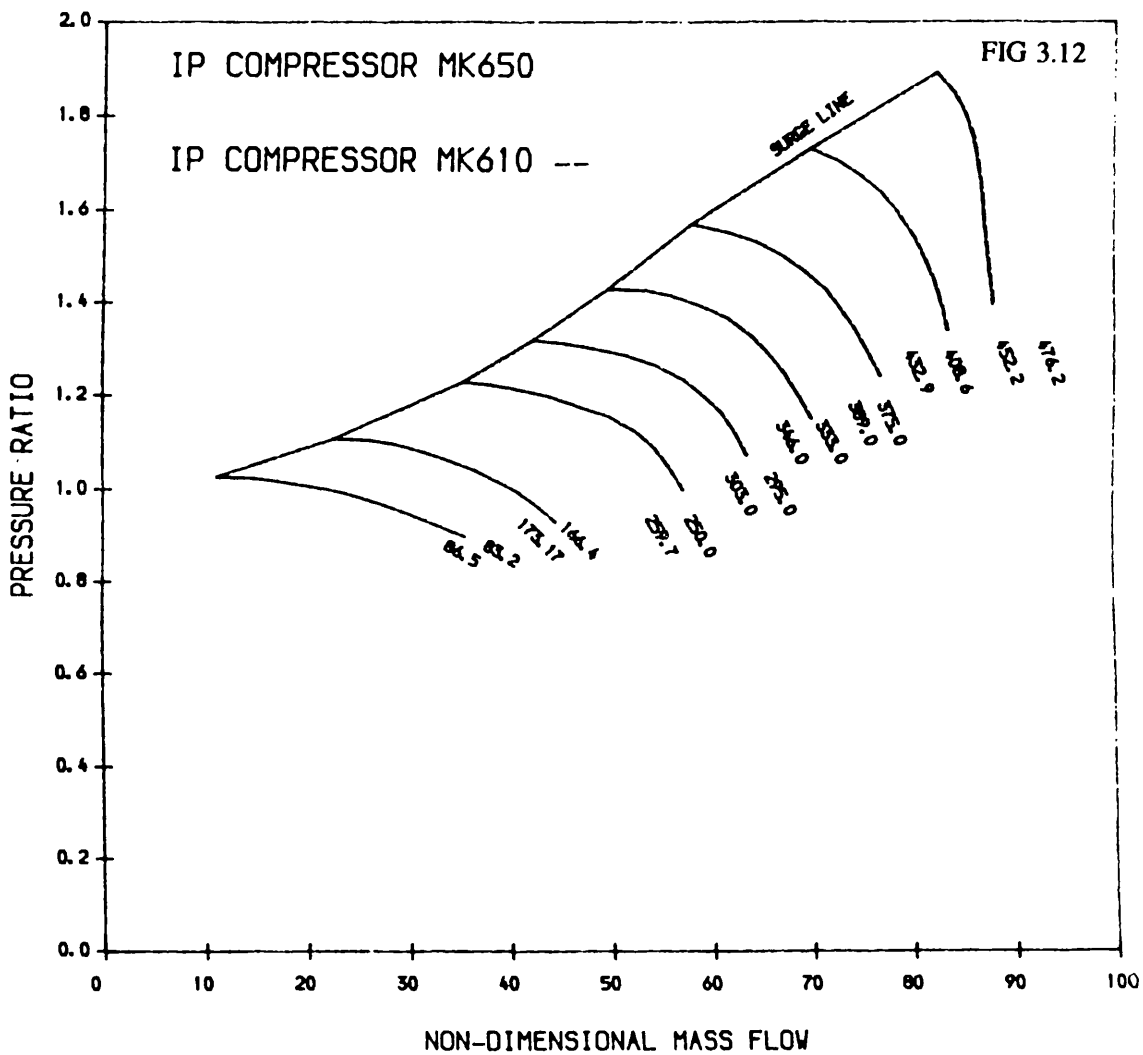


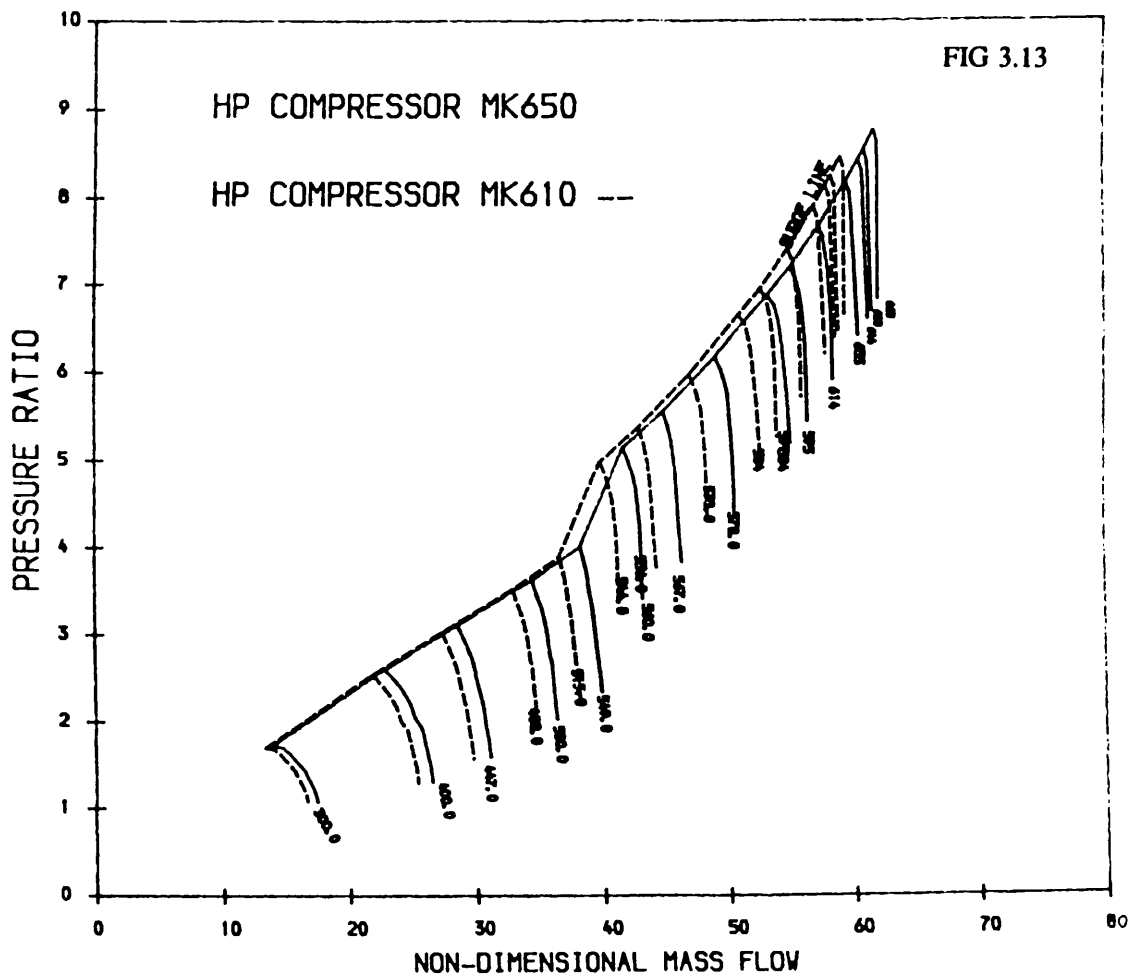
TAY 12 LOBE MIXER UNIT

FIG 3.9





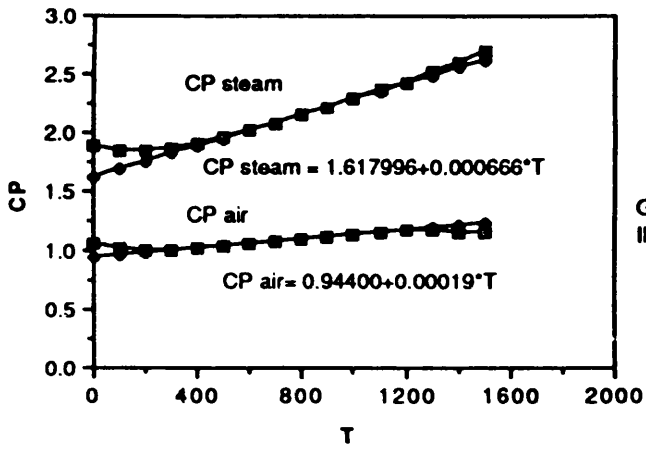




ROLLS-ROYCE TEST RESULTS

LP SHAFT SPEED RPM	DROPLET SPEED FT/S	% OF WATER INTO BYPASS	
		EXPERIMENTAL	METHOD TWO
1820	206	94.90%	89.40%
2263	211	94.80%	92.90%
2764	215	95.50%	100%
4130	218	97.40%	100%

TABLE 4.2



GRAPHS COINCIDE IN THE
INTERVAL 400 < TEMP < 1400

FIG 4.1

ENGINE PARAMETERS	CLEAN ENGINE	REF EVAP AT 26	REF EVAP AT 3	FIRST STAGE IP DRAG	THIRD STAGE IP DRAG	FIRST STAGE IP DRAG	FAN DRAG
NI.	7520.34	7523.87	7337.81	7501.56	7463.85	7498.35	7474.96
NI	11904.52	11526.94	11662.34	11913.45	11931.5	11827.11	11926.23
15M	1082.76	1006	1023.4	1083.71	1085.6	1084.23	1085.04
DELTA NI.	0	3.3	-182.73	-18.98	-36.7	-22.19	45.58
DELTA NI	0	-377.58	-242.2	8.93	26.98	-77.41	21.71
DELTA 15M	0	-76.76	-59.36	0.95	2.84	1.47	2.34

FUEL FLOW = 0.84 KGS

ENGINE PARAMETERS	CLEAN ENGINE	REF EVAP AT 26	REF EVAP AT 3	FIRST STAGE IP DRAG	THIRD STAGE IP DRAG	FIRST STAGE HP DRAG	FAN DRAG
NL	7573.27	7575.35	7994.81	7534.31	7516.18	7551.88	7527.79
NH	11964.5	11610.25	11715.55	11973.6	11992.5	11885.7	11966.49
TSM	1092.71	1016.97	1032.4	1093.7	1095.64	1093.99	1095.01
DELTA NL	0	2.08	-178.46	-18.96	-57.1	-21.4	-45.48
DELTA NH	0	-354.25	-248.95	9.1	28	-78.8	21.99
DELTA TSM	0	-75.74	-60.31	0.99	2.93	1.28	2.32

FUEL FLOW = 0.84 KG/S

ENGINE PARAMETERS	CLEAN ENGINE	REF EVAP AT 26	REF EVAP AT 13	FIRST STAGE IP DRAG	THIRD STAGE IP DRAG	FIRST STAGE HP DRAG	FAN DRAG
NL	7843.22	7838.35	7683.46	7825.52	7788.65	7825.36	7799.54
NH	12329.8	12148.6	12025.21	12344.23	12374.99	12219.37	12365.92
TSM	1146.11	1075.42	1085.06	1147.09	1149.1	1146.73	1148.51
DELTA NL	0	-4.87	-159.76	-17.7	-54.57	-17.86	-43.68
DELTA NH	0	-18.12	-304.6	14.43	45.19	-110.43	36.12
DELTA TSM	0	-70.7	-61.05	0.98	2.99	0.62	2.4

FUEL FLOW = 0.97 EGS

TABLE 5.3

FUEL FLOW = 0.84 KG/S

ENGINE PARAMETERS	CFE AN ENGINE	1% REDUCTION IN HP TURBINE CAPACITY	EVAPORATION AT 3	EVAPORATION AT 26
NH	11904.5	11926.4	11662.3	11526.94
NL	7520.5	7522.6	7337.8	7523.87
AIHEQV	125.22	125.26	121.73	125.48
RCMPL	1.5427	1.543	1.5125	1.543
ETISCL	0.9187	0.9186	0.9259	0.9182
ZNDLP	441.31	441.44	430.59	441.51
BETACL	7.49	7.49	7.61	7.54
AIHEQV	375.67	375.79	365.18	376.44
RCMPO	1.7149	1.7154	1.6703	1.7108
ETISCO	0.863	0.863	0.8662	0.8632
ZNDLPC	441.31	441.44	430.59	441.51
BETACO	5.07	5.07	5.07	5.2
AI24RR	82.09	82.13	80	83.81
RCMPI	1.5077	1.5061	1.5014	1.3904
ETISCL	0.7981	0.7971	0.8107	0.7023
ZNDIPC	412.64	412.74	404.03	412.8
BETACL	6.99	7.03	6.62	9.19
AIHERR	118.4	118.49	113.53	120.92
RCMPC	2.3258	2.3239	2.2708	2.1455
AI27RR	57.72	57.81	56.39	60.49
RCMPH	7.0331	7.1193	6.9478	7.7158
ETISCH	0.8674	0.8665	0.8733	0.8531
ZNDHPC	607.84	608.99	598.59	634.79
BETACH	4.02	3.7	3.08	3.75
NDMASSF AT 26	57.72	57.81	56.39	60.49
T26BEV	383.57	383.526	379.594	378.59
T26	383.57	383.526	379.594	325.71
P26	242.314	242.118	236.587	223.529
AIMS26	46.983	47.017	45.05	47.98
AIMS27	46.983	47.017	45.05	48.988
NDMASSF AT 4	1	0.99	1	1
T5M	1082.76	1082.36	1023.4	1006
T4	1442.66	1444.56	1365.66	1343.56
P4	1626.042	1644.835	1567.814	1645.8
GasMS4	40.785	40.814	40.149	42.489
T3BEV	696.465	699.16	685.221	615.419
T3	696.465	699.16	615.391	615.419
P3	1704.214	1723.713	1643.754	1724.715
AIMS3	59.946	59.974	39.31	41.65

TABLE 5.4

FUEL FLOW = 0.86 KG/S

ENGINE PARAMETERS	CLEAN ENGINE	1% REDUCTION IN HP TURBINE CAPACITY	EVAPORATION AT 3	EVAPORATION AT 26
NH	11964.5	11986.237	11715.553	11610.247
NL	7573.27	7575.335	7394.815	7575.351
AIIEQV	126.2	126.24	122.8	126.41
RCMPL	1.5514	1.5517	1.5219	1.5516
ETISCI	0.9168	0.9167	0.9237	0.9164
ZNDLP	444.41	444.53	433.94	444.53
BETACI	7.45	7.45	7.57	7.49
AI0EQV	378.6	378.73	368.39	379.24
RCMPO	1.7289	1.7294	1.6846	1.7244
ETISCO	0.862	0.862	0.8652	0.8621
ZNDLPC	444.41	444.53	433.94	444.53
BETACO	5.04	5.04	5.06	5.17
AI24RR	82.49	82.53	80.67	84.12
RCMPI	1.5086	1.507	1.5112	1.3898
ETISCI	0.7938	0.7928	0.8087	0.696
ZNDIPC	415.12	415.22	406.72	415.22
BETACI	7.06	7.1	6.6	9.27
AI1ERR	119.53	119.62	115.07	121.91
RCMPC	2.3404	2.3385	2.2998	2.1564
AI27RR	57.99	58.08	56.57	60.8
RCMPH	7.0886	7.1755	6.9796	7.7811
ETISCI	0.866	0.8651	0.8725	0.8514
ZNDHPC	610.01	611.15	599.91	637.98
BETACH	4.03	3.71	3.1	3.83
NDMASSF AT 26	57.99	58.08	56.57	60.8
T26BEV	384.69	384.648	381.382	379.685
T26	384.69	384.648	381.382	327.168
P26	243.836	243.635	239.611	224.669
AIMS26	47.431	47.464	45.659	48.373
AIMS27	47.431	47.464	45.659	49.381
NDMASSF AT 4	1	0.99	1	1
T5M	1092.71	1092.33	1032.4	1016.97
T4	1455.55	1457.491	1377.217	1357.877
P4	1649.402	1668.429	1595.387	1668.395
GASMS4	41.186	41.214	40.687	42.843
T3BEV	700.454	703.175	689.467	620.12
T3	700.454	703.175	620.356	620.12
P3	1728.452	1748.192	1672.387	1748.157
AIMS3	40.327	40.354	39.827	41.984

TABLE 5.5

FUEL FLOW = 0.96 KG/S

ENGINE PARAMETERS	CLEAN ENGINE	1% REDUCTION IN HP TURBINE CAPACITY	EVAPORATION AT 3	EVAPORATION AT 26
NH	12329.8	12361.2	12025.21	12148.58
NL	7843.23	7845.64	7683.46	7838.35
AIIEQV	131.24	131.29	128.17	131.28
RCMPI	1.5959	1.5963	1.5696	1.595
ETISCI	0.9075	0.9074	0.9131	0.9674
ZNDLP	460.25	460.39	450.87	459.96
BETACL	7.26	7.26	7.35	7.29
AIOEQV	393.73	393.88	384.5	393.83
RCMPO	1.8041	1.8047	1.7609	1.7983
ETISCO	0.8574	0.8574	0.8599	0.8576
ZNDLPC	460.25	460.39	450.87	459.96
BETACO	4.81	4.82	4.9	4.93
AI24RR	84.46	84.51	83.09	85.64
RCMPI	1.5099	1.5074	1.5243	1.3846
ETISCI	0.7709	0.7695	0.7914	0.6643
ZNDIPC	427.76	427.88	420.29	427.53
BETACI	7.45	7.5	6.94	9.66
AI1ERR	125.28	125.38	121.57	126.96
RCMPC	2.4096	2.4062	2.3926	2.2083
AI27RR	59.46	59.58	57.93	62.44
RCMPH	7.3946	7.49	7.2534	8.1397
ETISCH	0.8578	0.8569	0.8651	0.841
ZNDIIPC	624.18	625.85	610.63	660.51
BETACH	4.17	3.88	3.18	4.25
NDMASSF AT 26	59.46	59.58	57.93	62.44
T26BEV	390.205	390.109	387.817	385.049
T26	390.205	390.109	387.817	334.35
P26	251.043	250.69	249.279	230.076
AIMS26	49.711	49.749	48.239	50.376
AIMS27	49.711	49.749	48.239	51.387
NDMASSF AT 4	1	0.99	1	1
T5M	1146.11	1146.34	1085.06	1075.42
T4	1524.77	1526.717	1445.042	1434.373
P4	1772.76	1793.329	1726.229	1788.587
GASMS4	43.234	43.266	42.99	44.658
T3BEV	721.592	724.428	710.817	645.039
T3	721.592	724.428	644.43	645.039
P3	1856.36	1877.666	1808.132	1872.754
AIMS3	42.265	42.297	41.013	43.689

TABLE 5.6

	Rolls-Royce observations for the case of water thermodynamics relative to clean engine	
delta NL	-40	
delta NH	-25	
delta TSM	-34	
delta FUEL	1.74%	
TICVWATER program simulation results		
NL	-40	
EVAP AT 26	0	0%
EVAP AT 3	-131.08	100%
IP DRAGS	-1/5 * 56.68	3 STAGE
HP DRAGS	-1/5 * 22.17	1 STAGE
DELTA FUEL FO	106.85	
NH	-38.85	
EVAP AT 26	0	0%
EVAP AT 3	-149.71	100%
IP DRAGS	1/5 * 26.96	3 STAGE
HP DRAGS	-1/5 * 77.48	1 STAGE
DELTA FUEL FO	120.96	
TSM	-45.31	
EVAP AT 26	0	0%
EVAP AT 3	-66.34	100%
IP DRAGS	1/5 * 2.85	3 STAGE
HP DRAGS	1/5 * 1.48	1 STAGE
DELTA FUEL FO	20.16	
FUEL INCREASE	4.69%	

TABLE 5.7

Rolls-Royce observations for the case of water thermodynamics relative to clean engine	
delta NL	
delta NH	-40
delta TSM	-25
delta FUEL FLOW	-34
	1.74%
TICVWATER program simulation results	
DELTA NL	-40
EVAP AT 26	1.998
EVAP AT 3	-52.432
IP DRAGS	-36.7
HP DRAGS	0
DELTA FUEL FOR NL	67.134
DELTA NH	-183.452
EVAP AT 26	-226.548
EVAP AT 3	-59.884
IP DRAGS	26.98
HP DRAGS	0
DELTA FUEL FOR NH	76
DELTA TSM	-57.092
EVAP AT 26	-46.056
EVAP AT 3	-26.536
IP DRAGS	2.84
HP DRAGS	0
DELTA FUEL FOR TSM	12.66
DELTA FUEL	2.94%

TABLE 5.8

		Rolls-Royce observations for the case of water	
		thermodynamics relative to clean engine	
delta NL			
delta NH	-40		
delta T5M	-25		
delta FUEL FLOW	-34		
	1.74%		
		TICVWATER program simulation results	
DELTA NL	-40		
EVAP AT 26	0.333		10%
EVAP AT 3	-117.972		90%
IP DRAGS	-56.7		3 STAGE
HP DRAGS	0		1 STAGE
DELTA FUEL FOR NL	134.339		
DELTA NH	44.322		
EVAP AT 26	-134.739		10%
EVAP AT 3	0		90%
IP DRAGS	26.98		3 STAGE
HP DRAGS	0		1 STAGE
DELTA FUEL FOR NH	152.081		
DELTA T5M	-39.195		
EVAP AT 26	-7.676		10%
EVAP AT 3	-59.706		90%
IP DRAGS	2.84		3 STAGE
HP DRAGS	0		1 STAGE
DELTA FUEL FOR T5M	25.3469		
DELTA FUEL	5.90%		

	Rolls-Royce observations for the case of water thermodynamics relative to clean engine	
delta NL		
delta NH	-40	
delta T5M	-25	
delta FUEL FLOW	-34	
	1.74%	
	TICVWATER program simulation results	
DELTA NL	-40	
EVAP AT 26	2.997	90%
EVAP AT 3	-18.273	10%
IP DRAGS	-56.7	3 STAGE
HP DRAGS	0	1 STAGE
DELTA FUEL FOR NL	31.549	
DELTA NH	-301.346	
EVAP AT 26	-339.822	90%
EVAP AT 3	-24.22	10%
IP DRAGS	26.98	3 STAGE
HP DRAGS	0	1 STAGE
DELTA FUEL FOR NH	35.716	
DELTA T5M	-66.228	
EVAP AT 26	-69.084	90%
EVAP AT 3	-5.936	10%
IP DRAGS	2.84	3 STAGE
HP DRAGS	0	1 STAGE
DELTA FUEL FOR T5M	5.952	
DELTA FUEL	1.38%	

TABLE 5.11

		Rolls-Royce observations for the case of water thermodynamics relative to clean engine	
	delta NL		
	delta NH	-40	
	delta TSM	-25	
	delta FUEL FLOW	-34	
		1.74%	
		TICVWATER program simulation results	
	DELTA NL	-40	
	EVAP AT 26	2.664	80%
	EVAP AT 3	-36.546	20%
	IP DRAGS	-56.7	3 STAGE
	HP DRAGS	0	1 STAGE
	DELTA FUEL FOR NL	50.582	
	DELTA NH	-248.95	
	EVAP AT 26	-283.4	80%
	EVAP AT 3	-49.79	20%
	IP DRAGS	26.98	3 STAGE
	HP DRAGS	0	1 STAGE
	DELTA FUEL FOR NH	57.263	
	DELTA TSM	-60.27	
	EVAP AT 26	-60.592	80%
	EVAP AT 3	-12.062	20%
	IP DRAGS	2.84	3 STAGE
	HP DRAGS	0	1 STAGE
	DELTA FUEL FOR TSM	9.544	
	DELTA FUEL	2.22%	

TABLE 5.12

		Rolls-Royce observations for the case of water thermodynamics relative to clean engine	
delta NL			
delta NH	-40		
delta T5M	-25		
delta FUEL FLOW	-34		
	1.74%		
	TICVWATER program simulation results		
DELTA NL	-40		
EVAP AT 26	1.665		50%
EVAP AT 3	-91.365		50%
IP DRAGS	-56.7		3 STAGE
HP DRAGS	0		1 STAGE
DELTA FUEL FOR NL	106.4		
DELTA NH	-162.457		
EVAP AT 26	-188.79		50%
EVAP AT 3	-121.1		50%
IP DRAGS	26.98		3 STAGE
HP DRAGS	0		1 STAGE
DELTA FUEL FOR NH	120.453		
DELTA T5M	-45.145		
EVAP AT 26	-38.38		50%
EVAP AT 3	-29.68		50%
IP DRAGS	2.84		3 STAGE
HP DRAGS	0		1 STAGE
DELTA FUEL FOR T5M	20.075		
DELTA FUEL	4.67%		

TABLE 5.13

	Rolls-Royce observations for the case of water thermodynamics relative to clean engine	
delta NL		
delta NH	-40	
delta T5M	-25	
delta FUEL FLOW	-34	
	1.74%	
	TICVWATER program simulation results	
DELTA NL	-40	
EVAP AT 26	1.332	40%
EVAP AT 3	-109.638	60%
IP DRAGS	-56.7	3 STAGE
HP DRAGS	0	1 STAGE
DELTA FUEL FOR NL	124.876	
DELTA NH	-155.963	
EVAP AT 26	-226.55	40%
EVAP AT 3	-96.88	60%
IP DRAGS	26.98	3 STAGE
HP DRAGS	0	1 STAGE
DELTA FUEL FOR NH	140.485	
DELTA T5M	-43.546	
EVAP AT 26	-46.056	40%
EVAP AT 3	-23.744	60%
IP DRAGS	2.84	3 STAGE
HP DRAGS	0	1 STAGE
DELTA FUEL FOR T5M	23.414	
DELTA FUEL	5.48%	

TABLE 5.14

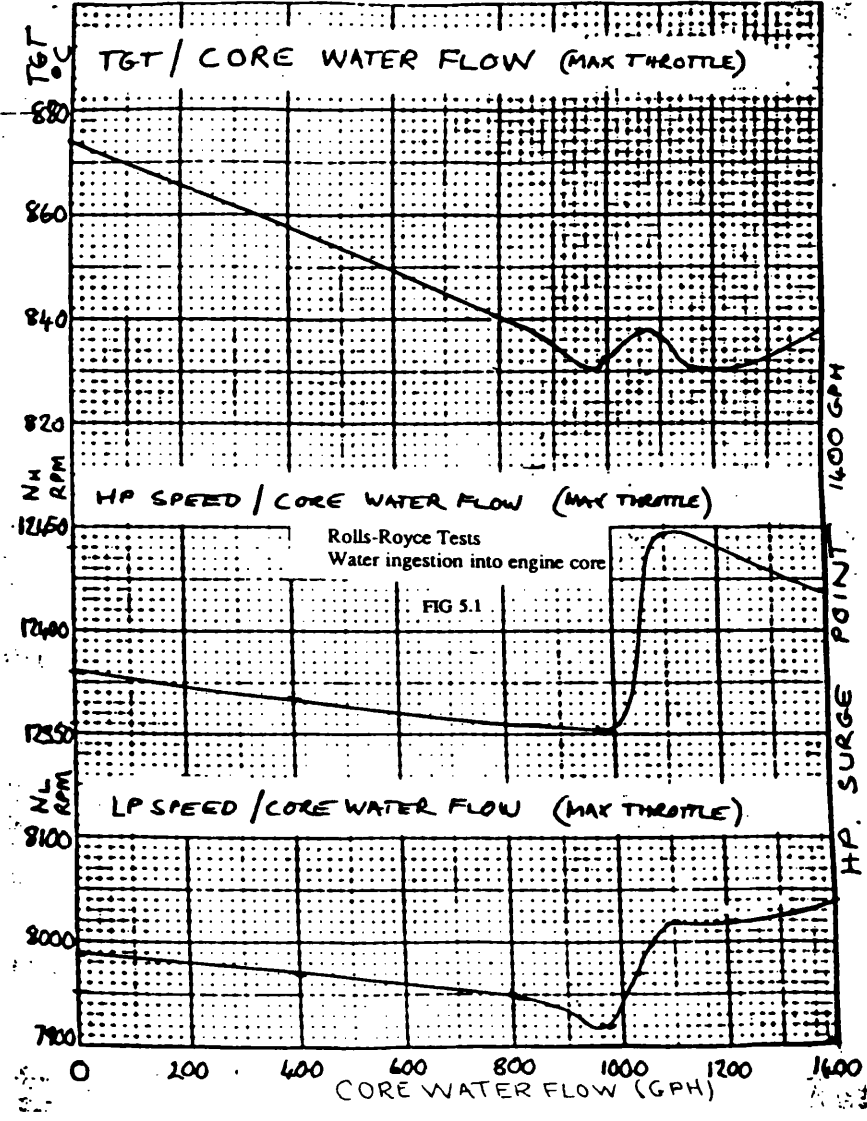
	Rollis-Royce observations for the case of water thermodynamics relative to clean engine	
delta NL		
delta NH	-40	
delta T5M	-25	
delta FUEL FLOW	-34	
	1.74%	
	TIC/VWATER program simulation results	
DELTA NL	-40	
EVAP AT 26	0.8325	25%
EVAP AT 3	-137.0475	75%
IP DRAGS	-56.7	3 STAGE
HP DRAGS	-0.2219	1 STAGE
DELTA FUEL FOR NL	153.1369	
DELTA NH	-76.4766	
EVAP AT 26	-94.395	25%
EVAP AT 3	-181.65	75%
IP DRAGS	26.98	3 STAGE
HP DRAGS	-0.7741	1 STAGE
DELTA FUEL FOR NH	173.3625	
DELTA T5M	-33.7893	
EVAP AT 26	-20.355	25%
EVAP AT 3	-45.315	75%
IP DRAGS	2.84	3 STAGE
HP DRAGS	0.147	1 STAGE
DELTA FUEL FOR T5M	28.8937	
DELTA FUEL	6.72%	

TABLE 5.15

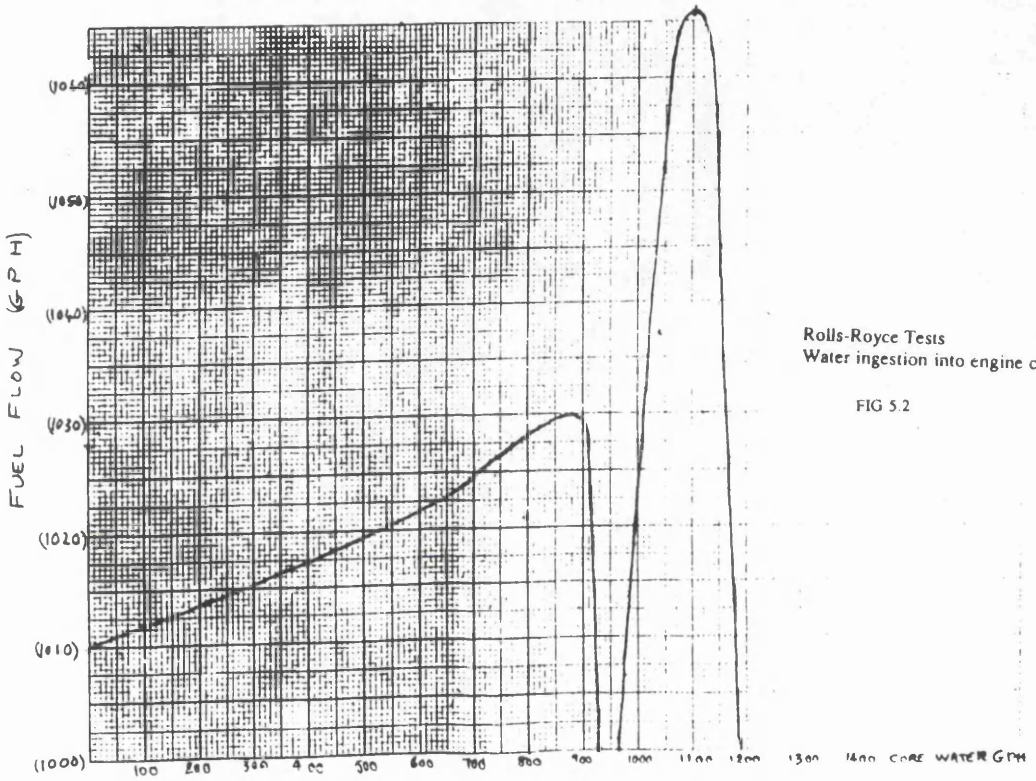
	Rolls-Royce observations for the case of water thermodynamics relative to clean engine	
delta NL		
delta NH	-40	
delta T5M	-25	
delta FUEL FLOW	-34	
	1.74 %	
TICVWATER program simulation results		
DELTA NL	-40	
EVAP AT 26	0.333	10%
EVAP AT 3	-164.457	90%
IP DRAGS	-56.7	3 STAGE
HP DRAGS	-0.2219	1 STAGE
DELTA FUEL FOR NL	181.0459	
DELTA NH	-24.5321	
EVAP AT 26	-37.758	10%
EVAP AT 3	-217.98	90%
IP DRAGS	26.98	3 STAGE
HP DRAGS	-0.7741	1 STAGE
DELTA FUEL FOR NH	205	
DELTA T5M	-23.954	
EVAP AT 26	-7.676	10%
EVAP AT 3	-53.424	90%
IP DRAGS	2.84	3 STAGE
HP DRAGS	0.147	1 STAGE
DELTA FUEL FOR T5M	34.159	
DELTA FUEL	7.94%	

TABLE 5.16

-TAY 650-15 CONSTANT MAX THROTTLE
INCREASING CORE WATER FLOW



CONSTANT, MAX CONDITIONS CORE WATER FLOW INCREASING



Rolls-Royce Tests
Water ingestion into engine co

FIG 5.2

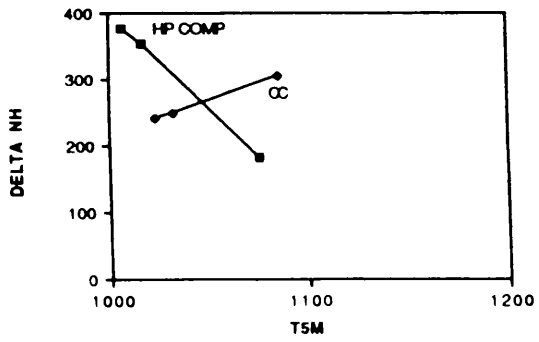
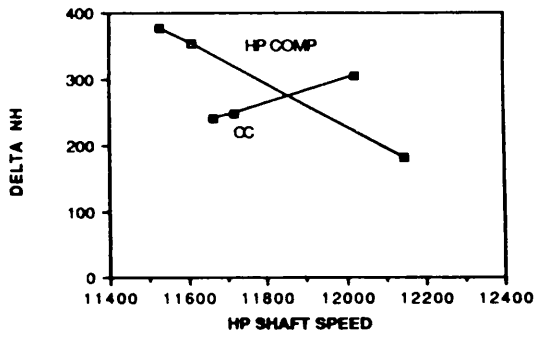
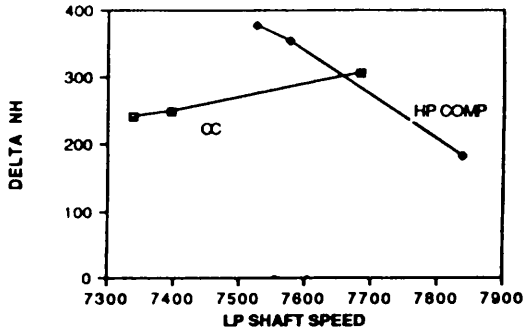


FIG 5.3

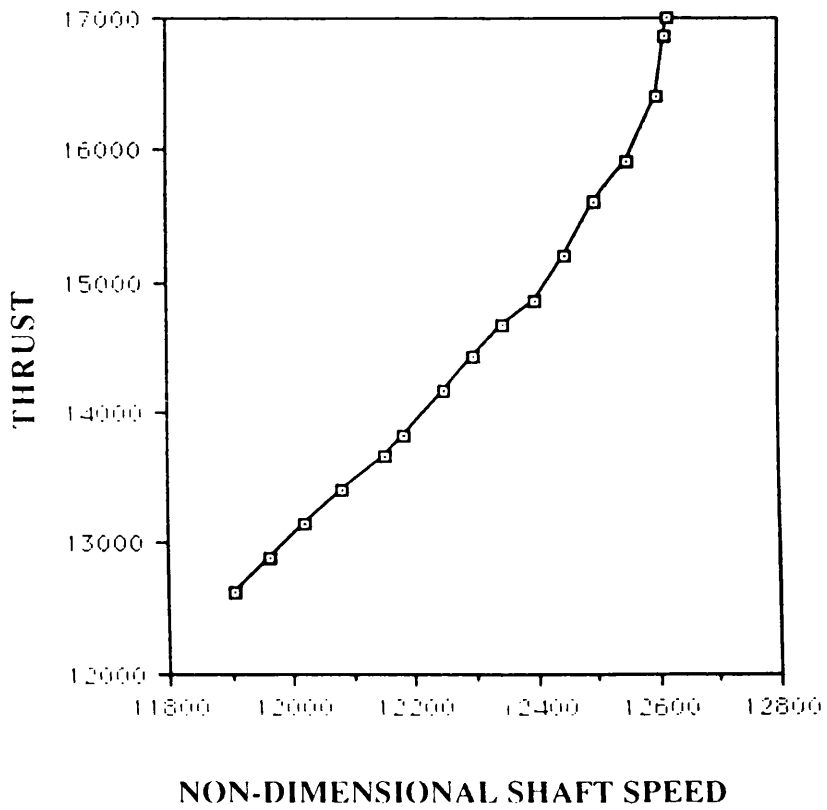
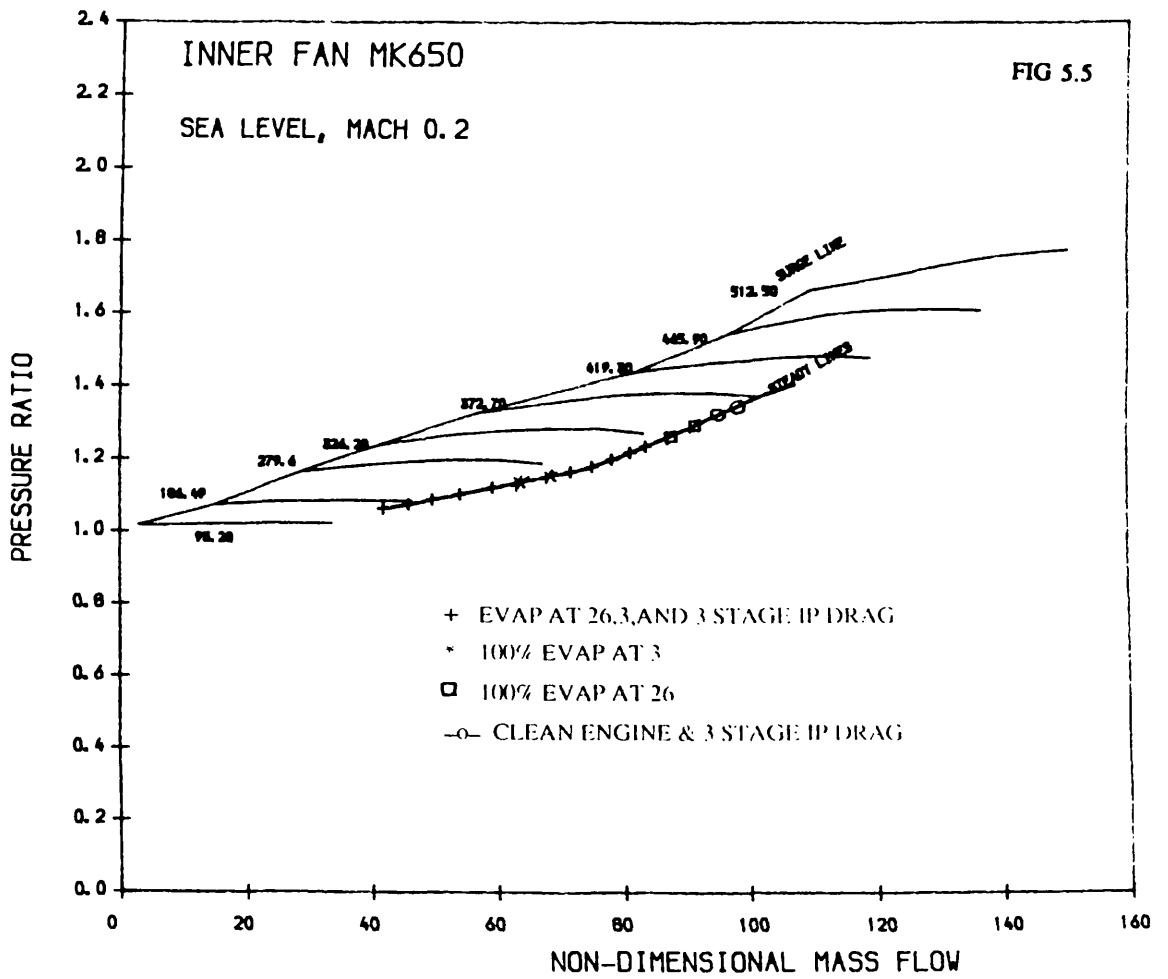
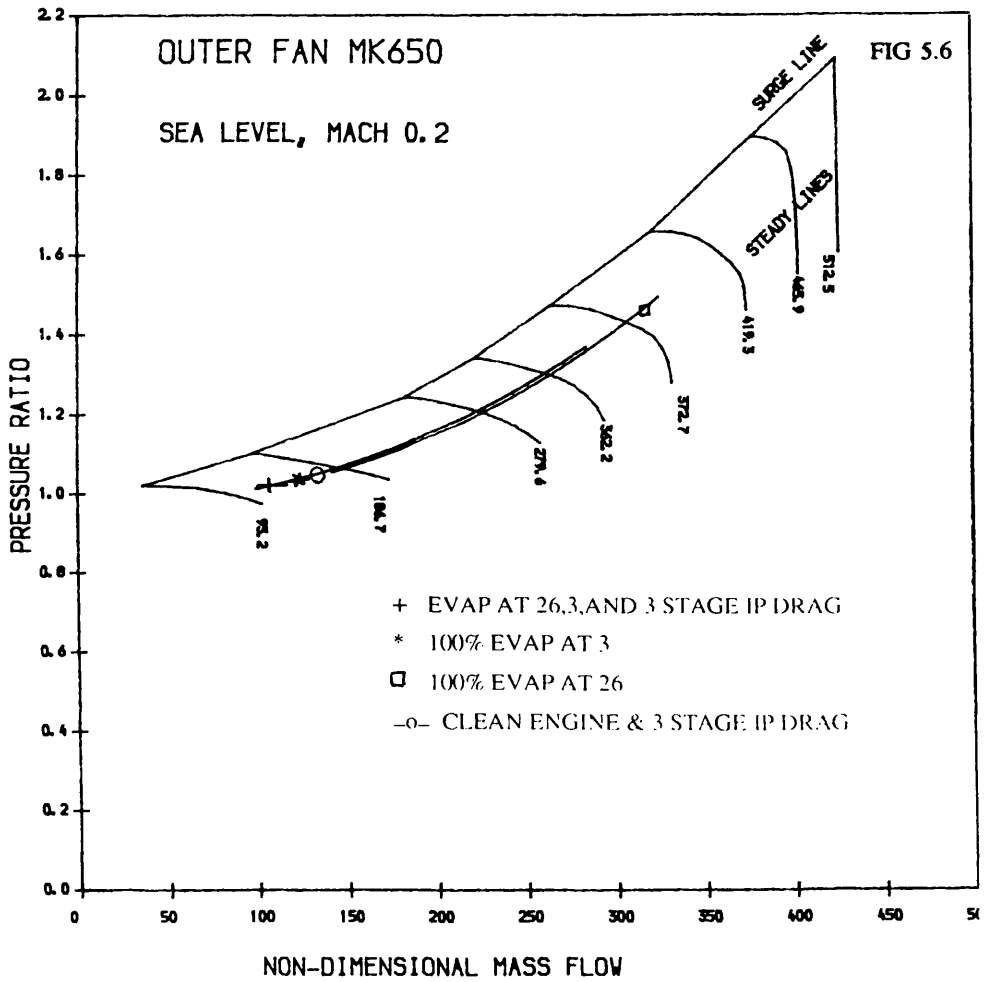


FIG 5.4





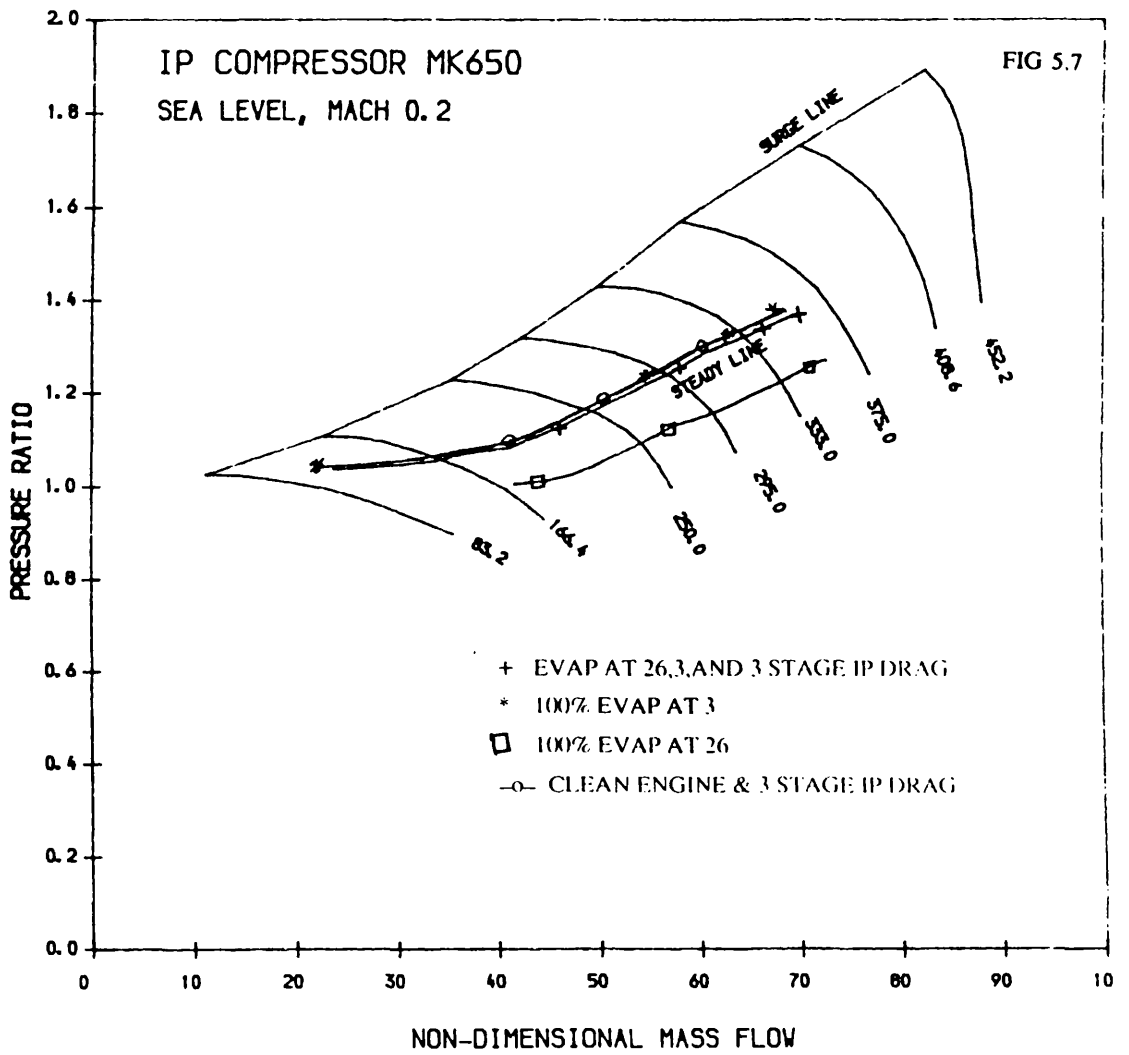
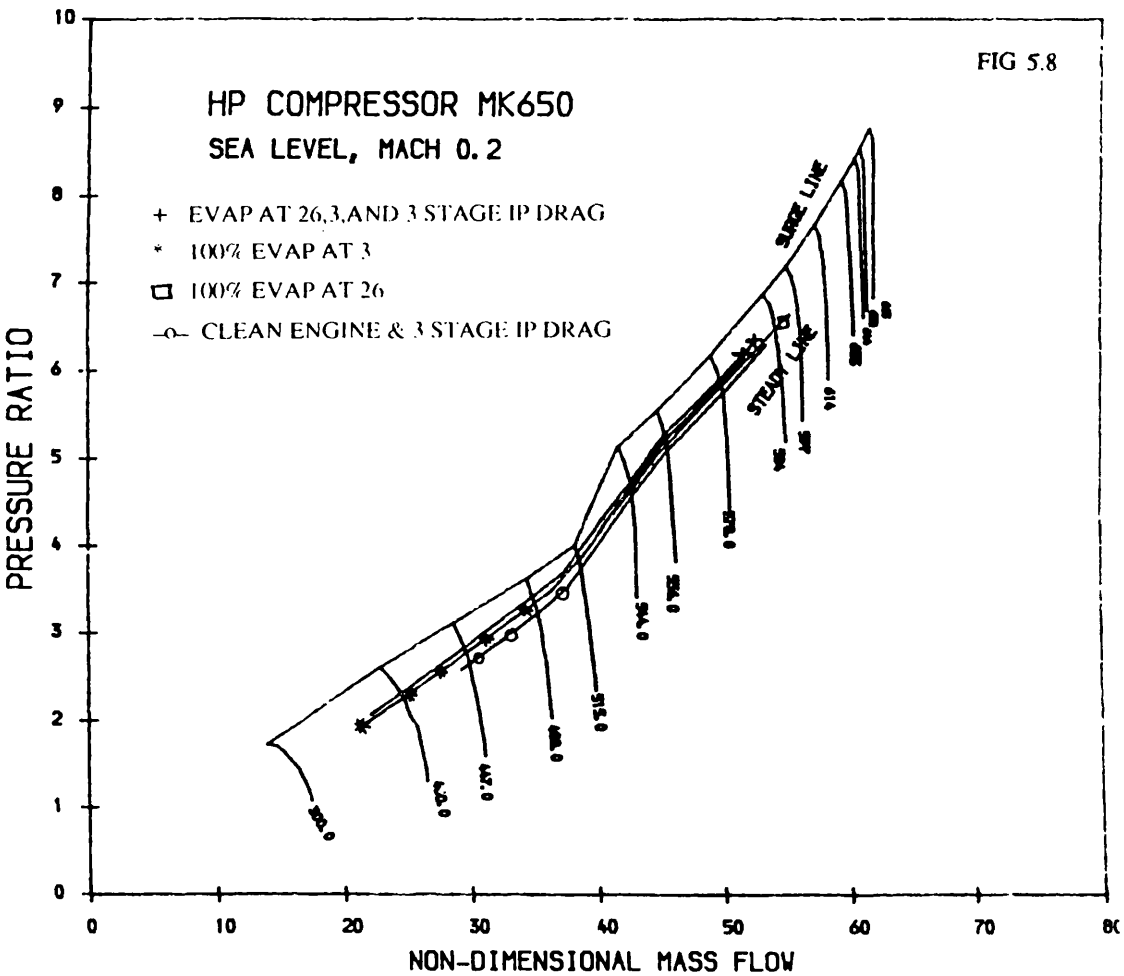


FIG 5.8



FUEL FLOW = 0.12 KG/S , ALTITUDE=20,000 FT, MACH=0.8

ENGINE PARAMETERS	CLEAN ENGINE	EVAPORATION AT 7	EVAPORATION AT 26,3,7 WITH DRAGS
NH	9392.737	9462.513	9184.741
NI	4705.235	5027.051	4477.264
AIIEQV	89.82	95.09	89.76
RCMPL	1.157	1.1892	1.141
ETISCL	0.8951	0.887	0.8775
ZNDLP	280.98	300.2	267.37
BETACL	14.61	14.11	15.41
AIIEQV	269.62	285.42	269.42
RCMPO	1.098	1.1012	1.0513
ETISCO	0.7167	0.7094	0.6344
ZNDLPC	280.98	300.2	267.37
BETACO	11.43	11.87	13.14
AI24RR	49.23	50.49	47.26
RCMPI	1.2386	1.284	1.2122
ETISCI	0.8357	0.8334	0.837
ZNDIPC	274.48	291.91	261.67
BETACI	4.43	3.88	4.49
AI1ERR	55.66	58.38	52.78
RCMPC	1.4334	1.5269	1.3831
AI27RR	40.67	40.48	39.58
RCMPII	3.8986	3.7969	3.9317
ETISCIH	0.8317	0.8309	0.8354
ZNDIIPC	528.3	526.54	522.57
BETACH	4.41	4.52	2.77
AIMS26	15.33	16.08	14.537
T26BEV	316.095	322.966	312.609
T26	316.095	322.966	308.668
P26	101.866	108.51	98.288
AIMS27	15.33	16.08	14.56
T5M	659.48	651.71	646.86
T4	879.317	870.325	841.623
P4	377.478	391.602	367.314
GASMS4	12.115	12.63	11.508
T3BEV	493.267	499.68	482.435
T3	493.267	499.68	438.589
P3	367.136	411.996	386.442
AIMS3	11.996	12.512	11.39

TABLE 6.1

FUEL FLOW = 0.20 KG/S , ALTITUDE 20,000 FT , MACH=0.8

ENGINE PARAMETERS	CLEAN ENGINE	EVAPORATION AT 7	EVAPORATION AT 26,3,7 WITH DRAGS
NH	10079.844	10118.08	9885.96
NL	5586.055	5783.62	5323.36
AIIEQV	99.31	103.5	97.12
RCMPL	1.263	1.2915	1.2249
ETISCL	0.898	0.8998	0.8896
ZNDLP	333.58	345.38	317.89
BETACL	11.79	11.67	12.85
AIIEQV	298.09	310.67	291.51
RCMPO	1.2296	1.2224	1.1558
ETISCO	0.8278	0.8019	0.7702
ZNDLPC	333.58	345.38	317.89
BETACO	9.31	10.09	10.62
AI24RR	58.01	58.69	55.6
RCMPI	1.3493	1.39	1.3097
ETISCI	0.8339	0.8318	0.8337
ZNDIPC	321.39	331.62	307.68
BETACI	4.48	3.97	4.59
AIIERR	70.6	72.78	65.92
RCMPC	1.7042	1.7951	1.6043
AI27RR	44.63	44.06	43.7
RCMPH	4.8163	4.6642	4.952
ETISCH	0.8465	0.8435	0.8477
ZNDHPC	551.15	548.54	548.44
BETACH	4.38	4.72	3.17
AIMS26	19.445	20.046	18.156
T26BEV	334.475	340.234	328.155
T26	334.475	340.234	324.698
P26	121.107	127.565	114.007
AIMS27	19.445	20.046	18.181
T5M	760.12	755.8	760.95
P4	1018.667	1013.119	995.538
P4	554.418	565.54	536.613
GASMS4	16.542	16.915	15.58
T3BEV	552.21	556.675	540.792
T3	552.21	556.675	504.192
P3	583.29	594.993	564.559
AIMS3	16.333	16.915	15.38

TABLE 6.2

FUEL FLOW = 0.32 KG/S , ALTITUDE 20,000 FT , MACH=0.8

ENGINE PARAMETERS	CLEAN ENGINE	EVAPORATION AT 7	EVAPORATION AT 26,3,7 WITH DRAGS
NH	10653.84	10671.779	10475.771
NL	6367.928	6503.961	6089.195
AI1EQV	110.76	114.85	107.44
RCMPL	1.3821	1.3996	1.3391
ETISCL	0.9201	0.9199	0.9097
ZNDLP	380.27	388.39	363.63
BETACL	9.84	10.02	10.78
AI0EQV	332.47	344.74	322.51
RCMPO	1.4096	1.4	1.3155
ETISCO	0.8769	0.8583	0.8502
ZNDLPC	380.27	388.39	363.63
BETACO	7.6	8.86	8.9
AI24RR	68.06	68.41	65.21
RCMPI	1.4157	1.4494	1.3859
ETISCI	0.8332	0.8331	0.8343
ZNDIPC	361.62	368.62	347.31
BETACI	5.52	5.12	5.41
AI1ERR	89.45	90.87	83.41
RCMPC	1.9566	2.0286	1.8558
AI27RR	50.31	49.59	48.92
RCMPII	5.7705	5.6348	5.9197
ETISCIH	0.8634	0.8619	0.8627
ZNDIHC	570.39	568	567.72
BETACH	3.97	4.05	2.05
AIMS26	24.637	25.03	22.974
T26BEV	348.879	353.008	343.35
T26	348.879	353.008	340.293
P26	139.043	144.162	131.885
AIMS27	24.637	25.03	23.002
TSM	872.98	869.1	883
T4	1169.768	1164.287	1155.028
P4	763.227	772.774	742.511
GASMS4	21.266	21.6	20.124
T3BEV	602.094	605.059	592.417
T3	602.094	605.059	559.876
P3	802.352	812.32	780.716
AIMS3	20.946	21.283	19.805

TABLE 6.3

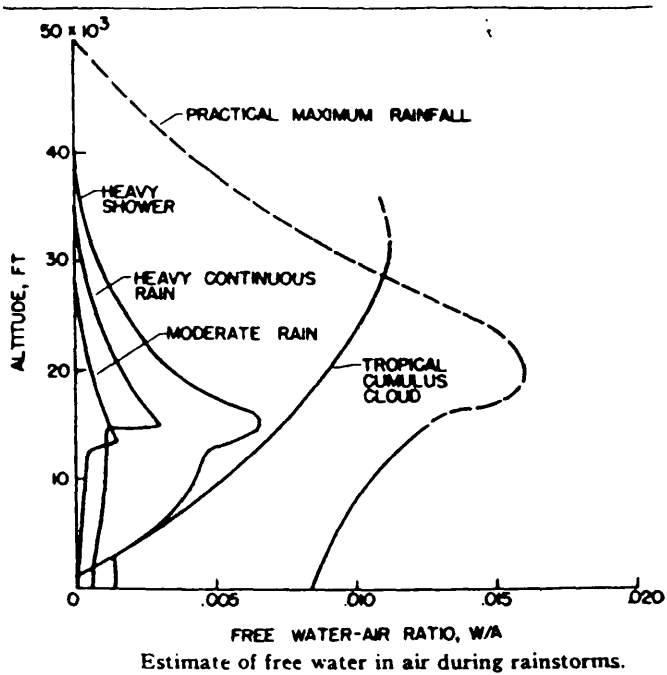
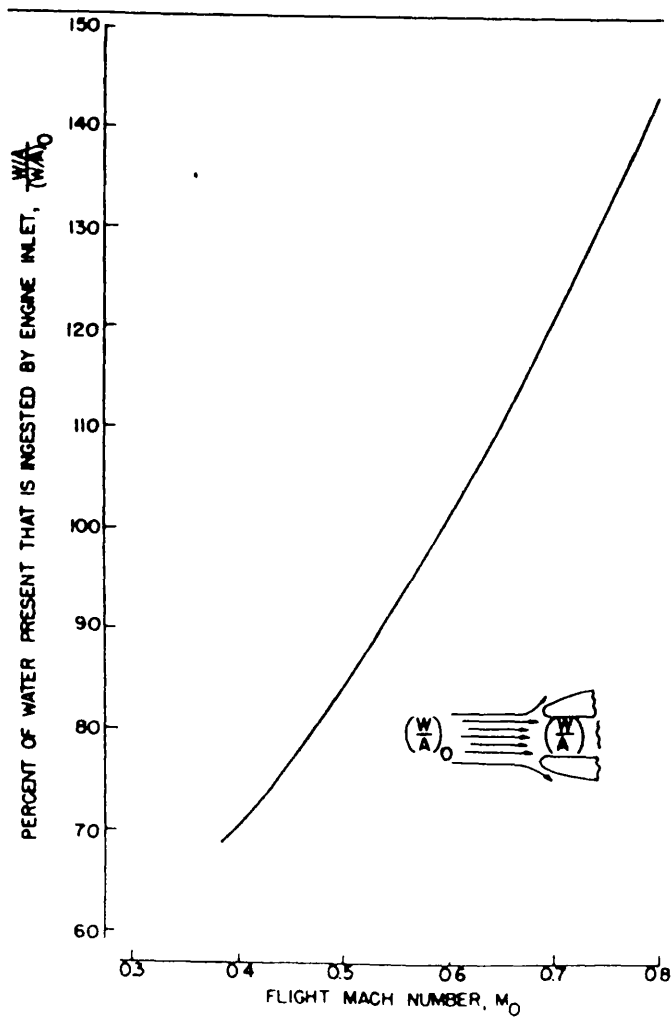
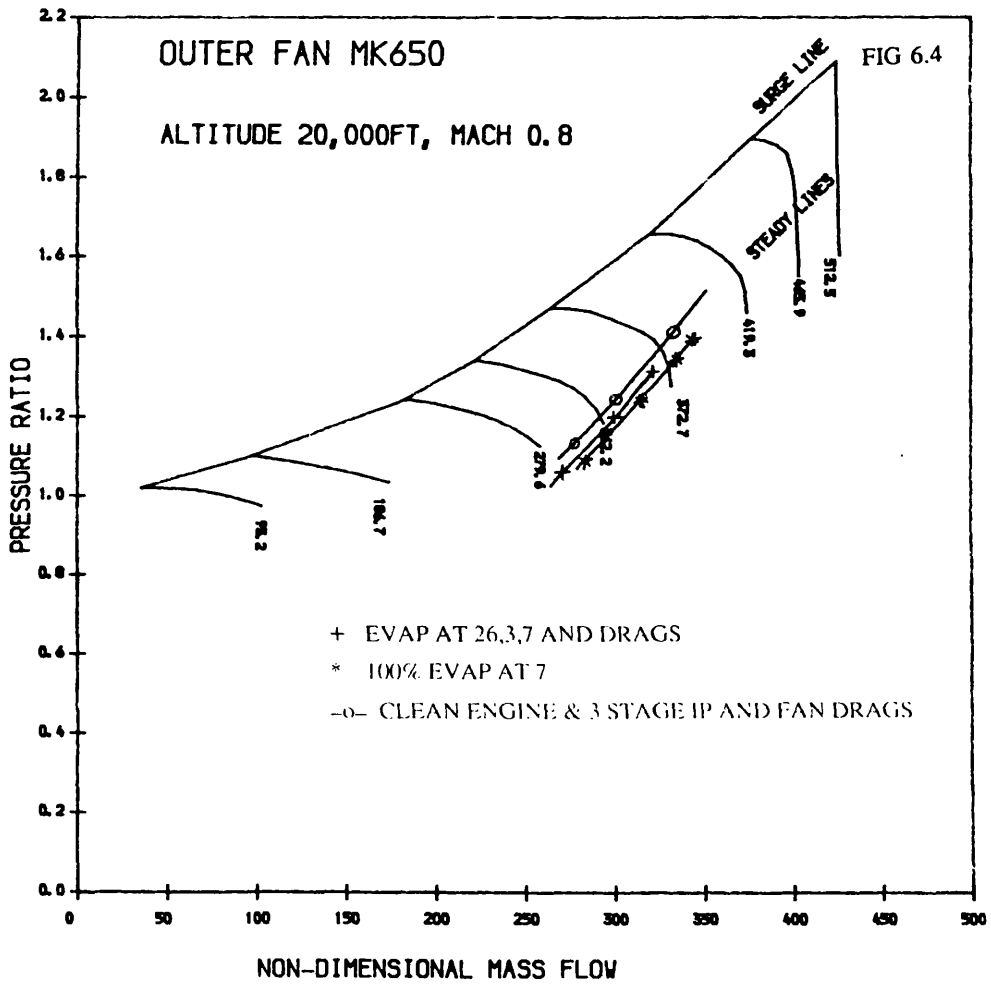


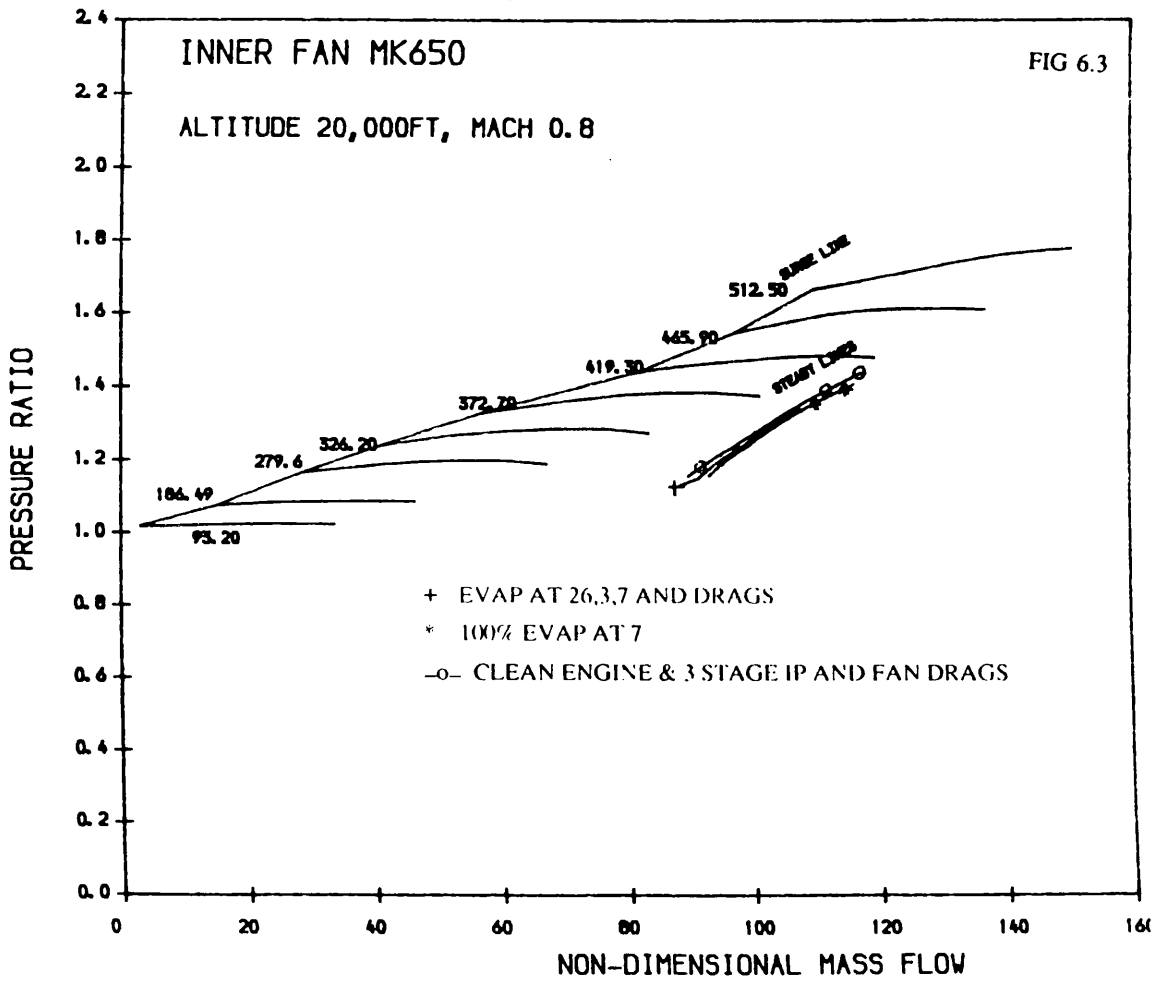
FIG 6.1

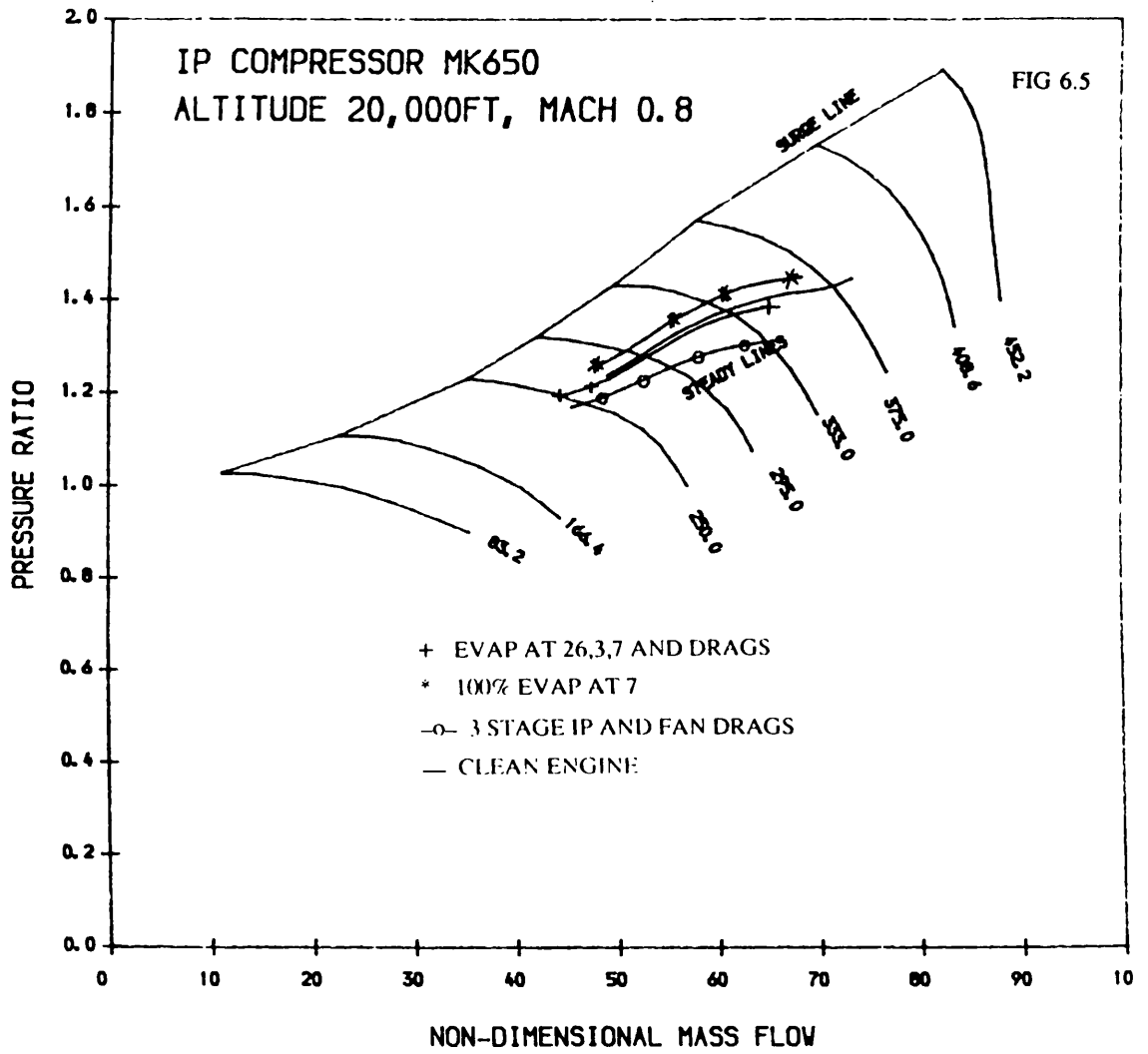


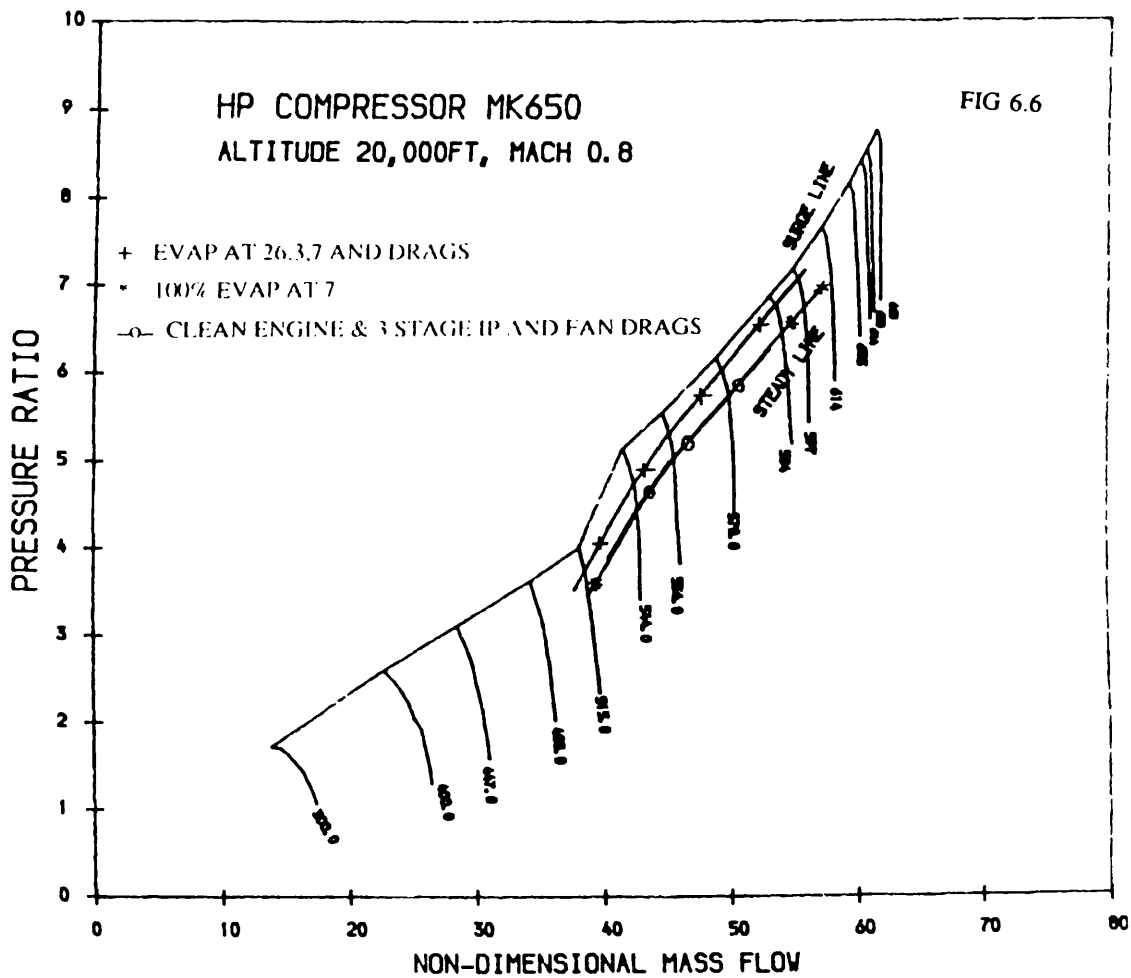
Free water ingestion by engine inlet. Air scoop area, 2 sq. ft.: Based on constant engine airflow of 80 lbs. per sec.

FIG 6.2









GLASGOW
 UNIVERSITY
 LIBRARY